Title

Precise test of lepton flavour universality in \(\varvec{W}\)-boson decays into muons and electrons in \(\varvec{pp}\) collisions at \(\varvec{\sqrt{s}}=13\,\text {T}\text {e}\hspace{-1.00006pt}\text {V} \) with the ATLAS detector

Journal

The European Physical Journal C, 84(10)

ISSN

1434-6044

Authors

Aad, G
Aakvaag, E
Abbott, B
et al.

Publication Date

2024-10-01

DOI

10.1140/epjc/s10052-024-13070-4

Eur. Phys. J. C (2024) 84:993
https://doi.org/10.1140/epjc/s10052-024-13070-4

THE EUROPEAN PHYSICAL JOURNAL C

Regular Article - Experimental Physics

Precise test of lepton flavour universality in W-boson decays into muons and electrons in pp collisions at $\sqrt{s} = 13$ TeV with the ATLAS detector

ATLAS Collaboration*

CERN, 1211 Geneva 23, Switzerland

Received: 6 March 2024 / Accepted: 29 June 2024

Abstract The ratio of branching ratios of the W boson to muons and electrons, $R_W^{\mu/e} = \mathcal{B}(W \to \mu\nu)/\mathcal{B}(W \to e\nu)$, has been measured using 140 fb^{-1} of pp collision data at $\sqrt{s} = 13$ TeV collected with the ATLAS detector at the LHC, probing the universality of lepton couplings. The ratio is obtained from measurements of the $t\bar{t}$ production cross-section in the ee, $e\mu$ and $\mu\mu$ dilepton final states. To reduce systematic uncertainties, it is normalised by the square root of the corresponding ratio $R_Z^{\mu\mu/ee}$ for the Z boson measured in inclusive $Z \to ee$ and $Z \to \mu\mu$ events. By using the precise value of $R_Z^{\mu\mu/ee}$ determined from e^+e^- colliders, the ratio $R_W^{\mu/e}$ is determined to be

$$R_W^{\mu/e} = 0.9995 \pm 0.0022\,(\text{stat}) \pm 0.0036\,(\text{syst}) \pm 0.0014\,(\text{ext}).$$

The three uncertainties correspond to data statistics, experimental systematics and the external measurement of $R_Z^{\mu\mu/ee}$, giving a total uncertainty of 0.0045, and confirming the Standard Model assumption of lepton flavour universality in W-boson decays at the 0.5% level.

Contents

1 Introduction

The assumption of lepton flavour universality, i.e. that the couplings of the charged leptons e, μ and τ to the electroweak gauge bosons are independent of the lepton masses, is a key axiom of the Standard Model of particle physics. This assumption has been tested over a wide range of momentum transfers by studying ratios of partial decay widths (or equivalently, ratios of branching ratios) of various particles to electrons, muons and taus. After correction for mass, phase space and radiative effects, these ratios of decays into leptons of generations i and j are proportional to g_i^2/g_j^2, where g_i is the coupling of lepton i ($= e, \mu, \tau$). The equality of these couplings has been tested to the 0.1–0.2% level in decays of τ leptons, π and K mesons (see for example Ref. [1]). More recently, hints of departures from lepton flavour universality at the level of a few standard deviations were seen in the so-called flavour anomalies in b-hadron decays, e.g. in the processes $B \to D^{(*)}\tau\nu$ vs. $B \to D^{(*)}\ell\nu$ (with $\ell = e$ or μ) [2–7], and in the loop-induced process $b \to s\ell\ell$. However, the latest measurement of $b \to s\ell\ell$ in $B \to K^{(*)}\mu^+\mu^-$ vs. $B \to K^{(*)}e^+e^-$ decays from the LHCb collaboration is in agreement with lepton flavour universality [8], and definitive conclusions have yet to be established.

At high momentum transfer, the branching ratios for the leptonic decays of the W boson to e, μ and τ are expected to be equal to very high precision, given the small sizes of the lepton masses compared to the W boson mass. This assumption has been tested in the production of W-boson pairs in e^+e^- collisions at LEP2, in the production of single W bosons at the Tevatron and Large Hadron Collider (LHC), and by exploiting the two W bosons produced in $t\bar{t}$ events at the LHC. The most precise measurement of $R_W^{\mu/e}$, the ratio of branching ratios for $W \to \mu\nu$ and $W \to e\nu$, was performed by the CMS collaboration with $pp \to t\bar{t}$ events at $\sqrt{s} = 13$ TeV. This analysis made use of a global fit to lepton and jet multiplicities, together with kinematic variables and the identification of jets originating from b-

* e-mail: atlas.publications@cern.ch

quarks, and achieved a precision of 0.9% [9]. Measurements of $pp \rightarrow W$ cross-sections in the $W \rightarrow e\nu$ and $W \rightarrow \mu\nu$ decay channels from the ATLAS and LHCb experiments [10,11], and measurements in $e^+e^- \rightarrow W^+W^-$ events from the ALEPH, DELPHI, L3 and OPAL experiments at LEP2 [12] also contribute significantly to the combined value of $R_W^{\mu/e} = 1.002 \pm 0.006$ determined by the Particle Data Group [13].

This paper describes a measurement of $R_W^{\mu/e}$ using W bosons produced from the decay of top quarks in $pp \rightarrow t\bar{t}$ events selected from the full Run 2 ATLAS pp collision data sample at $\sqrt{s} = 13$ TeV. Final states with two opposite-charge leptons (electrons or muons, $\ell = e$ or μ) and one or two jets tagged as likely to contain b-hadrons are selected, allowing $R_W^{\mu/e}$ to be derived from a comparison of the $t\bar{t}$ production cross-section measured in the ee, $e\mu$ and $\mu\mu$ channels. Many systematic uncertainties related to $t\bar{t}$ and background physics modelling cancel in this direct measurement of $R_W^{\mu/e}$, but it is still limited by uncertainties related to the identification of electrons and muons. The latter can be reduced by making a simultaneous measurement of the analogous ratio $R_Z^{\mu\mu/ee}$ for Z bosons, i.e. the ratio of branching ratios for $Z \rightarrow \mu\mu$ and $Z \rightarrow ee$, using inclusive $Z \rightarrow \ell\ell$ events in the same data sample. The main measured parameter of interest becomes $R_{WZ}^{\mu/e} = R_W^{\mu/e}/\sqrt{R_Z^{\mu\mu/ee}}$, and the final result is then obtained from $R_{WZ}^{\mu/e}$ and the precise measurement of $R_Z^{\mu\mu/ee} = 1.0009 \pm 0.0028$ from the LEP and SLD experiments [13,14], taken as an external input parameter. The $t\bar{t}$ and $Z \rightarrow \ell\ell$ cross-sections, $\sigma_{t\bar{t}}$ and $\sigma_{Z\rightarrow\ell\ell}$, are also measured as by-products of this procedure. The value of $\sigma_{t\bar{t}}$ is defined inclusively with respect to all $t\bar{t}$ final states, whereas $\sigma_{Z\rightarrow\ell\ell}$ is defined for decays into a single dilepton flavour $\ell\ell$.

The data and samples of Monte Carlo simulated events used in this analysis are described in Sect. 2, followed by the event reconstruction and selection in Sect. 3. The analysis method is described in Sect. 4, and supporting measurements of lepton isolation efficiencies are outlined in Sect. 5. Systematic uncertainties are detailed in Sect. 6 and the results in Sect. 7. Finally, the conclusion is given in Sect. 8.

2 Data and simulated event samples

The ATLAS detector [15–17] at the LHC covers nearly the entire solid angle around the collision point. It consists of an inner tracking detector surrounded by a thin superconducting solenoid producing a 2T axial magnetic field, electromagnetic and hadronic calorimeters, and an external muon spectrometer incorporating three large toroidal magnet assemblies. The analysis was performed on samples of proton–proton collision data collected at $\sqrt{s} = 13$ TeV in 2015–18, corresponding to an integrated luminosity of $140.1 \pm 1.2\,\text{fb}^{-1}$ after data quality requirements [18,19]. Events were required to pass a single-electron or single-muon trigger [20,21], with transverse momentum (p_{T}) thresholds that were progressively raised during the data-taking period.[1] The electron trigger reached the efficiency plateau region for electrons with reconstructed $p_{\text{T}} > 25$ GeV in 2015 and for $p_{\text{T}} > 27$ GeV for 2016–18, the corresponding thresholds for the muon trigger being 21 GeV for 2015 and 27.3 GeV thereafter. Each triggered event also includes the signals from on average 33 superimposed inelastic pp collisions, referred to as pileup.

Monte Carlo simulated event samples were used to develop the analysis procedures, to evaluate signal and background contributions, and to compare with data. Samples were processed using either the full ATLAS detector simulation [22] based on GEANT4 [23], or with a faster simulation making use of parameterised showers in the calorimeters [24]. The effects of pileup were simulated by generating additional inelastic pp collisions with PYTHIA8 (v8.186) [25] using the A3 set of parameter values (tune) [26] and overlaying them on the primary simulated events, so as to match the distribution of the number of inelastic events per bunch crossing observed in the data. These combined events were then processed using the same reconstruction and analysis chain as the data [27]. Small corrections were applied to lepton and jet energy scales [28–30], and to lepton and b-tagging efficiencies [31–33], in order to improve agreement with the response observed in data. Further topology-specific lepton isolation corrections were applied as discussed in Sect. 5.

The baseline simulated $t\bar{t}$ sample was produced with the POWHEG-BOX v2 event generator [34–37] (referred to hereafter as POWHEG), which implements matrix-elements at next-to-leading-order (NLO) in the strong coupling constant α_{s}, using the NNPDF3.0 NLO parton distribution function (PDF) set [38]. The parton shower, hadronisation and underlying event modelling was performed using PYTHIA8 (v8.210) with the NNPDF2.3 LO PDF set [39], the A14 tune [40], and additional parameters configured as described in Ref. [41]. Modelling uncertainties were assessed by using alternative samples generated using MADGRAPH5_AMC@NLO (referred to hereafter as AMC@NLO) [42] interfaced to PYTHIA8, and POWHEG interfaced to HERWIG7.1 [43,44], as discussed in Ref. [45]. Further variations were obtained from the baseline POWHEG + PYTHIA8 sample, by using event weights to

[1] ATLAS uses a right-handed coordinate system with its origin at the nominal interaction point in the centre of the detector, and the z-axis along the beam line. Pseudorapidity is defined in terms of the polar angle θ as $\eta = -\ln\tan\theta/2$, and transverse momentum is defined relative to the beam line as $p_{\text{T}} = p\sin\theta$. The azimuthal angle around the beam line is denoted by ϕ, and distances in (η, ϕ) space by $\Delta R = \sqrt{(\Delta\eta)^2 + (\Delta\phi)^2}$.

change the quantum chromodynamics (QCD) factorisation and renormalisation scales, and the amounts of initial and final state radiation. The top quark mass was set to $m_t = 172.5$ GeV, the $W \to \ell\nu$ branching ratio to the Standard Model prediction of 0.1082 for each lepton flavour (e, μ and τ) [46], and EvtGen [47] was used to handle the decays of b- and c-flavoured hadrons. The $t\bar{t}$ samples were normalised to a reference cross-section of $832 \pm 35^{+20}_{-29}$ pb, where the first uncertainty corresponds to PDF uncertainties and the second to QCD scale uncertainties. This value was calculated at next-to-next-to-leading-order (NNLO) accuracy in α_s, including the resummation of next-to-next-to-leading-logarithmic (NNLL) soft gluon terms [48], using Top++ 2.0 [49] as described in Ref. [50]. The associated production of a W boson and a top quark (Wt) is a background in the $t\bar{t}$ cross-section measurement but contributes sensitivity to $R_W^{\mu/e}$, as it gives rise to final states with two real W bosons. It was simulated with Powheg + Pythia8 with the same setup as for the $t\bar{t}$ sample. The interference between the $t\bar{t}$ and Wt amplitudes was modelled using the diagram removal scheme [51,52]. The Wt cross-section was taken to be 79.3 ± 2.2 (PDF) $^{+1.9}_{-1.8}$ (QCD scale) pb, based on an NLO calculation with the addition of third-order corrections resumming NNLL soft gluon contributions [53].

The dilepton plus b-tagged jet signature can also arise from Z-boson production with additional jets. In the $t\bar{t}$ measurement, this background was modelled using Sherpa 2.2.11 [54] for $Z \to ee/\mu\mu$ and Sherpa 2.2.14 for $Z \to \tau\tau$, with NLO matrix elements for up to two partons, and leading-order matrix elements for up to five partons, calculated with the Comix [55] and OpenLoops [56] libraries and matched with the Sherpa parton shower [57] using the MEPS@NLO prescription [58–61]. The samples include the off-shell Z/γ^* and interference contribution and have dilepton invariant mass $m_{\ell\ell} > 10$ GeV. They were generated using the NNPDF3.0 PDF set and normalised to an NNLO cross-section prediction [62]. For the inclusive $Z \to \ell\ell$ selections used in the normalisation measurement of $R_Z^{\mu\mu/ee}$, where jets are less important, $Z \to \ell\ell$ events were modelled using Powheg v1 [63] interfaced to Pythia8 (v8.186) with the AZNLO tune [64] and the CT10 PDF set [65], including Z/γ^* and interference contributions, and generating events with dilepton invariant mass $m_{\ell\ell} > 60$ GeV. These events were reweighted to data as a function of $p_T^{\ell\ell}$ in order to improve the modelling of the reconstructed Z-boson transverse momentum spectrum, and the samples were normalised to a reference cross-section of $\sigma_{Z\to\ell\ell} = 1951$ pb, based on predictions from Fewz [66].

Smaller contributions to both selections arise from diboson production (WW, WZ and ZZ), which was modelled using Sherpa 2.2.2, analogously to Z + jets production. Production of $t\bar{t}$ in association with a leptonically decaying W, Z or Higgs boson, or an additional $t\bar{t}$ pair, gives a negligible contribution to the opposite-charge dilepton samples, but is significant in the same-charge control samples used to assess the background from misidentified leptons in the $t\bar{t}$ selection. These processes were modelled at NLO using Powheg + Pythia8 or aMC@NLO + Pythia8. Additional background arises from events where at least one lepton is not a prompt lepton from a W or Z decay (including via leptonic τ decays), but is a misidentified lepton, i.e. a non-prompt lepton from the decay of a bottom or charm hadron, an electron from a photon conversion, a hadronic jet misidentified as an electron, or a muon produced from the decay in flight of a pion or kaon. Events with one prompt and one misidentified lepton can arise from $t\bar{t}$ or Wt events with one hadronically decaying W boson (modelled as described above), W + jets production (modelled with Sherpa 2.2.1) or t-channel single top quark production (modelled with Powheg + Pythia8). Processes with two misidentified leptons (e.g. from inclusive $b\bar{b}$ or $c\bar{c}$ production) are negligible for the $t\bar{t}$ selection, and the corresponding background in the inclusive $Z \to \ell\ell$ selection was modelled from data without relying on the simulation of such processes (see Sect. 4).

3 Event reconstruction and selection

This analysis makes use of reconstructed electrons, muons and b-tagged jets. Electron candidates were reconstructed from a localised cluster of energy deposits in the electromagnetic calorimeter matched to a track in the inner detector, passing the 'Medium' likelihood-based requirement of Ref. [28]. They were required to have transverse momentum $p_T > 20$ GeV and pseudorapidity $|\eta| < 2.47$, excluding the transition region between the barrel and endcap electromagnetic calorimeters, $1.37 < |\eta| < 1.52$, and to be consistent with originating from the signal primary vertex. The latter was defined as the reconstructed vertex with the highest sum of p_T^2 of associated tracks. To reduce background from non-prompt electrons, electron candidates were further required to pass the 'Tight' isolation requirements of Ref. [28], based on the amount of summed calorimeter energy and track transverse momentum close to the electron. Muon candidates were reconstructed by combining tracks from the inner detector with matching tracks reconstructed in the muon spectrometer, and were required to have $p_T > 20$ GeV, $|\eta| < 2.5$ and to satisfy the 'Medium' requirements of Ref. [32]. Muons were also required to be consistent with the signal primary vertex and to satisfy the 'Tight' isolation requirements of Ref. [32].

Jets were reconstructed using the anti-k_t algorithm [67,68] with radius parameter $R = 0.4$, starting from particle-flow objects that combine information from topological clusters of calorimeter energy deposits and inner-detector tracks [69]. After calibration using information from both simulation and data [30], jets were required to have $p_T > 25$ GeV

Table 1 Summary of the common object selection, and event selections for $t\bar{t}$ and Z final states

Object selection		
Electrons	$p_T > 27.3\,\text{GeV}$, $\lvert\eta\rvert < 1.37$ or $1.52 < \lvert\eta\rvert < 2.47$	
Muons	$p_T > 27.3\,\text{GeV}$, $\lvert\eta\rvert < 2.5$	
b-tagged jets	$p_T > 30.0\,\text{GeV}$, $\lvert\eta\rvert < 2.5$, b-tagging DL1r 70%	
Event selection	$t\bar{t} \to \ell\ell b\bar{b}\nu\bar{\nu}$	$Z \to \ell\ell$
Dilepton flavour ($\ell^+\ell^-$)	ee, $e\mu$, $\mu\mu$	ee, $\mu\mu$
Dilepton invariant mass	$m_{\ell\ell} > 30\,\text{GeV}$	$66\,\text{GeV} < m_{\ell\ell} < 116\,\text{GeV}$
b-tagged jet multiplicity	1 or 2	–

and $|\eta| < 2.5$, and jets with $p_T < 60\,\text{GeV}$ and $|\eta| < 2.4$ were subject to additional pileup rejection criteria using the multivariate jet-vertex tagger (JVT) [70]. To prevent double counting of electron energy deposits as jets, the closest jet to an electron candidate was removed if it was within $\Delta R = 0.2$ of the electron. Furthermore, to reduce the contribution of leptons from heavy-flavour hadron decays inside jets, leptons within $\Delta R = 0.4$ of selected jets were discarded, unless the lepton was a muon and the jet had fewer than three associated tracks, in which case the jet was discarded. Jets likely to contain b-hadrons were tagged using the DL1r algorithm [33,71], a multivariate discriminant based on deep-learning techniques making use of track impact parameters and reconstructed secondary vertices. A tagger working point with an efficiency of 70% for tagging b-quark jets from top-quark decays in simulated $t\bar{t}$ events was used, corresponding to rejection factors of about 380 against light quark and gluon jets, and 10 against jets originating from charm quarks.

Selected events were required to have exactly two leptons (electrons or muons) passing the requirements above, of opposite charges, with at least one of the leptons being matched to a corresponding electron or muon trigger signature. The leptons were additionally required to have $p_T > 27.3\,\text{GeV}$, to further reduce the contribution of events with misidentified leptons, and to ensure all leptons were above the muon trigger p_T threshold. For the $t\bar{t}$ selection (ee, $e\mu$ and $\mu\mu$), events were additionally required to satisfy $m_{\ell\ell} > 30\,\text{GeV}$ and to have exactly one or exactly two b-tagged jets with $p_T > 30\,\text{GeV}$. For the inclusive $Z \to \ell\ell$ selection, only ee and $\mu\mu$ events were retained, with $66\,\text{GeV} < m_{\ell\ell} < 116\,\text{GeV}$, and no requirements were made on jet or b-tagged jet multiplicity. Table 1 summarises the event selection.

The numbers of leptons in simulated $t\bar{t}$ events passing the ee and $\mu\mu$ $t\bar{t}$ selections are shown as the points and dashed red lines in Fig. 1a. The distributions are different, due mainly to the smaller electron efficiency in the forward region at high $|\eta|$, the gap in electron acceptance at $1.37 < |\eta| < 1.52$, and the reduction in muon acceptance at $\eta \approx 0$ due to detector services. The electron and muon efficiencies also evolve differently with p_T. To minimise physics modelling uncertainties in the measurement of $R_W^{\mu/e}$, it is important that the kinematic dependencies of the electron and muon identification efficiencies are as similar as possible. This was achieved by applying an η- and p_T-dependent weight to each muon, as shown in Fig. 1b. The weights were derived so as to equalise the two-dimensional distributions of lepton p_T and η in simulated ee and $\mu\mu$ $t\bar{t}$ events, and normalised so that the total number of selected events is similar in the two channels. The effect on the muon η distribution is shown by the blue solid line in Fig. 1a. The muon efficiency loss at $\eta \approx 0$ was compensated over a wide region corresponding to a single bin with $|\eta| < 0.5$ to avoid giving muons at $\eta \approx 0$ large weights, but the physics modelling effects in this region are small. The muon efficiency weighting affects the event counts in the $t\bar{t} \to \mu\mu$ and $e\mu$ selections, and the inclusive $Z \to \mu\mu$ selection. It was applied to both data and simulation, and is included in all distributions, event counts and efficiencies shown in this paper.

Figure 2 shows comparisons of data and simulation for selected events in the ee (left column) and $\mu\mu$ (right column) channels, additionally requiring $|m_{\ell\ell} - m_Z| > 10\,\text{GeV}$ to reduce the Z + jets contribution. The simulation prediction uses the reference values for the $t\bar{t}$ and Z cross-sections given in Sect. 2 and assumes $R_W^{\mu/e} = R_Z^{\mu\mu/ee} = 1$. The baseline prediction shown by the black histogram uses POWHEG + PYTHIA8 $t\bar{t}$ events, which are known not to reproduce the top quark p_T spectrum measured in data [72] or predicted by NNLO calculations [73]. The red dotted line shows the prediction from POWHEG + PYTHIA8 reweighted using a linear function of top quark p_T as discussed in Ref. [50] in order to better describe the measurement of Ref. [72]. The green dashed line shows the prediction using $t\bar{t}$ events generated with POWHEG + HERWIG7.

Figure 2a, b shows the multiplicity of b-tagged jets, $N_{b-\text{tag}}$, with the simulation normalised to the same integrated luminosity as the data; the simulation describes the data well for $N_{b-\text{tag}} \leq 2$, but shows a deficit for $N_{b-\text{tag}} \geq 3$. Figure 2c-f shows the lepton p_T and $|\eta|$ distributions for the $t\bar{t}$-dominated samples with at least one b-tagged jet, normalising the simulation to the same number of selected events as the data to focus on shape comparisons. The samples with

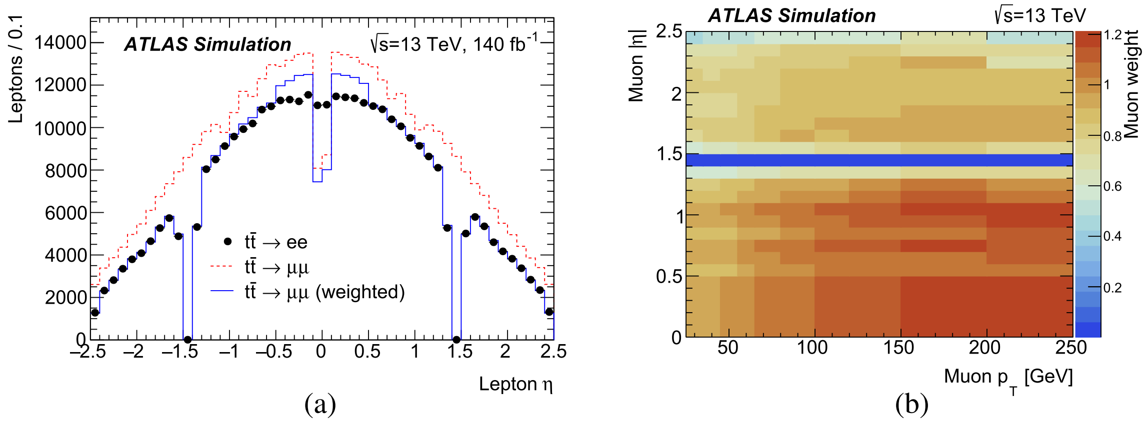

Fig. 1 **a** Number of selected leptons as a function of η in simulated $t\bar{t}$ events with at least one b-tagged jet in the ee (points) and $\mu\mu$ (red dashed line) channels, and number of selected leptons in the $\mu\mu$ channel after muon weighting (blue solid line); **b** muon efficiency weights as a function of $|\eta|$ and p_{T}

POWHEG + PYTHIA8 and POWHEG + HERWIG7 $t\bar{t}$ events both predict a harder p_{T} spectrum than the data, but the top-quark p_{T}-reweighted sample agrees well, as also seen in Ref. [50]. Similar features are seen in the $e\mu$ selection. The lepton p_{T} and $|\eta|$ distributions in the ee and $\mu\mu$ samples are similar (apart from at $\eta \approx 0$), demonstrating the effect of the muon efficiency weighting described above.

4 Analysis method

The $t\bar{t}$ cross-section was measured in each dilepton channel by fitting the numbers of selected events with one or two b-tagged jets to predictions based on the assumed $t\bar{t}$ cross-section, leptonic selection efficiencies $\epsilon_{\ell\ell}$ and estimated non-$t\bar{t}$ background. In the same-flavour channels, the dilepton invariant mass $m_{\ell\ell}$ was also exploited to separate signal events from the dominant Z + jets background. This method allows the efficiency $\epsilon_b^{\ell\ell'}$ for reconstructing and b-tagging a b-jet from the top quark decay to be determined from the data (separately for $\ell\ell' = ee$, $e\mu$ and $\mu\mu$), and minimises selection efficiency uncertainties due to the modelling of additional jets from QCD radiation in the $t\bar{t}$ events.

Following Ref. [50], the inclusive $t\bar{t}$ cross-section was determined in the $e\mu$ channel from the number of opposite-charge events with one ($N_1^{e\mu}$) or two ($N_2^{e\mu}$) b-tagged jets. The two event counts satisfy the tagging equations

$$\begin{aligned} N_1^{e\mu} &= L\sigma_{t\bar{t}}\,\epsilon_{e\mu} g_{e\mu}^{t\bar{t}}\, 2\epsilon_b^{e\mu}(1 - C_b^{e\mu}\epsilon_b^{e\mu}) \\ &\quad + \sum_{k=\mathrm{bkg}} s_1^k g_{e\mu}^k\, N_1^{e\mu,k} \text{ and} \\ N_2^{e\mu} &= L\sigma_{t\bar{t}}\,\epsilon_{e\mu} g_{e\mu}^{t\bar{t}}\, C_b^{e\mu}(\epsilon_b^{e\mu})^2 \\ &\quad + \sum_{k=\mathrm{bkg}} s_2^k g_{e\mu}^k\, N_2^{e\mu,k}, \end{aligned} \quad (1)$$

where L is the integrated luminosity of the sample, $\epsilon_{e\mu}$ is the efficiency for a $t\bar{t}$ event to pass the opposite-charge $e\mu$ selection (including the simulated values of the $W \to \ell\nu$ branching ratios), and $g_{e\mu}^{t\bar{t}}$ expresses possible deviations of these branching ratios from their simulated values. The parameter $C_b^{e\mu} \approx 1$ is a correlation coefficient that accounts for the fact that the tagging probabilities of the two b-quark jets from the top decays are not completely independent. It was evaluated from simulation as $C_b^{e\mu} = 4N_{e\mu}^{t\bar{t}}N_2^{t\bar{t}}/(N_1^{t\bar{t}} + 2N_2^{t\bar{t}})^2$, where $N_{e\mu}^{t\bar{t}}$ is the number of selected $e\mu$ $t\bar{t}$ events and $N_1^{t\bar{t}}$ and $N_2^{t\bar{t}}$ are the numbers of such events with one and two b-tagged jets [50]. Background contributions to N_1 and N_2 were divided into four sources indexed by k: Wt, Z + jets, dibosons and events with at least one misidentified lepton. The estimate of each background k was scaled by a factor s_n^k for events with $n = 1$ or 2 b-tagged jets, and additionally scaled by $g_{e\mu}^k$ to allow for changes in the W or Z leptonic branching ratios.

In the same-flavour channels, the events were divided into six bins of $m_{\ell\ell}$ to separate the $t\bar{t}$ signal from the large Z + jets background. The bins were indexed by subscript m, with lower bin boundaries at 30, 71, 81, 101, 111 and 151 GeV, the last bin including all events with $m_{\ell\ell} > 151$ GeV. Using the extension of the tagging formalism introduced in Ref. [74], the numbers of opposite-charge $\ell\ell$ events in each bin m with one and two b-tagged jets, $N_{1,m}^{\ell\ell}$ and $N_{2,m}^{\ell\ell}$ can then be expressed as

$$\begin{aligned} N_{1,m}^{\ell\ell} &= L\sigma_{t\bar{t}}\,\epsilon_{\ell\ell}\, g_{\ell\ell}^{t\bar{t}}\, 2\epsilon_b^{\ell\ell}(1 - C_b^{\ell\ell}\epsilon_b^{\ell\ell})\, f_{1,m}^{\ell\ell,t\bar{t}} \\ &\quad + \sum_{k=\mathrm{bkg}} s_1^k g_{\ell\ell}^k\, f_{1,m}^{\ell\ell,k} N_1^{\ell\ell,k} \text{ and} \\ N_{2,m}^{\ell\ell} &= L\sigma_{t\bar{t}}\,\epsilon_{\ell\ell}\, g_{\ell\ell}^{t\bar{t}}\, C_b^{\ell\ell}(\epsilon_b^{\ell\ell})^2\, f_{2,m}^{\ell\ell,t\bar{t}} \\ &\quad + \sum_{k=\mathrm{bkg}} s_2^k g_{\ell\ell}^k\, f_{2,m}^{\ell\ell,k} N_2^{\ell\ell,k}, \end{aligned} \quad (2)$$

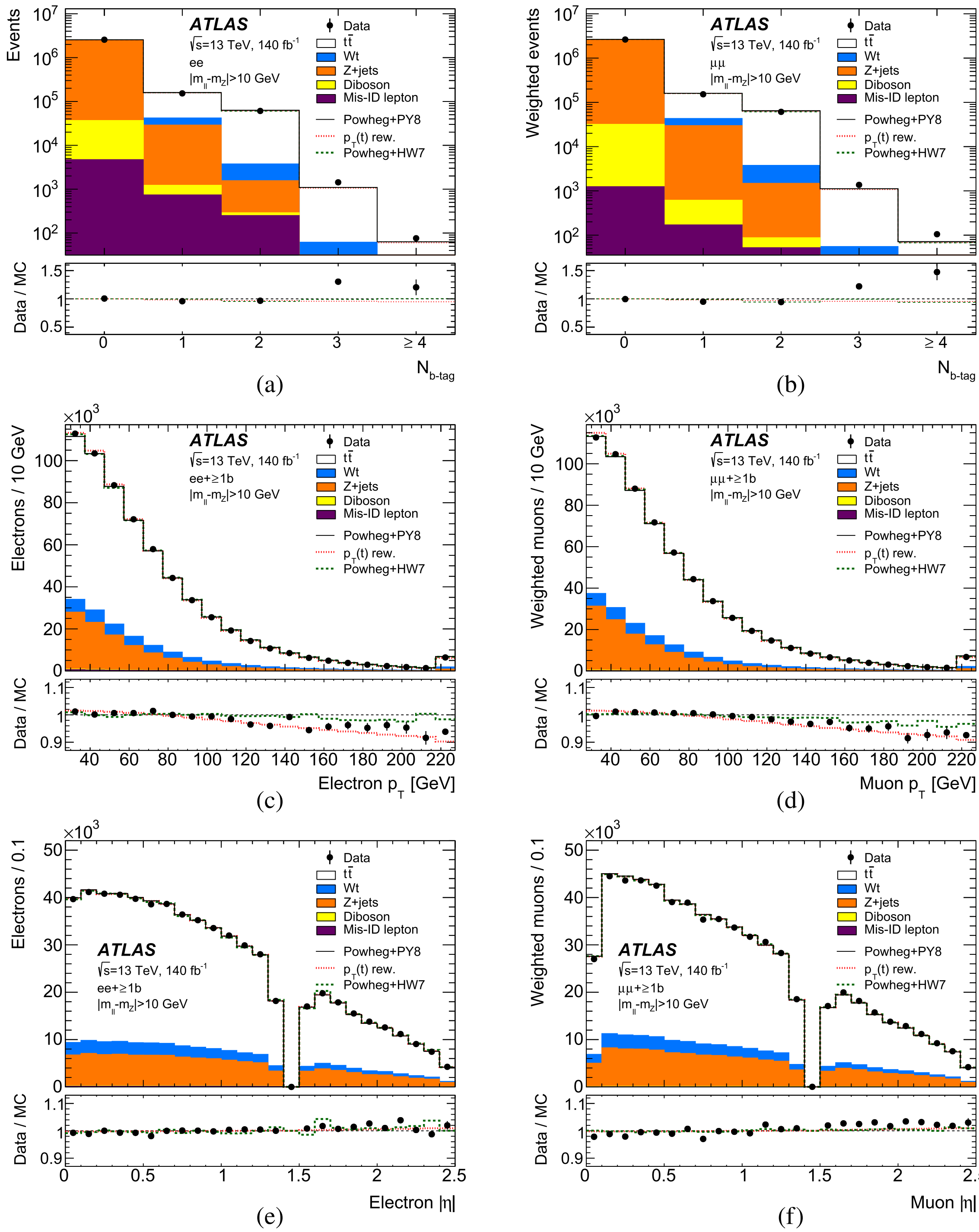

Fig. 2 Distributions of **a**, **b** the number of b-tagged jets in selected opposite-sign dilepton events with $|m_{\ell\ell} - m_Z| > 10\,\text{GeV}$ (without applying the b-tagged jet multiplicity requirement), together with **c**, **d** the lepton transverse momentum and **e**, **f** the lepton pseudorapidity in such events with at least one b-tagged jet, showing ee (left column) and weighted $\mu\mu$ (right column) events separately. The data is shown by the points with statistical error bars, compared to the prediction from simulation normalised to the data integrated luminosity in **a**, **b** and to the same number of selected events in **c**–**f**. The predicted contributions from $t\bar{t}$, Wt, $Z+$jets, dibosons and events with misidentified leptons are shown separately. The red dotted line shows the prediction with the reweighted top quark p_{T} distribution, and the green dashed line that with POWHEG + HERWIG7 $t\bar{t}$ events instead of POWHEG + PYTHIA8. The lower plots show the ratio of data to the baseline simulation, and the ratios of the alternative simulation predictions to the baseline. The last bins include the overflows in plots (**a**–**d**)

with separate selection efficiencies $\epsilon_{\ell\ell}$ and correlation coefficients $C_b^{\ell\ell}$ for each same-flavour channel ($\ell\ell = ee$ or $\mu\mu$). The coefficients $f_{1,m}^{\ell\ell,k}$ and $f_{2,m}^{\ell\ell,k}$ describe the $m_{\ell\ell}$ distributions, giving the fractions of events that appear in each mass bin, separately for each dilepton flavour $\ell\ell$, event source k and b-tagged jet multiplicity (1 or 2).

This analysis allows the branching ratios $\mathcal{B}(W \to e\nu)$ and $\mathcal{B}(W \to \mu\nu)$ to differ via a parameter Δ_W, whilst keeping their average fixed to $\overline{W} = 0.1082$, the Standard Model prediction used in the simulation. In this model

$$R_W^{\mu/e} = \frac{\mathcal{B}(W \to \mu\nu)}{\mathcal{B}(W \to e\nu)} = \frac{\overline{W}(1+\Delta_W)}{\overline{W}(1-\Delta_W)}\,, \tag{3}$$

so that $\Delta_W = (R_W^{\mu/e}-1)/(R_W^{\mu/e}+1)$. The selected $t\bar{t}$ dilepton samples also include events where one or both leptons arise from a $W \to \tau \to e/\mu$ decay, and the branching ratios for $W \to \tau\nu$, $\tau \to e\nu\bar{\nu}$ and $\tau \to \mu\nu\bar{\nu}$ were kept fixed at the values in the simulation. With these assumptions, the factors $g_{\ell\ell'}^{t\bar{t}}$ in Eqs. (1) and (2) are given by

$$\begin{aligned} g_{ee}^{t\bar{t}} &= f_{0\tau}^{ee}(1-\Delta_W)^2 &&+ f_{1\tau}^{ee}(1-\Delta_W) &&+ f_{2\tau}^{ee} \\ g_{e\mu}^{t\bar{t}} &= f_{0\tau}^{e\mu}(1-\Delta_W)(1+\Delta_W) &&+ f_{1\tau}^{e\mu} &&+ f_{2\tau}^{e\mu}\,, \\ g_{\mu\mu}^{t\bar{t}} &= f_{0\tau}^{\mu\mu}(1+\Delta_W)^2 &&+ f_{1\tau}^{\mu\mu}(1+\Delta_W) &&+ f_{2\tau}^{\mu\mu} \end{aligned} \tag{4}$$

where the parameters $f_{n\tau}^{\ell\ell'}$ give the fractions in each selected dilepton sample where n leptons resulted from $W \to \tau \to e/\mu$ rather than direct $W \to e/\mu$ decays. These fractions were taken from simulation, and are around $f_{0\tau}^{\ell\ell'} = 0.88$, $f_{1\tau}^{\ell\ell'} = 0.11$ and $f_{2\tau}^{\ell\ell'} = 0.004$ for all three dilepton flavour combinations. Increasing $f_{1\tau}^{\ell\ell'}$ by 1.3% and $f_{2\tau}^{\ell\ell'}$ by 2.6%, corresponding to the uncertainty of 1.3% in $\mathcal{B}(W \to \tau\nu)/\mathcal{B}(W \to \mu\nu)$ measured in Ref. [75], has a negligible effect on the fitted value of $R_W^{\mu/e}$ from this analysis.

The estimates of the Wt and diboson backgrounds $N_n^{\ell\ell',k}$ in Eqs. (1) and (2) (with $k = Wt$ or diboson) were taken directly from simulation, with s_n^k fixed to unity. However, since Wt events have two real W bosons and the diboson background is dominated by WW production, the corresponding values of $g_{\ell\ell'}^k$ were set equal to $g_{\ell\ell'}^{t\bar{t}}$ given by Eq. (4), effectively treating these backgrounds as signal for the determination of $R_W^{\mu/e}$. The normalisation factors $s_1^{Z+\text{jets}}$ and $s_2^{Z+\text{jets}}$ for the Z + jets background were determined from data, exploiting the binning of the same-flavour dilepton events in $m_{\ell\ell}$, and applying the same factors to all three dilepton channels. However, the introduction of the normalisation measurement of $R_Z^{\mu\mu/ee}$ also affects the Z + jets background estimate. Potential deviations of $R_Z^{\mu\mu/ee}$ from unity were described by a parameter Δ_Z, related to $R_Z^{\mu\mu/ee}$ by

$$R_Z^{\mu\mu/ee} = \frac{\mathcal{B}(Z \to \mu\mu)}{\mathcal{B}(Z \to ee)} = \frac{\overline{Z}(1+\Delta_Z)}{\overline{Z}(1-\Delta_Z)}\,, \tag{5}$$

where $\overline{Z}$ is the average $Z \to \ell\ell$ branching ratio and $\Delta_Z = (R_Z^{\mu\mu/ee}-1)/(R_Z^{\mu\mu/ee}+1)$, in analogy to Eq. (3). Potential biases in the modelling of the lepton isolation efficiency in the busy hadronic environment of $Z + b$-jet events (in particular differences between electrons and muons as discussed in Sect. 5) were taken into account by an additional ratio $R_{Z+b}^{\mu\mu/ee}$ and associated parameter $\Delta_{Z+b} = (R_{Z+b}^{\mu\mu/ee}-1)/(R_{Z+b}^{\mu\mu/ee}+1)$. With these ingredients, the values of $g_{\ell\ell'}^k$ for Z + jets events are given by

$$\begin{aligned} g_{ee}^{Z+\text{jets}} &= (1-\Delta_Z)(1-\Delta_{Z+b}) \\ g_{e\mu}^{Z+\text{jets}} &= 1 \\ g_{\mu\mu}^{Z+\text{jets}} &= (1+\Delta_Z)(1+\Delta_{Z+b}) \end{aligned}\,. \tag{6}$$

The contributions to the backgrounds in Eqs. (1) and (2) from events with misidentified leptons were evaluated using a partially data-driven method, as discussed below.

The factors $g_{\ell\ell'}^{t\bar{t}}$ giving sensitivity to the W-boson branching ratios are related to Δ_W and hence $R_W^{\mu/e}$ by Eqs. (3) and (4). However, to reduce sensitivity to uncertainties in the electron and muon identification efficiencies, the fit was not performed with $R_W^{\mu/e}$ directly, but instead using $R_{WZ}^{\mu/e}$ and $R_Z^{\mu\mu/ee}$, where

$$R_{WZ}^{\mu/e} = \frac{R_W^{\mu/e}}{\sqrt{R_Z^{\mu\mu/ee}}} = \frac{\mathcal{B}(W \to \mu\nu)}{\mathcal{B}(W \to e\nu)} \cdot \sqrt{\frac{\mathcal{B}(Z \to ee)}{\mathcal{B}(Z \to \mu\mu)}}\,. \tag{7}$$

The normalisation to $\sqrt{R_Z^{\mu\mu/ee}}$ ensures that the numerator and denominator of $R_{WZ}^{\mu/e}$ each contain one power of the electron and muon efficiencies, reducing the sensitivity of $R_{WZ}^{\mu/e}$ to uncertainties on these efficiencies. The value of $R_Z^{\mu\mu/ee}$ needed in Eq. (7) was determined from the event counts in the inclusive $Z \to \ell\ell$ selection, N_Z^{ee} and $N_Z^{\mu\mu}$, given by

$$\begin{aligned} N_Z^{ee} &= L\,\sigma_{Z\to\ell\ell}\,\epsilon_{Z\to ee}(1-\Delta_Z) + \sum_{k=\text{bkg}} s_Z^k\, N_Z^{ee,k} \quad \text{and} \\ N_Z^{\mu\mu} &= L\,\sigma_{Z\to\ell\ell}\,\epsilon_{Z\to\mu\mu}(1+\Delta_Z) + \sum_{k=\text{bkg}} s_Z^k\, N_Z^{\mu\mu,k}\,, \end{aligned} \tag{8}$$

where $\epsilon_{Z\to ee}$ and $\epsilon_{Z\to\mu\mu}$ are the selection efficiencies in simulation assuming equal branching ratios for $Z \to ee$ and $Z \to \mu\mu$, and the factors involving Δ_Z express the effects of deviations of $R_Z^{\mu\mu/ee}$ from unity. Five sources of backgrounds were considered, indexed by k: dibosons, $Z \rightarrow \tau\tau \rightarrow ee/\mu\mu$, $t\bar{t}$, Wt and events with misidentified leptons. The first four were estimated from simulation, with the $t\bar{t}$ background being scaled according to the fitted value of $\sigma_{t\bar{t}}$ via its normalisation $s_Z^{t\bar{t}}$, and all other s_Z^k values were fixed to unity. The misidentified-lepton background was estimated from data as discussed below.

All fit parameters were determined simultaneously using a single maximum likelihood fit to the observed event counts $N_1^{e\mu}$ and $N_2^{e\mu}$ in the $e\mu$ channel, the observed counts in each dilepton invariant mass bin $N_{1,m}^{\ell\ell}$ and $N_{2,m}^{\ell\ell}$ for each same-flavour channel, and the observed counts N_Z^{ee} and $N_Z^{\mu\mu}$ in the inclusive $Z \rightarrow \ell\ell$ selections, as summarised in Table 2. A Gaussian likelihood formulation was used, taking into account the probability distributions of the weighted event counts in the $\mu\mu$ and $e\mu$ channels. The fit has ten free parameters: the four parameters of interest $\sigma_{t\bar{t}}$, $\sigma_{Z\rightarrow\ell\ell}$, $R_{WZ}^{\mu/e}$ and $R_Z^{\mu\mu/ee}$, the three b-tagged jet efficiencies $\epsilon_b^{\ell\ell'}$, the scale factors $s_1^{Z+\text{jets}}$ and $s_2^{Z+\text{jets}}$ for the Z + jets background, and the Z + jets isolation efficiency parameter $R_{Z+b}^{\mu\mu/ee}$. Apart from the integrated luminosity L and the misidentified lepton backgrounds, all other quantities were determined from simulation, namely the efficiencies $\epsilon_{\ell\ell'}$, $\epsilon_{Z\rightarrow ee}$ and $\epsilon_{Z\rightarrow\mu\mu}$, b-tagging correlations $C_b^{\ell\ell'}$, τ fractions $f_{n\tau}^{\ell\ell'}$, background counts $N_1^{\ell\ell',k}$, $N_2^{\ell\ell',k}$ and $N_Z^{\ell\ell,k}$, and mass distributions $f_{1,m}^{\ell\ell,k}$ and $f_{2,m}^{\ell\ell,k}$. In the baseline simulation, the $t\bar{t}$ dilepton selection efficiencies are $\epsilon_{ee} = 0.316\%$, $\epsilon_{e\mu} = 0.639\%$ and $\epsilon_{\mu\mu} = 0.314\%$, the correlation coefficients $C_b^{\ell\ell'}$ are about 1.003 for all dilepton flavours, and the Z selection efficiencies are $\epsilon_{Z\rightarrow ee}$=16.8% and $\epsilon_{Z\rightarrow\mu\mu}$=17.3%. The fitted Z cross-section and $R_Z^{\mu\mu/ee}$ are constrained by the inclusive $Z \rightarrow \ell\ell$ selection, $\sigma_{t\bar{t}}$ is mainly determined from the $e\mu$ channel, and $R_{WZ}^{\mu/e}$, $s_1^{Z+\text{jets}}$, $s_2^{Z+\text{jets}}$ and $R_{Z+b}^{\mu\mu/ee}$ are mainly determined from the same-flavour $t\bar{t}$ selections. Around 1% of the events in the inclusive $Z \rightarrow \ell\ell$ selections are also included in the same-flavour $t\bar{t}$ selections, but this overlap has a negligible effect on the analysis. The analysis procedure was validated using simulation-based pseudo-experiments with various input values of $\sigma_{t\bar{t}}$, $\sigma_{Z\rightarrow\ell\ell}$, $R_W^{\mu/e}$ and $R_Z^{\mu\mu/ee}$. These tests verified that the fit gives correct uncertainty estimates and that any residual biases are much smaller than the data statistical uncertainty.

The background from events with misidentified leptons in the $t\bar{t}$ selection was estimated using same-sign (SS) control samples, selected as described in Sect. 3 but requiring two leptons of the same rather than opposite electric charges. In an extension of the method described in Ref. [50], the misidentified lepton background $N_j^{i,\text{mis-id}}$ in invariant mass bin i (using a single bin for the $e\mu$ channel) with j b-tagged jets, was estimated from the number of SS events in data, $N_j^{i,\text{d,SS}}$, after subtracting the number of prompt SS events $N_j^{i,\text{prompt,SS}}$ estimated using simulation, and then scaling by the ratio R_j^i of misidentified-lepton events in the opposite-sign (OS) and SS samples in simulation:

$$N_j^{i,\text{mis-id}} = R_j^i (N_j^{i,\text{d,SS}} - N_j^{i,\text{prompt,SS}})$$
$$R_j^i = \frac{N_j^{i,\text{mis-id,OS}}}{N_j^{i,\text{mis-id,SS}}}. \quad (9)$$

To reduce the pollution of the SS ee and $e\mu$ samples from true OS events where an electron charge sign was misreconstructed (particularly for $m_{\ell\ell}$ close to the $Z \rightarrow ee$ resonance), electrons in the SS sample were required to be accepted by a charge misidentification boosted decision tree (BDT) [28] that reduces the rate of electron charge misidentification by up to an order of magnitude. The values of R_j^i are sensitive to the composition of the misidentified lepton background in simulation, and the corresponding uncertainty was assessed by removing the photon conversion, misidentified hadron and muon decay in flight contributions in turn, and recalculating R_j^i. The modelling of the charge misidentification BDT was studied using $Z \rightarrow ee$ events. An uncertainty of 25% on the prompt SS contribution was assumed, covering the uncertainties in the dominant contributing processes ($t\bar{t}$+W, Z and H, and WZ) and in the rate of electron charge misidentification. The misidentified lepton background was evaluated to contribute 0.4–1.2% of the ee opposite-sign sample (depending on $m_{\ell\ell}$ and the b-tagged jet multiplicity), 0.2–0.8% of the $e\mu$ sample and less than 0.4% of the $\mu\mu$ sample. The estimates from data are compatible with the predictions from simulation within the evaluated uncertainties of 30–70%. The simulation was also found to provide a good description of data SS control samples where the isolation requirements were inverted to increase the misidentified lepton contributions.

The misidentified lepton background in the $Z \rightarrow \ell\ell$ selection was estimated from data in the region 66 GeV $< m_{\ell\ell} <$ 81 GeV and 101 GeV $< m_{\ell\ell} <$ 116 GeV by defining two orthogonal control samples (B and C) enriched in misidentified leptons. The B samples were defined by requiring the lower-p_T lepton to fail the isolation requirement, and in the

Table 2 Summary of the fitted distributions, showing the distribution variable, number of bins and event count nomenclature for each sample of selected events

Event selection	Variable	Bins	Event count
$e\mu$+1 or 2 b-tagged jets	$N_{b\text{-tag}}$	2	$N_1^{e\mu}$, $N_2^{e\mu}$
ee+1 b-tagged jet	$m_{\ell\ell}$	6	$N_{1,m}^{ee}$
ee+2 b-tagged jets	$m_{\ell\ell}$	6	$N_{2,m}^{ee}$
$\mu\mu$+1 b-tagged jet	$m_{\ell\ell}$	6	$N_{1,m}^{\mu\mu}$
$\mu\mu$+2 b-tagged jets	$m_{\ell\ell}$	6	$N_{2,m}^{\mu\mu}$
$Z \rightarrow ee$ or $\mu\mu$	Channel	2	N_Z^{ee}, $N_Z^{\mu\mu}$

case of electrons also requiring it to fail the Medium identification requirement but pass a looser requirement. The C samples were defined by requiring the two leptons to have the same rather than opposite electric charges. To reduce the background from genuine $Z \rightarrow ee$ events where one electron charge sign was mismeasured, both electrons were required to be accepted by the charge misidentification BDT. A third control sample (D) was defined by applying both B and C requirements. Assuming the B and C requirements to be uncorrelated, the number $N_{\mathrm{A}}^{\mathrm{mis-id}}$ of misidentified lepton events in the A (signal) sample was then estimated from $N_{\mathrm{A}}^{\mathrm{mis-id}} = f N_{\mathrm{B}}^{\mathrm{mis-id}} N_{\mathrm{C}}^{\mathrm{mis-id}} / N_{\mathrm{D}}^{\mathrm{mis-id}}$ where $N_{\mathrm{X}}^{\mathrm{mis-id}}$ is the number of observed events in region X ($X = B, C$ or D) after subtracting the prompt lepton contribution using simulation, and the factor $f = (50\,\mathrm{GeV})/(15\,\mathrm{GeV} + 15\,\mathrm{GeV}) = 5/3$ linearly interpolates the estimate over the complete mass range $66\,\mathrm{GeV} < m_{\ell\ell} < 116\,\mathrm{GeV}$. The misidentified lepton contributions were found to be $0.39 \pm 0.37\%$ of the $Z \rightarrow ee$ sample and $0.06 \pm 0.27\%$ of the $Z \rightarrow \mu\mu$ sample, estimating the systematic uncertainties by using a tighter anti-isolation requirement in the B and D samples.

5 Lepton isolation efficiency measurements

The efficiency of the isolation requirements applied to the leptons was measured directly in data using a tag-and-probe methodology, separately for the $Z \rightarrow \ell\ell$ and busier $t\bar{t} \rightarrow \ell\ell$ environments, and for all leptons with $p_{\mathrm{T}} > 20\,\mathrm{GeV}$. In the $Z \rightarrow \ell\ell$ measurements, opposite-sign ee and $\mu\mu$ pairs were selected, requiring the tag lepton to satisfy the identification and isolation cuts described in Sect. 3 and to be matched to a corresponding trigger signature. The probe lepton was only required to satisfy the identification cuts, and the isolation efficiency was measured from the fraction of probe leptons with dilepton invariant mass in the range $80\,\mathrm{GeV} < m_{\ell\ell} < 102\,\mathrm{GeV}$ that pass the isolation requirement, after correcting for the background from non-prompt leptons, which reaches up to 1% in the samples failing the isolation requirement at low lepton p_{T}. This background was estimated using a template fit to the $m_{\ell\ell}$ distribution, with the templates for prompt leptons obtained from simulation, and those from misidentified lepton events obtained from control samples with modified selection cuts. The isolation efficiencies were measured as a function of lepton p_{T} for four bins in $|\eta|$. The data results are compared to the corresponding isolation efficiencies predicted by the Powheg + Pythia8 and Sherpa $Z \rightarrow \ell\ell$ simulation samples in Fig. 3a, b. The data efficiencies in the lowest bin used in the analysis ($25\,\mathrm{GeV} < p_{\mathrm{T}} < 30\,\mathrm{GeV}$) are around 80–85%, increasing to 99% at high lepton p_{T}. The Powheg + Pythia8 simulation underestimates the electron efficiency by around 2% at low p_{T}, whereas the muon efficiency is overestimated by 1%. The Sherpa simulation also underestimates the electron efficiency by about 2% at low p_{T}, but overestimates the muon efficiency by about 3%.

The corresponding efficiencies in the $t\bar{t}$ environment were measured using $e\mu$ events with at least one b-tagged jet. Here, an invariant mass cut cannot be applied to suppress misidentified lepton background and the fraction of background in the probe lepton samples failing isolation reaches 25–30% in the samples with one b-tagged jet, but remains below 10% when two b-tagged jets are present. This background was estimated using same-charge events in a similar way as for the main analysis selection discussed in Sect. 4. The efficiencies were measured as a function of lepton p_{T} for $|\eta| < 1.5$ and $|\eta| > 1.5$, combining the results from the one b-tagged and two b-tagged jet samples, which were found to be consistent. The results from data are compared with the baseline Powheg + Pythia8 $t\bar{t}$ simulation in Fig. 3c, d. In data, the efficiencies vary from around 80% at $p_{\mathrm{T}} = 25\,\mathrm{GeV}$ to 97–98% at high p_{T}, and the simulation underestimates the efficiency at low p_{T} for electrons, and overestimates it for muons, similar to the $Z \rightarrow \ell\ell$ case.

The ratios of data to simulation efficiencies shown in Fig. 3 were used to define multiplicative efficiency corrections (scale factors) that were applied to simulation on a per-lepton basis. The systematic uncertainties on the $Z \rightarrow \ell\ell$ scale factors were assessed by varying selection cuts for the fit and control regions, leading to uncertainties of less than 0.05% on the values of $\epsilon_{Z\rightarrow ee}$ and $\epsilon_{Z\rightarrow\mu\mu}$. The systematic uncertainties on the $t\bar{t}$ scale factors include the modelling of prompt-lepton contributions to the same-charge samples, the extrapolation of misidentified leptons from same- to opposite-charge and the modelling of the electron charge misassignment, giving uncertainties of around 0.1% per lepton. The isolation efficiency scale factors calculated for Powheg + Pythia8 $t\bar{t}$ events were applied to all simulated events passing the $t\bar{t}$ selections, including the Z + jets events simulated with Sherpa. However, the results from inclusive $Z \rightarrow \mu\mu$ events shown in Fig. 3b suggest that the modelling of the muon isolation efficiency in Sherpa Z + jets events may require different corrections to those measured for Powheg + Pythia8 $t\bar{t}$ events. A potential extra difference in lepton isolation efficiencies between $Z(\rightarrow ee)$ + jets and $Z(\rightarrow \mu\mu)$ + jets was therefore included in the likelihood fit, represented by the floating parameter $R_{Z+b}^{\mu\mu/ee}$ appearing via Δ_{Z+b} in Eq. (6).

6 Systematic uncertainties

Systematic uncertainties arise from uncertainties in the quantities appearing in Eqs. (1), (2) and (8). Each systematic uncertainty was evaluated by calculating the effect on all input parameters ($\epsilon_{\ell\ell'}$, $C_b^{\ell\ell'}$, $\epsilon_{Z\rightarrow\ell\ell}$, background estimates etc.) simultaneously and repeating the fit, rather than includ-

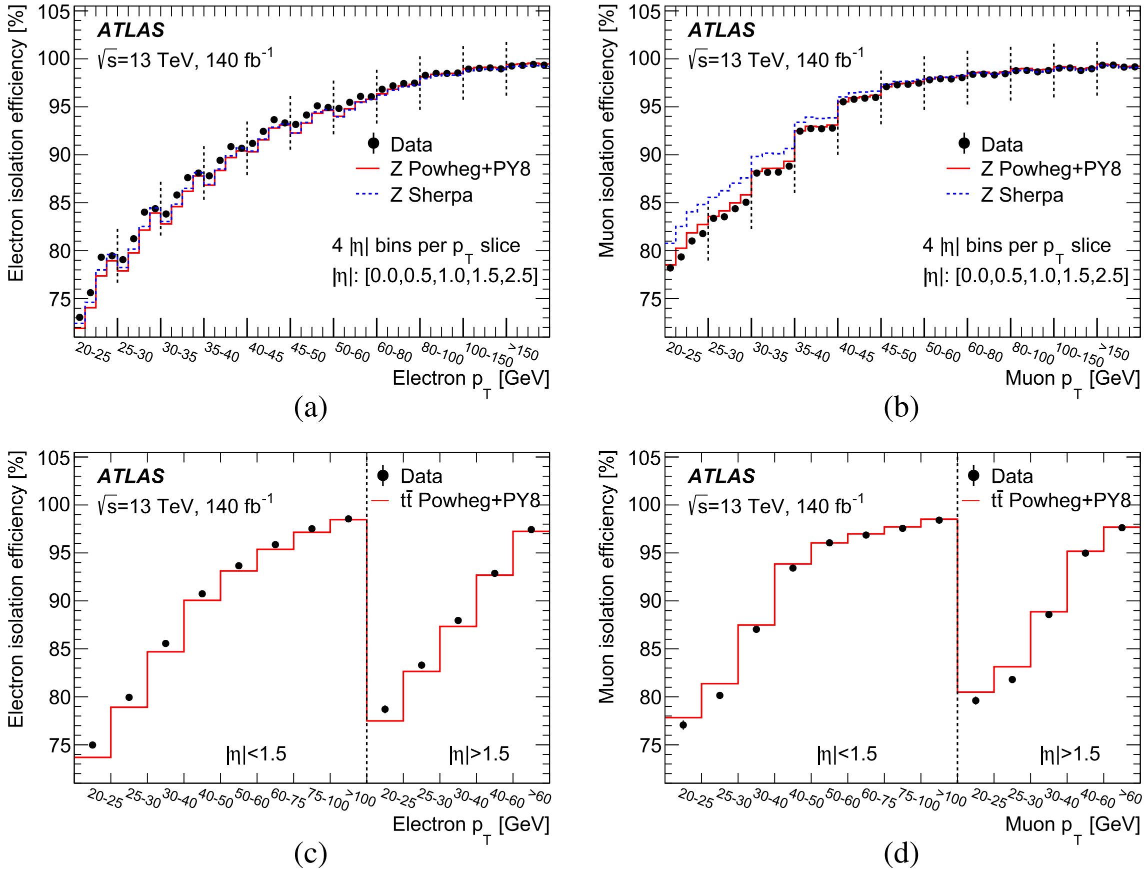

Fig. 3 Lepton isolation efficiencies measured for **a**, **c** electrons and **b**, **d** muons as functions of lepton p_{T} and $|\eta|$. The data is shown by the points with error bars and the simulation by the histograms. The upper plots show measurements in $Z \rightarrow \ell\ell$ events, with four η bins (with boundaries at $|\eta| = 0$, 0.5, 1.0, 1.5 and 2.5) shown sequentially for each p_{T} slice. The lower plots show measurements in $t\bar{t} \rightarrow e\mu$ events, separately for leptons with $|\eta| < 1.5$ in the leftmost bins and $|\eta| > 1.5$ in the rightmost bins. The data is compared to Powheg + Pythia8 simulation (without isolation efficiency scale factors) for both Z and $t\bar{t}$ events, and additionally to Sherpa Z events

ing the systematic uncertainty as a nuisance parameter in the fit in a profile likelihood approach. For some sources of uncertainty, e.g. lepton efficiencies and PDF variations, the effects on the different input quantities are only partially correlated, and this was taken into account by using the full covariance matrix expressing the dependence of the fit result on each parameter and their correlations. The resulting systematic uncertainties on $\sigma_{t\bar{t}}$, $\sigma_{Z\rightarrow\ell\ell}$, $R^{\mu/e}_{WZ}$ and $R^{\mu\mu/ee}_{Z}$ are discussed below, and summarised in Table 5 in Sect. 7. The methodologies generally follow those described in Ref. [50].

$t\bar{t}$ modelling: The values of $\epsilon_{\ell\ell'}$, $C_b^{\ell\ell'}$, $f_{n\tau}^{\ell\ell'}$ and $f_{j,m}^{\ell\ell,t\bar{t}}$ depend on the choice of $t\bar{t}$ simulation model. The uncertainty due to the choice of generator (in particular the matrix-element matching algorithm) was assessed by using the sample generated with aMC@NLO + Pythia8 instead of Powheg + Pythia8, and the parton shower, hadronisation and underlying event modelling uncertainty was assessed by using the Powheg + Herwig7.1 sample. Uncertainties due to initial- and final-state radiation were assessed by using event weights to vary the QCD renormalisation and factorisation scales in the matrix element independently by factors of two up and down from their default values, by changing the h_{damp} parameter from $1.5m_t$ to $3m_t$ and symmetrising the resulting uncertainty [45], by using the Var3c A14 tune variations [40], and by changing the renormalisation and factorisation scales used in the parton shower, again by factors of two up and down. Since some of these variations also induce changes in the amount of activity close to the leptons, they affect the simulated lepton isolation efficiencies. These variations were therefore evaluated without applying lepton isolation cuts, to avoid double-counting differences absorbed in the lepton isolation efficiency scale factors described in Sect. 5. The fraction of $t\bar{t}$ events with at least three b-jets at generator level was also varied by ±50%, motivated by the discrepancies seen for $N_{b-\mathrm{tag}} \geq 3$ in Fig. 2a, b, and the top quark mass was varied by ± 1 GeV.

Top quark p_{T} modelling: As none of the considered $t\bar{t}$ modelling variations reproduce the data lepton p_{T} distribution, the full effect of the top quark p_{T} reweighting shown as the red dotted line in Fig. 2c, d was included as a systematic uncertainty.

Parton distribution functions: The PDF uncertainties were evaluated using the 30 eigenvectors of the PDF4LHC15 meta-PDF set [76], taking into account the differing effects on the $t\bar{t}$, Wt, Z + jets and inclusive Z processes and their correlations. The uncertainties from the PDF4LHC15 eigenvectors are larger than the shifts induced by reweighting the simulation samples (generated with NNPDF3.0 or CT10 PDFs) to the central predictions of PDF4LHC15.

Single top modelling: The uncertainties on modelling the Wt background were assessed using alternative samples generated with aMC@NLO + Pythia8 and Powheg + Herwig7.0 [77], by varying the renormalisation and factorisation scales and by using the Var3c tune variations, in the same way as for $t\bar{t}$ events. The Wt cross-section was varied by the QCD scale uncertainty of 2.4%, the PDF-related cross-section uncertainty being already accounted for coherently with the $t\bar{t}$ and Z PDF variations.

Single-top/$t\bar{t}$ interference: The uncertainty in modelling the interference between the Wt and $t\bar{t}$ final states was assessed by using the diagram subtraction scheme [51,52] instead of the baseline diagram removal scheme.

Z (+jets) modelling: Uncertainties in the Z + jets background in the $t\bar{t}$ selection were evaluated by changing the QCD factorisation and renormalisation scales in the Sherpa samples by factors of two up and down from their default values, separately or together and excluding variations in opposite directions. The Sherpa samples were also used to evaluate corresponding variations in $\epsilon_{Z\to ee}$ and $\epsilon_{Z\to\mu\mu}$ for the inclusive $Z\to\ell\ell$ selection. Simultaneous changes of both scales were found to have the largest effects on both $R^{\mu/e}_{WZ}$ and $R^{\mu\mu/ee}_{Z}$, and were used to define the corresponding uncertainty. Half the effect of the $p_{\mathrm{T}}^{\ell\ell}$ weighting applied to the Powheg + Pythia8 inclusive $Z\to\ell\ell$ samples was included as an additional Z modelling uncertainty.

Diboson modelling: The normalisation of the diboson contribution was varied by 20%, covering uncertainties in the cross-sections and acceptances. Alternative samples generated using Powheg + Pythia8 instead of Sherpa were also considered.

Lepton energy/momentum scale and resolution: The electron energy scale and muon momentum scale and corresponding resolution were determined using $Z\to ee$ and $Z\to\mu\mu$ decays as discussed in Refs. [28,29], and were varied within the corresponding uncertainties.

Lepton identification: The lepton identification efficiencies were measured using tag-and-probe techniques applied to $Z\to ee$ and $Z\to\mu\mu$ events [31,32], as functions of lepton p_{T} and η for electrons, and η and ϕ for muons. The corresponding uncertainties are only partially correlated across p_{T}, η and ϕ, and the information was propagated to $\epsilon_{\ell\ell'}$ and $\epsilon_{Z\to\ell\ell}$ (and their correlations) by generating multiple sets of scale factor replicas whose variations represent the full uncertainty model. The uncertainties due to electron charge misidentification were studied using $Z\to ee$ events and taken into account using the same technique.

Lepton isolation: The lepton isolation efficiency uncertainties discussed in Sect. 5 were also propagated using scale factor replicas, and taken to be uncorrelated between electrons and muons, and between the $t\bar{t}$ and $Z\to\ell\ell$ selections.

Lepton trigger: The lepton trigger efficiencies were also measured in $Z\to ee$ and $Z\to\mu\mu$ events using tag-and-probe techniques [20,21], and were varied within the corresponding uncertainties.

Jet energy scale and resolution: The jet energy scale was determined using a combination of simulation, test beam and in-situ measurements, and the jet energy resolution was studied using di-jet balance techniques [30]. The modelling of the pileup jet veto using the JVT requirement was studied using jets in $Z\to\mu\mu$ events [70].

***b*-tagging efficiency/mistag:** The efficiency for reconstructing and tagging b-jets in $t\bar{t}$ events was measured in situ via the fit parameters $\epsilon_b^{\ell\ell'}$. However, the background yields and tagging correlations depend on the b-tagging efficiencies and mistag rates predicted by simulation, with the corresponding scale factors and uncertainties determined using $t\bar{t}$ and Z + jets events as described in Refs. [33,78,79].

Misidentified leptons: The uncertainties on the misidentified lepton backgrounds were evaluated as discussed in Sect. 4, and were taken to be uncorrelated between electrons and muons, and between the $t\bar{t}$ and $Z\to\ell\ell$ selections.

Table 3 Observed numbers of opposite-charge dilepton events (weighted events for the $e\mu$ and $\mu\mu$ channels) with one (upper block) and two (lower block) b-tagged jets in the $t\bar{t}$ selection in data, together with the estimated event counts from the fit prediction, including the associated statistical and systematic uncertainties. The five columns show the ee channel with $|m_{\ell\ell} - m_Z| > 10$ GeV (off-Z) and $|m_{\ell\ell} - m_Z| < 10$ GeV (on-Z), the $e\mu$ channel, and the $\mu\mu$ channel including off-Z and on-Z selections. The uncertainties in the total predictions are smaller than the individual component uncertainties due to correlations induced by the fit

Event counts	$N^{ee}_{1,\text{off}-Z}$	$N^{ee}_{1,\text{on}-Z}$	$N^{e\mu}_{1}$	$N^{\mu\mu}_{1,\text{off}-Z}$	$N^{\mu\mu}_{1,\text{on}-Z}$
Data	222,304	442,108	405,437	223,085	448,105
$t\bar{t}$	154,800 ± 1700	24,830 ± 850	361,000 ± 4200	152,500 ± 1800	24,070 ± 860
Wt	17,500 ± 1600	2770 ± 240	41500 ± 3800	17,800 ± 1700	2730 ± 250
Z + jets	46,880 ± 400	410,700 ± 2000	859 ± 21	51,010 ± 780	418,000 ± 2000
Diboson	770 ± 160	3940 ± 840	790 ± 280	770 ± 160	3880 ± 830
Mis-ID leptons	1300 ± 500	360 ± 260	1740 ± 610	390 ± 150	172 ± 87
Total prediction	221,280 ± 550	442,600 ± 1100	405,900 ± 1800	222,390 ± 670	448,900 ± 1100
Event counts	$N^{ee}_{2,\text{off}-Z}$	$N^{ee}_{2,\text{on}-Z}$	$N^{e\mu}_{2}$	$N^{\mu\mu}_{2,\text{off}-Z}$	$N^{\mu\mu}_{2,\text{on}-Z}$
Data	85936	37704	198502	86169	38512
$t\bar{t}$	79,750 ± 920	13,340 ± 480	191,000 ± 1800	79,770 ± 830	13,180 ± 450
Wt	2860 ± 760	400 ± 110	6700 ± 1600	2940 ± 740	423 ± 90
Z + jets	2675 ± 68	23,610 ± 590	78 ± 2	3095 ± 87	24110 ± 600
Diboson	67 ± 23	550 ± 110	29 ± 8	71 ± 30	570 ± 110
Mis-ID leptons	400 ± 290	96 ± 59	720 ± 520	350 ± 160	104 ± 56
Total prediction	85,760 ± 360	38,000 ± 190	198,510 ± 440	86,230 ± 300	38,380 ± 210

Simulation statistics: The limited size of the Monte Carlo simulation samples primarily affects the predictions of $\epsilon_{\ell\ell'}$ and $C_b^{\ell\ell'}$, and the fractions $f_{j,m}^{\ell\ell,Z\text{+jets}}$ of the Z + jets background entering each invariant mass bin. The uncertainties in $\epsilon_{\ell\ell'}$ and $C_b^{\ell\ell'}$ were taken into account by repeating the fit with each parameter shifted by its uncertainty in turn. The uncertainties in $f_{j,m}^{\ell\ell,Z\text{+jets}}$ were accounted for directly in the Gaussian likelihood terms that compare the data counts with the prediction in each invariant mass bin.

Integrated luminosity: The integrated luminosity of the dataset was evaluated using the LUCID2 detector [80], complemented by measurements from the inner detector and calorimeters, and has an uncertainty of 0.83% [18].

Beam energy: The LHC beam energy is known to a precision of 0.1%, which translates into small uncertainties on $\sigma_{t\bar{t}}$ and $\sigma_{Z\to\ell\ell}$ as discussed in Ref. [50].

7 Fit results

Table 3 shows the number of observed events in each of the dilepton channels of the $t\bar{t}$ selection together with the results of the fit, broken down into the estimated contributions from $t\bar{t}$, Wt, Z + jets, diboson and misidentified leptons. The counts are shown separately for events with one and two b-tagged jets, and separately for events off (with $|m_{\ell\ell} - m_Z| > 10$ GeV) and on (with $|m_{\ell\ell} - m_Z| < 10$ GeV) the Z resonance in the same-flavour channels. The full $m_{\ell\ell}$ distributions are shown in Fig. 4. In the same-flavour samples with one b-tagged jet, the $t\bar{t}$ purity is about 70% and the background is dominated by Z + jets events. In the two b-tagged jets samples, the $t\bar{t}$ purity rises to 93%, with equal background contributions from Z + jets and Wt events. In the $e\mu$ channel, the Z + jets background is almost negligible, and the $t\bar{t}$ purity is 89% in the one b-tagged sample and 96% in the two b-tagged sample. Table 4 shows the corresponding event counts and predictions for the $Z \to \ell\ell$ selection; here the backgrounds are only around 0.5%.

Figure 4 shows that the fit generally models the data well, except for a data excess in the lowest $m_{\ell\ell}$ bin in all four same-flavour distributions, whose significance is however always less than two standard deviations. Part of this discrepancy can be attributed to the top-quark p_T mismodelling—the reweighted sample shown by the red dotted line in Fig. 2 also predicts a softer $m_{\ell\ell}$ distribution for $t\bar{t}$ events, as also observed for the $m_{\ell\ell}$ distribution in the $t\bar{t}$-dominated $e\mu$ channel. The effect of this reweighting defines the 'Top quark p_T modelling' uncertainty in Table 5 and is included in the cyan bands shown in Fig. 4.

The fit results for the cross-sections are

$$\sigma_{t\bar{t}} = 809.5 \pm 1.1 \pm 20.1 \pm 7.5 \pm 1.9 \,\text{pb},$$
$$\sigma_{Z\to\ell\ell} = 2019.4 \pm 0.2 \pm 20.7 \pm 16.8 \pm 1.8 \,\text{pb},$$

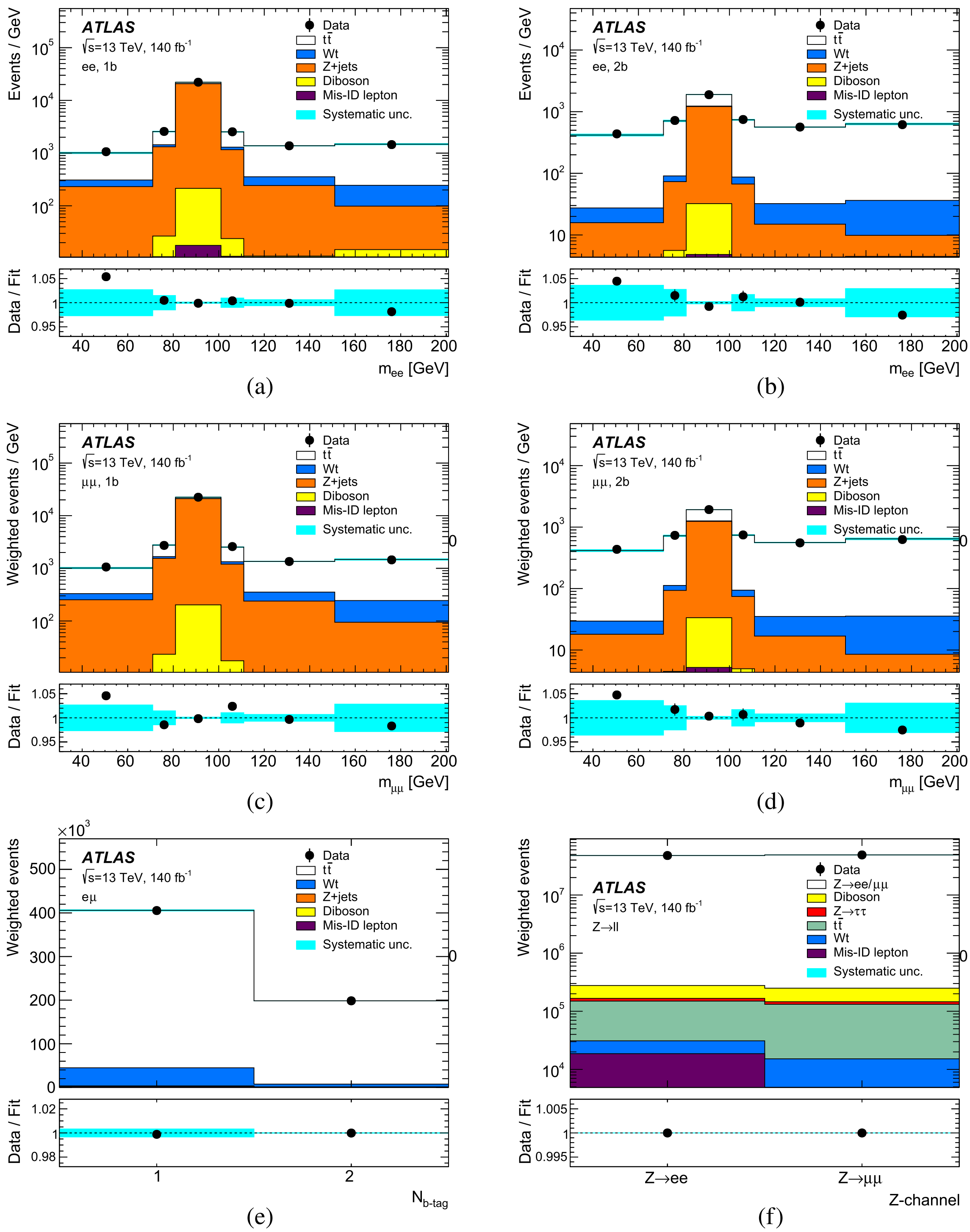

Fig. 4 Results of the fit to data, showing the invariant mass distributions for the one and two b-tagged jet samples in the **a**, **b** ee and **c**, **d** $\mu\mu$ channels, **e** the b-tagged jet multiplicity in the $e\mu$ channel, and **f** the number of events in the inclusive $Z \rightarrow \ell\ell$ selection. The data are shown by the points with statistical error bars, and are compared with the results of the fit, showing the scaled contributions from $t\bar{t}$, Wt, Z + jets, dibosons, $Z \rightarrow \tau\tau$ and events with misidentified leptons. The total systematic uncertainty of the fit prediction in each bin is shown by the cyan band. The lower panels show the ratios of data to the fit predictions. In the invariant mass distributions, the last bin includes the overflow with $m_{\ell\ell} > 200$ GeV but is normalised to the displayed bin width

Table 4 Observed numbers of opposite-charge dilepton events (weighted events for the $\mu\mu$ channel) in the inclusive $Z \rightarrow ee$ and $Z \rightarrow \mu\mu$ selections in data, together with the estimated event counts from the fit prediction, including the associated statistical and systematic uncertainties. The uncertainties in the total predictions are much smaller than the individual uncertainties due to correlations induced by the fit

Event counts Data	$Z \rightarrow ee$ 47,898,836	$Z \rightarrow \mu\mu$ 49,016,812
$Z \rightarrow \ell\ell$	47,621,000 ± 33,000	48,767,000 ± 29,000
Diboson	111,000 ± 22,000	104,000 ± 21,000
$Z \rightarrow \tau\tau$	16,850 ± 140	13,780 ± 110
$t\bar{t}$	119,000 ± 14,000	117,000 ± 14,000
Wt	12,380 ± 890	12,390 ± 880
Mis-ID leptons	19,000 ± 18,000	3000 ± 13,000
Total prediction	47,898,800 ± 6900	49,016,800 ± 6200

where the four uncertainties are due to data statistics, systematic effects, and the knowledge of the integrated luminosity and the LHC beam energy. As shown in Table 5, the $t\bar{t}$ cross-section result has a precision of 2.7%, dominated by the uncertainties from $t\bar{t}$ modelling, the top-quark p_T modelling and the integrated luminosity. It is compatible with the theoretical prediction discussed in Sect. 2 and with the result from the $e\mu$ channel alone reported in Ref. [81], taking into account the larger systematic uncertainty in this analysis due to the use of the same-flavour channels and the tighter lepton p_{T} requirement. The result for $\sigma_{Z\rightarrow\ell\ell}$ represents the inclusive cross-section for $Z/\gamma^* \rightarrow \ell\ell$ production for a single dilepton flavour with $m_{\ell\ell} > 60\,\mathrm{GeV}$. In order to compare with previous measurements, it was translated into a fiducial cross-section $\sigma^{\mathrm{fid}}_{Z\rightarrow\ell\ell}$ requiring two Born-level leptons with $p_{\mathrm{T}} > 25\,\mathrm{GeV}$ and $|\eta| < 2.5$, and $66 < m_{\ell\ell} < 116\,\mathrm{GeV}$. The relationship between the total and fiducial cross-sections is given by $\sigma^{\mathrm{fid}}_{Z\rightarrow\ell\ell} = A_Z\sigma_{Z\rightarrow\ell\ell}$, and the factor $A_Z = 0.3836 \pm 0.0005$ was evaluated from the Powheg + Pythia8 $Z \rightarrow \ell\ell$ sample, including the extrapolation to the lower lepton p_{T} requirement of $p_{\mathrm{T}} > 25\,\mathrm{GeV}$. The resulting fiducial cross-section is

$$\sigma^{\mathrm{fid}}_{Z\rightarrow\ell\ell} = 774.7 \pm 0.1 \pm 1.8 \pm 6.4 \pm 0.7\,\mathrm{pb}.$$

The systematic uncertainty is much smaller than that for $\sigma_{Z\rightarrow\ell\ell}$ because of strong reductions in the PDF and Z modelling uncertainties in the fiducial cross-section measurement. The result is compatible with that measured in Ref. [82].

The values of $\epsilon_b^{\ell\ell'}$ for the three dilepton channels were found to be compatible with the values expected from simulation, and are all close to 0.51. The Z + jets scaling parameters were measured to be $s_1^{Z+\mathrm{jets}} = 0.89 \pm 0.09$ and $s_2^{Z+\mathrm{jets}} = 1.12 \pm 0.32$, the uncertainties being dominated by the QCD scale variations in the Z + jets samples, which significantly change the predicted cross-sections. The Z + jets lepton isolation efficiency difference was fitted as $R^{\mu\mu/ee}_{Z+b} = 0.990 \pm 0.003$, compatible with the differences between Sherpa and Powheg + Pythia8 lepton isolation efficiencies shown for inclusive $Z \rightarrow \ell\ell$ events in Fig. 3.

The two ratios of branching ratios were fitted to be

$$R^{\mu/e}_{WZ} = 0.9990 \pm 0.0022 \pm 0.0036$$
$$R^{\mu\mu/ee}_{Z} = 0.9913 \pm 0.0002 \pm 0.0045$$

where the first uncertainties are statistical and the second systematic. A detailed breakdown of the uncertainties is shown in Table 5. The value of $R^{\mu\mu/ee}_{Z}$ is 1.9 standard deviations below unity, hinting at a potential bias in the electron or muon identification efficiencies. The normalisation of $R^{\mu/e}_{WZ}$ by $R^{\mu\mu/ee}_{Z}$ via Eq. (7) protects $R^{\mu/e}_{WZ}$ against such a bias, modulo differences in the lepton p_{T} and η distributions in dilepton $t\bar{t}$ and $Z \rightarrow \ell\ell$ events.

Consistent results were found when analysing the 2015–16, 2017 and 2018 datasets separately. The result for $R^{\mu/e}_{WZ}$ was found to be stable when tightening the lepton p_{T} requirement progressively up to $p_{\mathrm{T}} > 40\,\mathrm{GeV}$, and when tightening the η requirement to $|\eta| < 1.5$, in each case removing around 40% of the $t\bar{t}$ sample. It also changed by less than 0.01% when removing the lowest $m_{\ell\ell}$ bin from the fit, demonstrating insensitivity to the mismodelling shown in Fig. 4. This mismodelling is consistent between ee and $\mu\mu$ channels, as can be seen from Fig. 5, which shows the ratio of $\mu\mu$ to ee events in each invariant mass bin, cancelling any common mismodelling. The data and fit predictions for this ratio agree well in all $m_{\ell\ell}$ bins.

The measured value of $R^{\mu/e}_{WZ}$ was converted to $R^{\mu/e}_{W}$ by using the external measurement of $R^{\mu\mu/ee}_{Z-\mathrm{ext}} = 1.0009 \pm 0.0028$ from LEP and SLD [13,14], giving a result of

$$R^{\mu/e}_{W} = R^{\mu/e}_{WZ}\sqrt{R^{\mu\mu/ee}_{Z-\mathrm{ext}}} = 0.9995 \pm 0.0022\,(\mathrm{stat}) \pm 0.0036\,(\mathrm{syst}) \pm 0.0014\,(\mathrm{ext}),$$

where the three uncertainties correspond to data statistics, systematic uncertainties from this analysis, and the uncertainty on the value of $R^{\mu\mu/ee}_{Z-\mathrm{ext}}$ (considered uncorrelated), giving a total uncertainty of 0.0045. The result is consistent

Table 5 Breakdown of the statistical and systematic uncertainties on the measured cross-sections $\sigma_{t\bar{t}}$ and $\sigma_{Z\to\ell\ell}$, and on the ratios of branching ratios $R_{WZ}^{\mu/e}$ and $R_{Z}^{\mu\mu/ee}$

Uncertainty [%]	$\sigma_{t\bar{t}}$	$\sigma_{Z\to\ell\ell}$	$R_{WZ}^{\mu/e}$	$R_{Z}^{\mu\mu/ee}$
Data statistics	0.13	0.01	0.22	0.02
$t\bar{t}$ modelling	1.68	0.03	0.10	0.00
Top-quark p_{T} modelling	1.42	0.00	0.06	0.00
Parton distribution functions	0.67	0.68	0.15	0.03
Single-top modelling	0.65	0.00	0.05	0.00
Single-top/$t\bar{t}$ interference	0.54	0.00	0.09	0.00
Z (+jets) modelling	0.06	0.73	0.13	0.20
Diboson modelling	0.05	0.04	0.01	0.00
Electron energy scale/resolution	0.05	0.06	0.10	0.11
Electron identification	0.10	0.07	0.04	0.13
Electron charge misidentification	0.06	0.06	0.01	0.13
Electron isolation	0.09	0.02	0.08	0.04
Muon momentum scale/resolution	0.04	0.02	0.06	0.04
Muon identification	0.18	0.12	0.11	0.23
Muon isolation	0.09	0.01	0.07	0.01
Lepton trigger	0.09	0.12	0.01	0.23
Jet energy scale/resolution	0.08	0.00	0.03	0.00
b-tagging efficiency/mistag	0.14	0.00	0.00	0.00
Misidentified leptons	0.17	0.02	0.15	0.05
Simulation statistics	0.04	0.00	0.06	0.00
Integrated luminosity	0.93	0.83	0.00	0.00
Beam energy	0.23	0.09	0.00	0.00
Total uncertainty	2.66	1.32	0.42	0.45

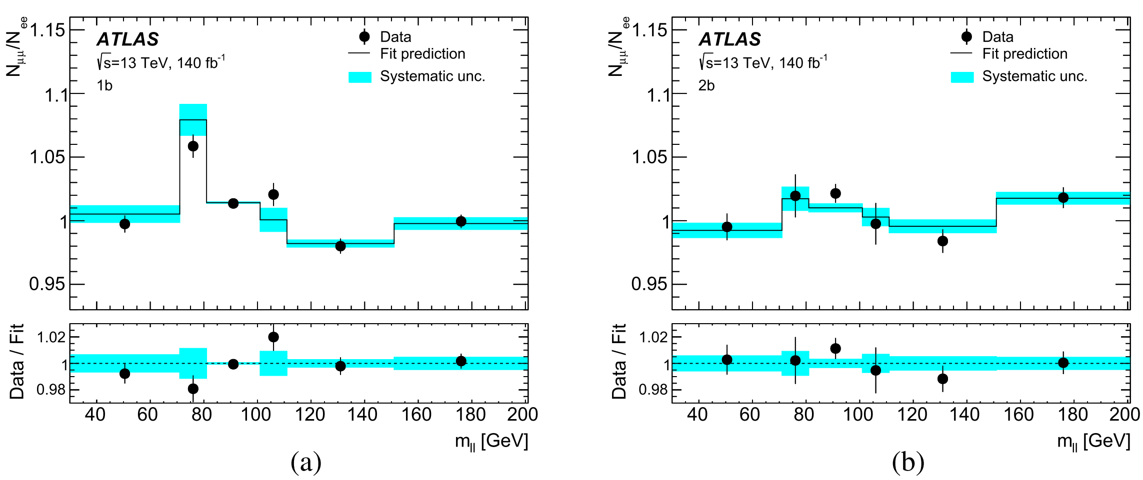

Fig. 5 Ratio of the number of events in the $\mu\mu$ channel divided by that in the ee channel as a function of dilepton invariant mass for events with **a** one and **b** two b-tagged jets. The ratio in data is shown by the points with statistical error bars, and the results of the fit prediction by the solid lines, with the cyan band indicating the systematic uncertainty

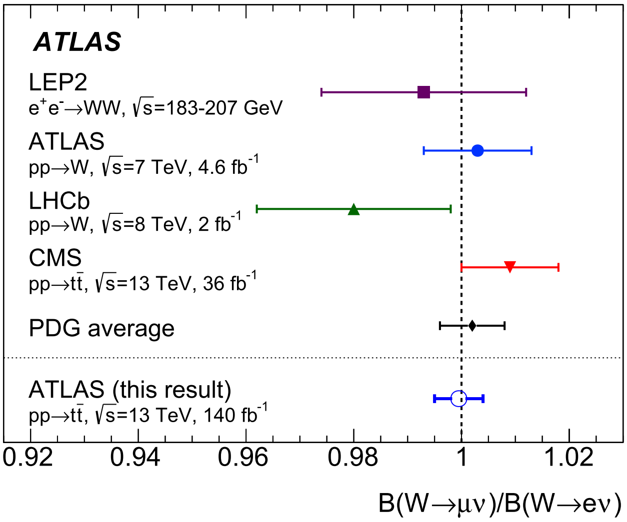

Fig. 6 Measurement of $R_W^{\mu/e} = \mathcal{B}(W \to \mu\nu)/\mathcal{B}(W \to e\nu)$ from this analysis compared to previous results from LEP2 and LHC experiments [9–12] and the Particle Data Group average [13]

with the assumption of lepton flavour universality and with previous measurements, and has higher precision than the previous world average [13]. The result is compared with previous measurements of $R_W^{\mu/e}$ in Fig. 6.

8 Conclusion

The ratio of branching ratios $R_W^{\mu/e} = \mathcal{B}(W \to \mu\nu)/\mathcal{B}(W \to e\nu)$ has been determined using the complete ATLAS Run 2 $\sqrt{s} = 13$ TeV pp collision data sample recorded at the LHC, by measuring the $t\bar{t}$ cross-section in the ee, $e\mu$ and $\mu\mu$ dilepton channels. Systematic uncertainties due to lepton identification and trigger efficiencies were minimised by normalising the result to a simultaneous measurement of $R_Z^{\mu\mu/ee} = \mathcal{B}(Z \to \mu\mu)/\mathcal{B}(Z \to ee)$, and utilising the high-precision measurement of $R_Z^{\mu\mu/ee}$ by the LEP and SLD collaborations. The resulting value of $R_W^{\mu/e} = 0.9995 \pm 0.0045$ is consistent with the assumption of lepton flavour universality. This is the most precise measurement of $R_W^{\mu/e}$ to date, with a smaller uncertainty than the previous world average.

Acknowledgements We thank CERN for the very successful operation of the LHC and its injectors, as well as the support staff at CERN and at our institutions worldwide without whom ATLAS could not be operated efficiently. The crucial computing support from all WLCG partners is acknowledged gratefully, in particular from CERN, the ATLAS Tier-1 facilities at TRIUMF/SFU (Canada), NDGF (Denmark, Norway, Sweden), CC-IN2P3 (France), KIT/GridKA (Germany), INFN-CNAF (Italy), NL-T1 (Netherlands), PIC (Spain), RAL (UK) and BNL (USA), the Tier-2 facilities worldwide and large non-WLCG resource providers. Major contributors of computing resources are listed in Ref. [83]. We gratefully acknowledge the support of ANPCyT, Argentina; YerPhI, Armenia; ARC, Australia; BMWFW and FWF, Austria; ANAS, Azerbaijan; CNPq and FAPESP, Brazil; NSERC, NRC and CFI, Canada; CERN; ANID, Chile; CAS, MOST and NSFC, China; Minciencias, Colombia; MEYS CR, Czech Republic; DNRF and DNSRC, Denmark; IN2P3-CNRS and CEA-DRF/IRFU, France; SRNSFG, Georgia; BMBF, HGF and MPG, Germany; GSRI, Greece; RGC and Hong Kong SAR, China; ISF and Benoziyo Center, Israel; INFN, Italy; MEXT and JSPS, Japan; CNRST, Morocco; NWO, Netherlands; RCN, Norway; MNiSW, Poland; FCT, Portugal; MNE/IFA, Romania; MESTD, Serbia; MSSR, Slovakia; ARRS and MIZŠ, Slovenia; DSI/NRF, South Africa; MICINN, Spain; SRC and Wallenberg Foundation, Sweden; SERI, SNSF and Cantons of Bern and Geneva, Switzerland; MOST, Taipei; TENMAK, Türkiye; STFC, United Kingdom; DOE and NSF, United States of America. Individual groups and members have received support from BCKDF, CANARIE, CRC and DRAC, Canada; PRIMUS 21/SCI/017, CERN-CZ and FORTE, Czech Republic; COST, ERC, ERDF, Horizon 2020, ICSC-NextGenerationEU and Marie Skłodowska-Curie Actions, European Union; Investissements d'Avenir Labex, Investissements d'Avenir Idex and ANR, France; DFG and AvH Foundation, Germany; Herakleitos, Thales and Aristeia programmes co-financed by EU-ESF and the Greek NSRF, Greece; BSF-NSF and MINERVA, Israel; Norwegian Financial Mechanism 2014-2021, Norway; NCN and NAWA, Poland; La Caixa Banking Foundation, CERCA Programme Generalitat de Catalunya and PROMETEO and GenT Programmes Generalitat Valenciana, Spain; Göran Gustafssons Stiftelse, Sweden; The Royal Society and Leverhulme Trust, United Kingdom. In addition, individual members wish to acknowledge support from CERN: European Organization for Nuclear Research (CERN PJAS); Chile: Agencia Nacional de Investigación y Desarrollo (FONDECYT 1190886, FONDECYT 1210400, FONDECYT 1230812, FONDECYT 1230987); China: National Natural Science Foundation of China (NSFC-12175119, NSFC 12275265, NSFC-12075060); Czech Republic: Czech Science Foundation (GACR-24-11373S), Ministry of Education Youth and Sports (FORTE CZ.02.01.01/00/22_008/0004632), PRIMUS Research Programme (PRIMUS/21/SCI/017); European Union: European Research Council (ERC - 948254, ERC 101089007), Horizon 2020 Framework Programme (MUCCA - CHIST-ERA-19-XAI-00), Italian Center for High Performance Computing, Big Data and Quantum Computing (ICSC, NextGenerationEU); France: Agence Nationale de la Recherche (ANR-20-CE31-0013, ANR-21-CE31-0013, ANR-21-CE31-0022), Investissements d'Avenir Labex (ANR-11-LABX-0012); Germany: Baden-Württemberg Stiftung (BW Stiftung-Postdoc Eliteprogramme), Deutsche Forschungsgemeinschaft (DFG-469666862, DFG-CR 312/5-2); Italy: Istituto Nazionale di Fisica Nucleare (ICSC, NextGenerationEU); Japan: Japan Society for the Promotion of Science (JSPS KAKENHI Grant No. 22KK0227, JSPS KAKENHI JP21H05085, JSPS KAKENHI JP22H01227, JSPS KAKENHI JP 22H04944); Netherlands: Netherlands Organisation for Scientific Research (NWO Veni 2020-VI.Veni.202.179); Norway: Research Council of Norway (RCN-314472); Poland: Polish National Agency for Academic Exchange (PPN/PPO/2020/1/00002/U/00001), Polish National Science Centre (NCN 2021/42/E/ST2/00350, NCN OPUS nr 2022/47/B/ST2/03059, NCN UMO-2019/34/E/ST2/00393, UMO-2020/37/B/ST2/01043, UMO-2021/40/C/ST2/00187, UMO-2022/47/O/ST2/00148, UMO-2023/49/B/ST2/04085); Slovenia: Slovenian Research Agency (ARIS grant J1-3010); Spain: Generalitat Valenciana (Artemisa, FEDER, IDIFEDER/2018/048), Ministry of Science and Innovation (MCIN and NextGenEU -PCI2022-135018-2, MICIN and FEDER -PID2021-125273NB, RYC2019-028510-I, RYC2020-030254-I, RYC2021-031273-I, RYC2022-038164-I), PROMETEO and GenT Programmes Generalitat Valenciana (CIDEGENT/2019/023, CIDEGENT/2019/027); Sweden: Swedish Research Council (Swedish Research Council 2023-04654, VR 2018-00482, VR 2022-03845, VR 2022-04683, VR 2023-03403, VR grant 2021-03651), Knut and Alice Wallenberg Foundation (KAW 2018.0157, KAW 2018.0458, KAW 2019.0447, KAW 2022.0358); Switzerland: Swiss National Science Foundation (SNSF-PCEFP2_194658); United Kingdom: Leverhulme

Trust (Leverhulme Trust RPG-2020-004), Royal Society (NIF-R1-231091); United States of America: Neubauer Family Foundation.

Data Availability Statement This manuscript has no associated data. [Author's comment: All ATLAS scientific output is published in journals, and preliminary results are made available in Conference Notes. All are openly available, without restriction on use by external parties beyond copyright law and the standard conditions agreed by CERN. Data associated with journal publications are also made available: tables and data from plots (e.g. cross section values, likelihood profiles, selection efficiencies, cross section limits, ...) are stored in appropriate repositories such as HEPDATA (http://hepdata.cedar.ac.uk/). ATLAS also strives to make additional material related to the paper available that allows a reinterpretation of the data in the context of new theoretical models. For example, an extended encapsulation of the analysis is often provided for measurements in the framework of RIVET (http://rivet.hepforge.org/). This information is taken from the ATLAS Data Access Policy, which is a public document that can be downloaded from http://opendata.cern.ch/record/413 [opendata.cern.ch].]

Code Availability Statement This manuscript has no associated code/software. [Author's comment: ATLAS collaboration software is open source, and all code necessary to recreate an analysis is publicly available. The Athena (http://gitlab.cern.ch/atlas/athena) software repository provides all code needed for calibration and uncertainty application, with configuration files that are also publicly available via Docker containers and cvmfs. The specific code and configurations written in support of this analysis are not public; however, these are internally preserved.]

Funded by SCOAP^3.

References

1. A. Pich, Precision Tau physics. Prog. Part. Nucl. Phys. **75**, 41 (2014). https://doi.org/10.1016/j.ppnp.2013.11.002. arXiv:1310.7922 [hep-ph]
2. BaBar Collaboration, Evidence for an excess of $\bar{B} \to D^{(*)}\tau^-\bar{\nu}_\tau$ decays. Phys. Rev. Lett. **109**, 101802 (2012). https://doi.org/10.1103/PhysRevLett.109.101802. arXiv:1205.5442 [hep-ex]
3. Belle Collaboration, Measurement of the branching ratio of $\bar{B} \to D^{(*)}\tau^-\bar{\nu}_\tau$ relative to $\bar{B} \to D^{(*)}\ell^-\bar{\nu}_\ell$ decays with hadronic tagging at Belle. Phys. Rev. D **92**, 072014 (2015). https://doi.org/10.1103/PhysRevD.92.072014. arXiv:1507.03233 [hep-ex]
4. Belle Collaboration, Measurement of the τ lepton polarization and $R(D^*)$ in the decay $\bar{B} \to D^*\tau^-\bar{\nu}_\tau$ with one-prong hadronic τ decays at Belle. Phys. Rev. D **97**, 012004 (2018). https://doi.org/10.1103/PhysRevD.97.012004. arXiv:1709.00129 [hep-ex]
5. Belle II Collaboration, A test of lepton flavor universality with a measurement of $R(D^*)$ using hadronic B tagging at the Belle II experiment. (2024). arXiv:2401.02840 [hep-ex]
6. LHCb Collaboration, Measurement of the ratios of branching fractions $\mathcal{R}(D^*)$ and $\mathcal{R}(D^0)$. Phys. Rev. Lett. **131**, 111802 (2023). https://doi.org/10.1103/PhysRevLett.131.111802. arXiv:2302.02886 [hep-ex]
7. LHCb Collaboration, Test of lepton flavor universality using $B^0 \to D^{*-}\tau^+\nu_\tau$ decays with hadronic τ channels. Phys. Rev. D **108**, 012018 (2023). https://doi.org/10.1103/PhysRevD.108.012018. arXiv:2305.01463 [hep-ex]
8. LHCb Collaboration, *Test of lepton universality in $b \to s\ell^+\ell^-$ decays*. Phys. Rev. Lett. **131**, 051803 (2023). https://doi.org/10.1103/PhysRevLett.131.051803. arXiv:2212.09152 [hep-ex]
9. CMS Collaboration, Precision measurement of the W boson decay branching fractions in proton–proton collisions at $\sqrt{s}$ = 13 TeV. Phys. Rev. D **105**, 072008 (2022). https://doi.org/10.1103/PhysRevD.105.072008. arXiv:2201.07861 [hep-ex]
10. ATLAS Collaboration, Precision measurement and interpretation of inclusive W^+, W^- and Z/γ^* production cross sections with the ATLAS detector. Eur. Phys. J. C **77**, 367 (2017). https://doi.org/10.1140/epjc/s10052-017-4911-9. arXiv:1612.03016 [hep-ex]
11. LHCb Collaboration, Measurement of forward $W \to e\nu$ production in pp collisions at $\sqrt{s}$ = 8 TeV. JHEP **10**, 030 (2016). https://doi.org/10.1007/JHEP10(2016)030. arXiv:1608.01484 [hep-ex]
12. S. Schael et al., Electroweak measurements in electron–positron collisions at W-boson-pair energies at LEP. Phys. Rep. **532**, 119 (2013). https://doi.org/10.1016/j.physrep.2013.07.004. arXiv:1302.3415
13. Particle Data Group, Review of particle physics. PTEP **2022**, 083C01 (2022). https://doi.org/10.1093/ptep/ptac097
14. S. Schael et al., Precision electroweak measurements on the Z resonance. Phys. Rep. **427**, 257 (2006). https://doi.org/10.1016/j.physrep.2005.12.006. arXiv:hep-ex/0509008
15. ATLAS Collaboration, The ATLAS Experiment at the CERN Large Hadron Collider, JINST **3**, S08003 (2008). https://doi.org/10.1088/1748-0221/3/08/S08003
16. B. Abbott et al., Production and integration of the ATLAS Insertable B-layer. JINST **13**, T05008 (2018). https://doi.org/10.1088/1748-0221/13/05/T05008. arXiv:1803.00844 [physics.ins-det]
17. ATLAS Collaboration, ATLAS Insertable B-Layer: Technical Design Report ATLAS-TDR-19; CERN-LHCC-2010-013 (2010). Addendum: ATLAS-TDR-19-ADD-1; CERN-LHCC-2012-009, 2012. https://cds.cern.ch/record/1291633. https://cds.cern.ch/record/1451888
18. ATLAS Collaboration, Luminosity determination in pp collisions at $\sqrt{s}$ = 13 TeV using the ATLAS detector at the LHC. Eur. Phys. J. C **83**, 982 (2023). https://doi.org/10.1140/epjc/s10052-023-11747-w. arXiv:2212.09379 [hep-ex]
19. ATLAS Collaboration, ATLAS data quality operations and performance for 2015–2018 data-taking. JINST **15**, P04003 (2020). https://doi.org/10.1088/1748-0221/15/04/P04003. arXiv:1911.04632 [physics.ins-det]
20. ATLAS Collaboration, Performance of electron and photon triggers in ATLAS during LHC Run 2. Eur. Phys. J. C **80**, 47 (2020). https://doi.org/10.1140/epjc/s10052-019-7500-2. arXiv:1909.00761 [hep-ex]
21. ATLAS Collaboration, Performance of the ATLAS muon triggers in Run 2. JINST **15**, P09015 (2020). https://doi.org/10.1088/1748-0221/15/09/p09015. arXiv:2004.13447 [physics.ins-det]
22. ATLAS Collaboration, The ATLAS simulation infrastructure. Eur. Phys. J. C **70**, 823 (2010). https://doi.org/10.1140/epjc/s10052-010-1429-9. arXiv:1005.4568 [physics.ins-det]
23. S. Agostinelli et al., GEANT4—a simulation toolkit. Nucl. Instrum. Methods A **506**, 250 (2003). https://doi.org/10.1016/S0168-9002(03)01368-8

24. ATLAS Collaboration, The simulation principle and performance of the ATLAS fast calorimeter simulation FastCaloSim, ATL-PHYS-PUB-2010-013 (2010). https://cds.cern.ch/record/1300517
25. T. Sjöstrand, S. Mrenna and P. Skands, A brief introduction to PYTHIA 8.1. Comput. Phys. Commun. **178**, 852 (2008). https://doi.org/10.1016/j.cpc.2008.01.036. arXiv:0710.3820 [hep-ph]
26. ATLAS Collaboration, The Pythia 8 A3 tune description of ATLAS minimum bias and inelastic measurements incorporating the Donnachie–Landshoff diffractive model. ATL-PHYS-PUB-2016-017 (2016). https://cds.cern.ch/record/2206965
27. ATLAS Collaboration, The ATLAS Collaboration Software and Firmware, ATL-SOFT-PUB-2021-001 (2021). https://cds.cern.ch/record/2767187
28. ATLAS Collaboration, Electron and photon performance measurements with the ATLAS detector using the 2015-2017 LHC proton–proton collision data. JINST **14**, P12006 (2019). https://doi.org/10.1088/1748-0221/14/12/P12006. arXiv:1908.00005 [hep-ex]
29. ATLAS Collaboration, Studies of the muon momentum calibration and performance of the ATLAS detector with pp collisions at $\sqrt{s}=13$ TeV. Eur. Phys. J. C **83**, 686 (2023). https://doi.org/10.1140/epjc/s10052-023-11584-x. arXiv:2212.07338 [hep-ex]
30. ATLAS Collaboration, Jet energy scale and resolution measured in proton–proton collisions at $\sqrt{s}=13$ TeV with the ATLAS detector. Eur. Phys. J. C **81**, 689 (2021). https://doi.org/10.1140/epjc/s10052-021-09402-3. arXiv:2007.02645 [hep-ex]
31. ATLAS Collaboration, Electron and photon efficiencies in LHC Run 2 with the ATLAS experiment. JHEP **2405**, 162 (2024). https://doi.org/10.1007/JHEP05(2024)162. arXiv:2308.13362 [hep-ex]
32. ATLAS Collaboration, Muon reconstruction and identification efficiency in ATLAS using the full Run 2 pp collision data set at $\sqrt{s}=13$ TeV. Eur. Phys. J. C **81**, 578 (2021). https://doi.org/10.1140/epjc/s10052-021-09233-2. arXiv:2012.00578 [hep-ex]
33. ATLAS Collaboration, ATLAS b-jet identification performance and efficiency measurement with $t\bar{t}$ events in pp collisions at $\sqrt{s}=13$ TeV. Eur. Phys. J. C **79**, 970 (2019). https://doi.org/10.1140/epjc/s10052-019-7450-8. arXiv:1907.05120 [hep-ex]
34. P. Nason, A new method for combining NLO QCD with shower Monte Carlo algorithms. JHEP **11**, 040 (2004). https://doi.org/10.1088/1126-6708/2004/11/040. arXiv:hep-ph/0409146
35. S. Frixione, P. Nason, C. Oleari, Matching NLO QCD computations with parton shower simulations: the POWHEG method. JHEP **11**, 070 (2007). https://doi.org/10.1088/1126-6708/2007/11/070. arXiv:0709.2092 [hep-ph]
36. S. Alioli, P. Nason, C. Oleari, E. Re, A general framework for implementing NLO calculations in shower Monte Carlo programs: the POWHEG BOX. JHEP **06**, 043 (2010). https://doi.org/10.1007/JHEP06(2010)043. arXiv:1002.2581 [hep-ph]
37. S. Frixione, G. Ridolfi, P. Nason, A positive-weight next-to-leading-order Monte Carlo for heavy flavour hadroproduction. JHEP **09**, 126 (2007). https://doi.org/10.1088/1126-6708/2007/09/126. arXiv:0707.3088 [hep-ph]
38. NNPDF Collaboration, Parton distributions for the LHC run II. JHEP **04**, 040 (2015). https://doi.org/10.1007/JHEP04(2015)040. arXiv:1410.8849 [hep-ph]
39. NNPDF Collaboration, Parton distributions with LHC data. Nucl. Phys. B **867**, 244 (2013). https://doi.org/10.1016/j.nuclphysb.2012.10.003. arXiv:1207.1303 [hep-ph]
40. ATLAS Collaboration, ATLAS Pythia 8 tunes to 7 TeV data, ATL-PHYS-PUB-2014-021 (2014). https://cds.cern.ch/record/1966419
41. ATLAS Collaboration, Studies on top-quark Monte Carlo modelling for Top2016, ATL-PHYS-PUB-2016-020 (2016). https://cds.cern.ch/record/2216168
42. J. Alwall et al., The automated computation of tree-level and next-to-leading order differential cross sections, and their matching to parton shower simulations. JHEP **07**, 079 (2014). https://doi.org/10.1007/JHEP07(2014)079. arXiv:1405.0301 [hep-ph]
43. M. Bähr et al., Herwig++ physics and manual. Eur. Phys. J. C **58**, 639 (2008). https://doi.org/10.1140/epjc/s10052-008-0798-9. arXiv:0803.0883 [hep-ph]
44. J. Bellm et al., Herwig 7.1 Release Note (2017). arXiv:1705.06919 [hep-ph]
45. ATLAS Collaboration, Study of top-quark pair modelling and uncertainties using ATLAS measurements at $\sqrt{s}=13$ TeV, ATL-PHYS-PUB-2020-023 (2020). https://cds.cern.ch/record/2730443
46. J. Erler, A. Freitas, Electroweak model and constraints on new physics, in Review of Particle Physics. PTEP **2022**, 083C01 (2022). https://doi.org/10.1093/ptep/ptac097
47. D.J. Lange, The EvtGen particle decay simulation package. Nucl. Instrum. Methods A **462**, 152 (2001). https://doi.org/10.1016/S0168-9002(01)00089-4
48. M. Czakon, P. Fiedler, A. Mitov, Total top-quark pair-production cross section at hadron colliders through $\mathcal{O}(\alpha_S^4)$. Phys. Rev. Lett. **110**, 252004 (2013). https://doi.org/10.1103/PhysRevLett.110.252004. arXiv:1303.6254 [hep-ph]
49. M. Czakon, A. Mitov, Top++: a program for the calculation of the top-pair cross-section at hadron colliders. Comput. Phys. Commun. **185**, 2930 (2014). https://doi.org/10.1016/j.cpc.2014.06.021. arXiv:1112.5675 [hep-ph]
50. ATLAS Collaboration, Measurement of the $t\bar{t}$ production cross-section and lepton differential distributions in $e\mu$ dilepton events from pp collisions at $\sqrt{s}=13$ TeV with the ATLAS detector. Eur. Phys. J. C **80**, 528 (2020). https://doi.org/10.1140/epjc/s10052-020-7907-9. arXiv:1910.08819 [hep-ex]
51. E. Re, Single-top Wt-channel production matched with parton showers using the POWHEG method. Eur. Phys. J. C **71**, 1547 (2011). https://doi.org/10.1140/epjc/s10052-011-1547-z. arXiv:1009.2450 [hep-ph]
52. C.D. White, S. Frixione, E. Laenen, F. Maltoni, Isolating Wt production at the LHC. JHEP **11**, 074 (2009). https://doi.org/10.1088/1126-6708/2009/11/074. arXiv:0908.0631 [hep-ph]
53. N. Kidonakis, N. Yamanaka, Higher-order corrections for tW production at high-energy hadron colliders. JHEP **05**, 278 (2021). https://doi.org/10.1007/JHEP05(2021)278. arXiv:2102.11300 [hep-ph]
54. E. Bothmann et al., Event generation with Sherpa 2.2. SciPost Phys. **7**, 034 (2019). https://doi.org/10.21468/SciPostPhys.7.3.034. arXiv:1905.09127 [hep-ph]
55. T. Gleisberg, S. Höche, Comix, a new matrix element generator. JHEP **12**, 039 (2008). https://doi.org/10.1088/1126-6708/2008/12/039. arXiv:0808.3674 [hep-ph]
56. F. Buccioni et al., OpenLoops 2. Eur. Phys. J. C **79**, 866 (2019). https://doi.org/10.1140/epjc/s10052-019-7306-2. arXiv:1907.13071 [hep-ph]
57. S. Schumann, F. Krauss, A parton shower algorithm based on Catani–Seymour dipole factorisation. JHEP **03**, 038 (2008). https://doi.org/10.1088/1126-6708/2008/03/038. arXiv:0709.1027 [hep-ph]
58. S. Höche, F. Krauss, M. Schönherr, F. Siegert, A critical appraisal of NLO+PS matching methods. JHEP **09**, 049 (2012). https://doi.org/10.1007/JHEP09(2012)049. arXiv:1111.1220 [hep-ph]
59. S. Catani, F. Krauss, B.R. Webber, R. Kuhn, QCD matrix elements + parton showers. JHEP **11**, 063 (2001). https://doi.org/10.1088/1126-6708/2001/11/063. arXiv:hep-ph/0109231
60. S. Höche, F. Krauss, M. Schönherr, F. Siegert, QCD matrix elements + parton showers. The NLO case. JHEP **04**, 027 (2013). https://doi.org/10.1007/JHEP04(2013)027. arXiv:1207.5030 [hep-ph]
61. S. Höche, F. Krauss, S. Schumann, F. Siegert, QCD matrix elements and truncated showers. JHEP **05**, 053 (2009). https://doi.org/10.1088/1126-6708/2009/05/053. arXiv:0903.1219 [hep-ph]
62. C. Anastasiou, L. Dixon, K. Melnikov, F. Petriello, High-precision QCD at hadron colliders: electroweak gauge boson rapid-

ity distributions at next-to-next-to leading order. Phys. Rev. D **69**, 094008 (2004). https://doi.org/10.1103/PhysRevD.69.094008. arXiv:hep-ph/0312266
63. S. Alioli, P. Nason, C. Oleari, E. Re, NLO vector-boson production matched with shower in POWHEG. JHEP **07**, 060 (2008). https://doi.org/10.1088/1126-6708/2008/07/060. arXiv:0805.4802 [hep-ph]
64. ATLAS Collaboration, Measurement of the Z/γ^* boson transverse momentum distribution in pp collisions at $\sqrt{s} = 7$ TeV with the ATLAS detector. JHEP **09**, 145 (2014). https://doi.org/10.1007/JHEP09(2014)145. arXiv:1406.3660 [hep-ex]
65. H.-L. Lai et al., New parton distributions for collider physics. Phys. Rev. D **82**, 074024 (2010). https://doi.org/10.1103/PhysRevD.82.074024. arXiv:1007.2241 [hep-ph]
66. R. Gavin, Y. Li, F. Petriello, S. Quackenbush, FEWZ 2.0: a code for hadronic Z production at next-to-next-to-leading order. Comput. Phys. Commun. **182**, 2388 (2011). https://doi.org/10.1016/j.cpc.2011.06.008. arXiv:1011.3540 [hep-ph]
67. M. Cacciari, G.P. Salam, G. Soyez, The anti-k_t jet clustering algorithm. JHEP **04**, 063 (2008). https://doi.org/10.1088/1126-6708/2008/04/063. arXiv:0802.1189 [hep-ph]
68. M. Cacciari, G.P. Salam, G. Soyez, FastJet user manual. Eur. Phys. J. C **72**, 1896 (2012). https://doi.org/10.1140/epjc/s10052-012-1896-2. arXiv:1111.6097 [hep-ph]
69. ATLAS Collaboration, Jet reconstruction and performance using particle flow with the ATLAS detector. Eur. Phys. J. C **77**, 466 (2017). https://doi.org/10.1140/epjc/s10052-017-5031-2. arXiv:1703.10485 [hep-ex]
70. ATLAS Collaboration, Performance of pile-up mitigation techniques for jets in pp collisions at $\sqrt{s} = 8$ TeV using the ATLAS detector. Eur. Phys. J. C **76**, 581 (2016). https://doi.org/10.1140/epjc/s10052-016-4395-z. arXiv:1510.03823 [hep-ex]
71. ATLAS Collaboration, ATLAS flavour-tagging algorithms for the LHC Run 2 pp collision dataset. Eur. Phys. J. C **83**, 681 (2023). https://doi.org/10.1140/epjc/s10052-023-11699-1. arXiv:2211.16345 [physics.data-an]
72. ATLAS Collaboration, Measurements of top-quark pair differential cross-sections in the lepton+jets channel in pp collisions at $\sqrt{s} = 13$ TeV using the ATLAS detector. JHEP **11**, 191 (2017). https://doi.org/10.1007/JHEP11(2017)191. arXiv:1708.00727 [hep-ex]
73. M. Czakon, D. Heymes, A. Mitov, High-precision differential predictions for top-quark pairs at the LHC. Phys. Rev. Lett. **116**, 082003 (2016). https://doi.org/10.1103/PhysRevLett.116.082003. arXiv:1511.00549 [hep-ph]
74. ATLAS Collaboration, Measurement of the $t\bar{t}$ production cross-section in pp collisions at $\sqrt{s} = 5.02$ TeV with the ATLAS detector. JHEP **06**, 138 (2023). https://doi.org/10.1007/JHEP06(2023)138. arXiv:2207.01354 [hep-ex]
75. ATLAS Collaboration, Test of the universality of τ and μ lepton couplings in W-boson decays with the ATLAS detector. Nat. Phys. **17**, 813 (2021). https://doi.org/10.1038/s41567-021-01236-w. arXiv:2007.14040 [hep-ex]
76. J. Butterworth et al., PDF4LHC recommendations for LHC Run II. J. Phys. G **43**, 023001 (2016). https://doi.org/10.1088/0954-3899/43/2/023001. arXiv:1510.03865 [hep-ph]
77. J. Bellm et al., Herwig 7.0/Herwig++ *3.0 release note*. Eur. Phys. J. C **76**, 196 (2016). https://doi.org/10.1140/epjc/s10052-016-4018-8. arXiv:1512.01178 [hep-ph]
78. ATLAS Collaboration, Measurement of the c-jet mistagging efficiency in $t\bar{t}$ events using pp collision data at $\sqrt{s} = 13$ TeV collected with the ATLAS detector. Eur. Phys. J. C **82**, 95 (2022). https://doi.org/10.1140/epjc/s10052-021-09843-w. arXiv:2109.10627 [hep-ex]
79. ATLAS Collaboration, Calibration of the light-flavour jet mistagging efficiency of the b-tagging algorithms with Z+jets events using 139 fb^{-1} of ATLAS proton–proton collision data at $\sqrt{s} = 13$ TeV. Eur. Phys. J. C **83**, 728 (2023). https://doi.org/10.1140/epjc/s10052-023-11736-z. arXiv:2301.06319 [hep-ex]
80. G. Avoni et al., The new LUCID-2 detector for luminosity measurement and monitoring in ATLAS. JINST **13**, P07017 (2018). https://doi.org/10.1088/1748-0221/13/07/P07017
81. ATLAS Collaboration, Inclusive and differential cross-sections for dilepton $t\bar{t}$ production measured in $\sqrt{s} = 13$ TeV pp collisions with the ATLAS detector. JHEP **07**, 141 (2023).https://doi.org/10.1007/JHEP07(2023)141. arXiv:2303.15340 [hep-ex]
82. ATLAS Collaboration, Precise measurements of W- and Z-boson transverse momentum spectra with the ATLAS detector using pp collisions at $\sqrt{s} = 5.02$ TeV and 13 TeV. (2024). arXiv:2404.06204 [hep-ex]
83. ATLAS Collaboration, ATLAS Computing Acknowledgements, ATL-SOFT-PUB-2023-001 (2023). https://cds.cern.ch/record/2869272

ATLAS Collaboration*

G. Aad[103], E. Aakvaag[16], B. Abbott[121], S. Abdelhameed[117a], K. Abeling[55], N. J. Abicht[49], S. H. Abidi[29], M. Aboelela[44], A. Aboulhorma[35e], H. Abramowicz[152], H. Abreu[151], Y. Abulaiti[118], B. S. Acharya[69a,69b,k], A. Ackermann[63a], C. Adam Bourdarios[4], L. Adamczyk[86a], S. V. Addepalli[26], M. J. Addison[102], J. Adelman[116], A. Adiguzel[21c], T. Adye[135], A. A. Affolder[137], Y. Afik[39], M. N. Agaras[13], J. Agarwala[73a,73b], A. Aggarwal[101], C. Agheorghiesei[27c], A. Ahmad[36], F. Ahmadov[38,x], W. S. Ahmed[105], S. Ahuja[96], X. Ai[62e], G. Aielli[76a,76b], A. Aikot[164], M. Ait Tamlihat[35e], B. Aitbenchikh[35a], M. Akbiyik[101], T. P. A. Åkesson[99], A. V. Akimov[37], D. Akiyama[169], N. N. Akolkar[24], S. Aktas[21a], K. Al Khoury[41], G. L. Alberghi[23b], J. Albert[166], P. Albicocco[53], G. L. Albouy[60], S. Alderweireldt[52], Z. L. Alegria[122], M. Aleksa[36], I. N. Aleksandrov[38], C. Alexa[27b], T. Alexopoulos[10], F. Alfonsi[23b], M. Algren[56], M. Alhroob[168], B. Ali[133], H. M. J. Ali[92], S. Ali[31], S. W. Alibocus[93], M. Aliev[33c], G. Alimonti[71a], W. Alkakhi[55], C. Allaire[66], B. M. M. Allbrooke[147], J. F. Allen[52], C. A. Allendes Flores[138f], P. P. Allport[20], A. Aloisio[72a,72b], F. Alonso[91], C. Alpigiani[139], Z. M. K. Alsolami[92], M. Alvarez Estevez[100], A. Alvarez Fernandez[101], M. Alves Cardoso[56], M. G. Alviggi[72a,72b], M. Aly[102], Y. Amaral Coutinho[83b], A. Ambler[105], C. Amelung[36], M. Amerl[102], C. G. Ames[110], D. Amidei[107], K. J. Amirie[156], S. P. Amor Dos Santos[131a], K. R. Amos[164], S. An[84], V. Ananiev[126], C. Anastopoulos[140], T. Andeen[11], J. K. Anders[36], S. Y. Andrean[47a,47b], A. Andreazza[71a,71b], S. Angelidakis[9], A. Angerami[41,z], A. V. Anisenkov[37], A. Annovi[74a], C. Antel[56], E. Antipov[146], M. Antonelli[53], F. Anulli[75a], M. Aoki[84], T. Aoki[154], M. A. Aparo[147], L. Aperio Bella[48], C. Appelt[18], A. Apyan[26], S. J. Arbiol Val[87], C. Arcangeletti[53], A. T. H. Arce[51], E. Arena[93], J.-F. Arguin[109], S. Argyropoulos[54], J.-H. Arling[48], O. Arnaez[4], H. Arnold[146], G. Artoni[75a,75b], H. Asada[112], K. Asai[119], S. Asai[154], N. A. Asbah[36], R. A. Ashby Pickering[168], K. Assamagan[29], R. Astalos[28a], K. S. V. Astrand[99], S. Atashi[160], R. J. Atkin[33a], M. Atkinson[163], H. Atmani[35f], P. A. Atmasiddha[129], K. Augsten[133], S. Auricchio[72a,72b], A. D. Auriol[20], V. A. Austrup[102], G. Avolio[36], K. Axiotis[56], G. Azuelos[109,ad], D. Babal[28b], H. Bachacou[136], K. Bachas[153,o], A. Bachiu[34], F. Backman[47a,47b], A. Badea[39], T. M. Baer[107], P. Bagnaia[75a,75b], M. Bahmani[18], D. Bahner[54], K. Bai[124], J. T. Baines[135], L. Baines[95], O. K. Baker[173], E. Bakos[15], D. Bakshi Gupta[8], V. Balakrishnan[121], R. Balasubramanian[115], E. M. Baldin[37], P. Balek[86a], E. Ballabene[23a,23b], F. Balli[136], L. M. Baltes[63a], W. K. Balunas[32], J. Balz[101], I. Bamwidhi[117b], E. Banas[87], M. Bandieramonte[130], A. Bandyopadhyay[24], S. Bansal[24], L. Barak[152], M. Barakat[48], E. L. Barberio[106], D. Barberis[57a,57b], M. Barbero[103], M. Z. Barel[115], K. N. Barends[33a], T. Barillari[111], M.-S. Barisits[36], T. Barklow[144], P. Baron[123], D. A. Baron Moreno[102], A. Baroncelli[62a], G. Barone[29], A. J. Barr[127], J. D. Barr[97], F. Barreiro[100], J. Barreiro Guimarães da Costa[14a], U. Barron[152], M. G. Barros Teixeira[131a], S. Barsov[37], F. Bartels[63a], R. Bartoldus[144], A. E. Barton[92], P. Bartos[28a], A. Basan[101], M. Baselga[49], A. Bassalat[66,b], M. J. Basso[157a], R. Bate[165], R. L. Bates[59], S. Batlamous[100], B. Batool[142], M. Battaglia[137], D. Battulga[18], M. Bauce[75a,75b], M. Bauer[36], P. Bauer[24], L. T. Bazzano Hurrell[30], J. B. Beacham[51], T. Beau[128], J. Y. Beaucamp[91], P. H. Beauchemin[159], P. Bechtle[24], H. P. Beck[19,n], K. Becker[168], A. J. Beddall[82], V. A. Bednyakov[38], C. P. Bee[146], L. J. Beemster[15], T. A. Beermann[36], M. Begalli[83d], M. Begel[29], A. Behera[146], J. K. Behr[48], J. F. Beirer[36], F. Beisiegel[24], M. Belfkir[117b], G. Bella[152], L. Bellagamba[23b], A. Bellerive[34], P. Bellos[20], K. Beloborodov[37], D. Benchekroun[35a], F. Bendebba[35a], Y. Benhammou[152], K. C. Benkendorfer[61], L. Beresford[48], M. Beretta[53], E. Bergeaas Kuutmann[162], N. Berger[4], B. Bergmann[133], J. Beringer[17a], G. Bernardi[5], C. Bernius[144], F. U. Bernlochner[24], F. Bernon[36,103], A. Berrocal Guardia[13], T. Berry[96], P. Berta[134], A. Berthold[50], S. Bethke[111], A. Betti[75a,75b], A. J. Bevan[95], N. K. Bhalla[54], S. Bhatta[146], D. S. Bhattacharya[167], P. Bhattarai[144], K. D. Bhide[54], V. S. Bhopatkar[122], R. M. Bianchi[130], G. Bianco[23a,23b], O. Biebel[110], R. Bielski[124], M. Biglietti[77a], C. S. Billingsley[44], M. Bindi[55], A. Bingul[21b], C. Bini[75a,75b], A. Biondini[93], G. A. Bird[32], M. Birman[170], M. Biros[134], S. Biryukov[147], T. Bisanz[49], E. Bisceglie[43a,43b], J. P. Biswal[135], D. Biswas[142], I. Bloch[48], A. Blue[59], U. Blumenschein[95], J. Blumenthal[101], V. S. Bobrovnikov[37], M. Boehler[54], B. Boehm[167], D. Bogavac[36], A. G. Bogdanchikov[37], C. Bohm[47a], V. Boisvert[96], P. Bokan[36], T. Bold[86a], M. Bomben[5], M. Bona[95], M. Boonekamp[136], C. D. Booth[96], A. G. Borbély[59], I. S. Bordulev[37], H. M. Borecka-Bielska[109], G. Borissov[92], D. Bortoletto[127], D. Boscherini[23b], M. Bosman[13], J. D. Bossio Sola[36], K. Bouaouda[35a], N. Bouchhar[164], L. Boudet[4], J. Boudreau[130], E. V. Bouhova-Thacker[92], D. Boumediene[40], R. Bouquet[57a,57b], A. Boveia[120], J. Boyd[36], D. Boye[29], I. R. Boyko[38], L. Bozianu[56], J. Bracinik[20], N. Brahimi[4], G. Brandt[172], O. Brandt[32], F. Braren[48], B. Brau[104], J. E. Brau[124], R. Brener[170], L. Brenner[115], R. Brenner[162], S. Bressler[170],

D. Britton[59], D. Britzger[111], I. Brock[24], R. Brock[108], G. Brooijmans[41], E. Brost[29], L. M. Brown[166], L. E. Bruce[61], T. L. Bruckler[127], P. A. Bruckman de Renstrom[87], B. Brüers[48], A. Bruni[23b], G. Bruni[23b], M. Bruschi[23b], N. Bruscino[75a,75b], T. Buanes[16], Q. Buat[139], D. Buchin[111], A. G. Buckley[59], O. Bulekov[37], B. A. Bullard[144], S. Burdin[93], C. D. Burgard[49], A. M. Burger[36], B. Burghgrave[8], O. Burlayenko[54], J. T. P. Burr[32], J. C. Burzynski[143], E. L. Busch[41], V. Büscher[101], P. J. Bussey[59], J. M. Butler[25], C. M. Buttar[59], J. M. Butterworth[97], W. Buttinger[135], C. J. Buxo Vazquez[108], A. R. Buzykaev[37], S. Cabrera Urbán[164], L. Cadamuro[66], D. Caforio[58], H. Cai[130], Y. Cai[14a,14e], Y. Cai[14c], V. M. M. Cairo[36], O. Cakir[3a], N. Calace[36], P. Calafiura[17a], G. Calderini[128], P. Calfayan[68], G. Callea[59], L. P. Caloba[83b], D. Calvet[40], S. Calvet[40], M. Calvetti[74a,74b], R. Camacho Toro[128], S. Camarda[36], D. Camarero Munoz[26], P. Camarri[76a,76b], M. T. Camerlingo[72a,72b], D. Cameron[36], C. Camincher[166], M. Campanelli[97], A. Camplani[42], V. Canale[72a,72b], A. C. Canbay[3a], E. Canonero[96], J. Cantero[164], Y. Cao[163], F. Capocasa[26], M. Capua[43a,43b], A. Carbone[71a,71b], R. Cardarelli[76a], J. C. J. Cardenas[8], G. Carducci[43a,43b], T. Carli[36], G. Carlino[72a], J. I. Carlotto[13], B. T. Carlson[130,p], E. M. Carlson[157a,166], J. Carmignani[93], L. Carminati[71a,71b], A. Carnelli[136], M. Carnesale[75a,75b], S. Caron[114], E. Carquin[138f], S. Carrá[71a], G. Carratta[23a,23b], A. M. Carroll[124], T. M. Carter[52], M. P. Casado[13,h], M. Caspar[48], F. L. Castillo[4], L. Castillo Garcia[13], V. Castillo Gimenez[164], N. F. Castro[131a,131e], A. Catinaccio[36], J. R. Catmore[126], T. Cavaliere[4], V. Cavaliere[29], N. Cavalli[23a,23b], Y. C. Cekmecelioglu[48], E. Celebi[21a], S. Cella[36], F. Celli[127], M. S. Centonze[70a,70b], V. Cepaitis[56], K. Cerny[123], A. S. Cerqueira[83a], A. Cerri[147], L. Cerrito[76a,76b], F. Cerutti[17a], B. Cervato[142], A. Cervelli[23b], G. Cesarini[53], S. A. Cetin[82], D. Chakraborty[116], J. Chan[17a], W. Y. Chan[154], J. D. Chapman[32], E. Chapon[136], B. Chargeishvili[150b], D. G. Charlton[20], M. Chatterjee[19], C. Chauhan[134], Y. Che[14c], S. Chekanov[6], S. V. Chekulaev[157a], G. A. Chelkov[38,a], A. Chen[107], B. Chen[152], B. Chen[166], H. Chen[14c], H. Chen[29], J. Chen[62c], J. Chen[143], M. Chen[127], S. Chen[154], S. J. Chen[14c], X. Chen[62c,136], X. Chen[14b,ac], Y. Chen[62a], C. L. Cheng[171], H. C. Cheng[64a], S. Cheong[144], A. Cheplakov[38], E. Cheremushkina[48], E. Cherepanova[115], R. Cherkaoui El Moursli[35e], E. Cheu[7], K. Cheung[65], L. Chevalier[136], V. Chiarella[53], G. Chiarelli[74a], N. Chiedde[103], G. Chiodini[70a], A. S. Chisholm[20], A. Chitan[27b], M. Chitishvili[164], M. V. Chizhov[38,ai], K. Choi[11], Y. Chou[139], E. Y. S. Chow[114], K. L. Chu[170], M. C. Chu[64a], X. Chu[14a,14e], J. Chudoba[132], J. J. Chwastowski[87], D. Cieri[111], K. M. Ciesla[86a], V. Cindro[94], A. Ciocio[17a], F. Cirotto[72a,72b], Z. H. Citron[170], M. Citterio[71a], D. A. Ciubotaru[27b], A. Clark[56], P. J. Clark[52], N. Clarke Hall[97], C. Clarry[156], J. M. Clavijo Columbie[48], S. E. Clawson[48], C. Clement[47a,47b], J. Clercx[48], Y. Coadou[103], M. Cobal[69a,69c], A. Coccaro[57b], R. F. Coelho Barrue[131a], R. Coelho Lopes De Sa[104], S. Coelli[71a], B. Cole[41], J. Collot[60], P. Conde Muiño[131a,131g], M. P. Connell[33c], S. H. Connell[33c], E. I. Conroy[127], F. Conventi[72a,ae], H. G. Cooke[20], A. M. Cooper-Sarkar[127], F. A. Corchia[23a,23b], A. Cordeiro Oudot Choi[128], L. D. Corpe[40], M. Corradi[75a,75b], F. Corriveau[105,v], A. Cortes-Gonzalez[18], M. J. Costa[164], F. Costanza[4], D. Costanzo[140], B. M. Cote[120], J. Couthures[4], G. Cowan[96], K. Cranmer[171], D. Cremonini[23a,23b], S. Crépé-Renaudin[60], F. Crescioli[128], M. Cristinziani[142], M. Cristoforetti[78a,78b], V. Croft[115], J. E. Crosby[122], G. Crosetti[43a,43b], A. Cueto[100], Z. Cui[7], W. R. Cunningham[59], F. Curcio[164], J. R. Curran[52], P. Czodrowski[36], M. M. Czurylo[36], M. J. Da Cunha Sargedas De Sousa[57a,57b], J. V. Da Fonseca Pinto[83b], C. Da Via[102], W. Dabrowski[86a], T. Dado[49], S. Dahbi[149], T. Dai[107], D. Dal Santo[19], C. Dallapiccola[104], M. Dam[42], G. D'amen[29], V. D'Amico[110], J. Damp[101], J. R. Dandoy[34], D. Dannheim[36], M. Danninger[143], V. Dao[146], G. Darbo[57b], S. J. Das[29,af], F. Dattola[48], S. D'Auria[71a,71b], A. D'Avanzo[72a,72b], C. David[33a], T. Davidek[134], I. Dawson[95], H. A. Day-hall[133], K. De[8], R. De Asmundis[72a], N. De Biase[48], S. De Castro[23a,23b], N. De Groot[114], P. de Jong[115], H. De la Torre[116], A. De Maria[14c], A. De Salvo[75a], U. De Sanctis[76a,76b], F. De Santis[70a,70b], A. De Santo[147], J. B. De Vivie De Regie[60], D. V. Dedovich[38], J. Degens[93], A. M. Deiana[44], F. Del Corso[23a,23b], J. Del Peso[100], F. Del Rio[63a], L. Delagrange[128], F. Deliot[136], C. M. Delitzsch[49], M. Della Pietra[72a,72b], D. Della Volpe[56], A. Dell'Acqua[36], L. Dell'Asta[71a,71b], M. Delmastro[4], P. A. Delsart[60], S. Demers[173], M. Demichev[38], S. P. Denisov[37], L. D'Eramo[40], D. Derendarz[87], F. Derue[128], P. Dervan[93], K. Desch[24], C. Deutsch[24], F. A. Di Bello[57a,57b], A. Di Ciaccio[76a,76b], L. Di Ciaccio[4], A. Di Domenico[75a,75b], C. Di Donato[72a,72b], A. Di Girolamo[36], G. Di Gregorio[36], A. Di Luca[78a,78b], B. Di Micco[77a,77b], R. Di Nardo[77a,77b], K. F. Di Petrillo[39], M. Diamantopoulou[34], F. A. Dias[115], T. Dias Do Vale[143], M. A. Diaz[138a,138b], F. G. Diaz Capriles[24], M. Didenko[164], E. B. Diehl[107], S. Díez Cornell[48], C. Diez Pardos[142], C. Dimitriadi[24,162], A. Dimitrievska[20], J. Dingfelder[24], I.-M. Dinu[27b], S. J. Dittmeier[63b], F. Dittus[36], M. Divisek[134], F. Djama[103], T. Djobava[150b], C. Doglioni[99,102], A. Dohnalova[28a], J. Dolejsi[134], Z. Dolezal[134], K. Domijan[86a], K. M. Dona[39], M. Donadelli[83d], B. Dong[108], J. Donini[40], A. D'Onofrio[72a,72b],

M. D'Onofrio[93], J. Dopke[135], A. Doria[72a], N. Dos Santos Fernandes[131a], P. Dougan[102], M. T. Dova[91], A. T. Doyle[59], M. A. Draguet[127], E. Dreyer[170], I. Drivas-koulouris[10], M. Drnevich[118], M. Drozdova[56], D. Du[62a], T. A. du Pree[115], F. Dubinin[37], M. Dubovsky[28a], E. Duchovni[170], G. Duckeck[110], O. A. Ducu[27b], D. Duda[52], A. Dudarev[36], E. R. Duden[26], M. D'uffizi[102], L. Duflot[66], M. Dührssen[36], I. Duminica[27g], A. E. Dumitriu[27b], M. Dunford[63a], S. Dungs[49], K. Dunne[47a,47b], A. Duperrin[103], H. Duran Yildiz[3a], M. Düren[58], A. Durglishvili[150b], B. L. Dwyer[116], G. I. Dyckes[17a], M. Dyndal[86a], B. S. Dziedzic[36], Z. O. Earnshaw[147], G. H. Eberwein[127], B. Eckerova[28a], S. Eggebrecht[55], E. Egidio Purcino De Souza[128], L. F. Ehrke[56], G. Eigen[16], K. Einsweiler[17a], T. Ekelof[162], P. A. Ekman[99], S. El Farkh[35b], Y. El Ghazali[35b], H. El Jarrari[36], A. El Moussaouy[35a], V. Ellajosyula[162], M. Ellert[162], F. Ellinghaus[172], N. Ellis[36], J. Elmsheuser[29], M. Elsawy[117a], M. Elsing[36], D. Emeliyanov[135], Y. Enari[154], I. Ene[17a], S. Epari[13], P. A. Erland[87], D. Ernani Martins Neto[87], M. Errenst[172], M. Escalier[66], C. Escobar[164], E. Etzion[152], G. Evans[131a], H. Evans[68], L. S. Evans[96], A. Ezhilov[37], S. Ezzarqtouni[35a], F. Fabbri[23a,23b], L. Fabbri[23a,23b], G. Facini[97], V. Fadeyev[137], R. M. Fakhrutdinov[37], D. Fakoudis[101], S. Falciano[75a], L. F. Falda Ulhoa Coelho[36], F. Fallavollita[111], G. Falsetti[43a,43b], J. Faltova[134], C. Fan[163], Y. Fan[14a], Y. Fang[14a,14e], M. Fanti[71a,71b], M. Faraj[69a,69b], Z. Farazpay[98], A. Farbin[8], A. Farilla[77a], T. Farooque[108], S. M. Farrington[52], F. Fassi[35e], D. Fassouliotis[9], M. Faucci Giannelli[76a,76b], W. J. Fawcett[32], L. Fayard[66], P. Federic[134], P. Federicova[132], O. L. Fedin[37,a], M. Feickert[171], L. Feligioni[103], D. E. Fellers[124], C. Feng[62b], M. Feng[14b], Z. Feng[115], M. J. Fenton[160], L. Ferencz[48], R. A. M. Ferguson[92], S. I. Fernandez Luengo[138f], P. Fernandez Martinez[13], M. J. V. Fernoux[103], J. Ferrando[92], A. Ferrari[162], P. Ferrari[114,115], R. Ferrari[73a], D. Ferrere[56], C. Ferretti[107], D. Fiacco[75a,75b], F. Fiedler[101], P. Fiedler[133], A. Filipčič[94], E. K. Filmer[1], F. Filthaut[114], M. C. N. Fiolhais[131a,131c,c], L. Fiorini[164], W. C. Fisher[108], T. Fitschen[102], P. M. Fitzhugh[136], I. Fleck[142], P. Fleischmann[107], T. Flick[172], M. Flores[33d,aa], L. R. Flores Castillo[64a], L. Flores Sanz De Acedo[36], F. M. Follega[78a,78b], N. Fomin[16], J. H. Foo[156], A. Formica[136], A. C. Forti[102], E. Fortin[36], A. W. Fortman[17a], M. G. Foti[17a], L. Fountas[9,i], D. Fournier[66], H. Fox[92], P. Francavilla[74a,74b], S. Francescato[61], S. Franchellucci[56], M. Franchini[23a,23b], S. Franchino[63a], D. Francis[36], L. Franco[114], V. Franco Lima[36], L. Franconi[48], M. Franklin[61], G. Frattari[26], Y. Y. Frid[152], J. Friend[59], N. Fritzsche[50], A. Froch[54], D. Froidevaux[36], J. A. Frost[127], Y. Fu[62a], S. Fuenzalida Garrido[138f], M. Fujimoto[103], K. Y. Fung[64a], E. Furtado De Simas Filho[83e], M. Furukawa[154], J. Fuster[164], A. Gabrielli[23a,23b], A. Gabrielli[156], P. Gadow[36], G. Gagliardi[57a,57b], L. G. Gagnon[17a], S. Gaid[161], S. Galantzan[152], E. J. Gallas[127], B. J. Gallop[135], K. K. Gan[120], S. Ganguly[154], Y. Gao[52], F. M. Garay Walls[138a,138b], B. Garcia[29], C. García[164], A. Garcia Alonso[115], A. G. Garcia Caffaro[173], J. E. García Navarro[164], M. Garcia-Sciveres[17a], G. L. Gardner[129], R. W. Gardner[39], N. Garelli[159], D. Garg[80], R. B. Garg[144], J. M. Gargan[52], C. A. Garner[156], C. M. Garvey[33a], V. K. Gassmann[159], G. Gaudio[73a], V. Gautam[13], P. Gauzzi[75a,75b], I. L. Gavrilenko[37], A. Gavrilyuk[37], C. Gay[165], G. Gaycken[48], E. N. Gazis[10], A. A. Geanta[27b], C. M. Gee[137], A. Gekow[120], C. Gemme[57b], M. H. Genest[60], A. D. Gentry[113], S. George[96], W. F. George[20], T. Geralis[46], P. Gessinger-Befurt[36], M. E. Geyik[172], M. Ghani[168], K. Ghorbanian[95], A. Ghosal[142], A. Ghosh[160], A. Ghosh[7], B. Giacobbe[23b], S. Giagu[75a,75b], T. Giani[115], P. Giannetti[74a], A. Giannini[62a], S. M. Gibson[96], M. Gignac[137], D. T. Gil[86b], A. K. Gilbert[86a], B. J. Gilbert[41], D. Gillberg[34], G. Gilles[115], L. Ginabat[128], D. M. Gingrich[2,ad], M. P. Giordani[69a,69c], P. F. Giraud[136], G. Giugliarelli[69a,69c], D. Giugni[71a], F. Giuli[36], I. Gkialas[9,i], L. K. Gladilin[37], C. Glasman[100], G. R. Gledhill[124], G. Glemža[48], M. Glisic[124], I. Gnesi[43b,e], Y. Go[29], M. Goblirsch-Kolb[36], B. Gocke[49], D. Godin[109], B. Gokturk[21a], S. Goldfarb[106], T. Golling[56], M. G. D. Gololo[33g], D. Golubkov[37], J. P. Gombas[108], A. Gomes[131a,131b], G. Gomes Da Silva[142], A. J. Gomez Delegido[164], R. Gonçalo[131a], L. Gonella[20], A. Gongadze[150c], F. Gonnella[20], J. L. Gonski[144], R. Y. González Andana[52], S. González de la Hoz[164], R. Gonzalez Lopez[93], C. Gonzalez Renteria[17a], M. V. Gonzalez Rodrigues[48], R. Gonzalez Suarez[162], S. Gonzalez-Sevilla[56], L. Goossens[36], B. Gorini[36], E. Gorini[70a,70b], A. Gorišek[94], T. C. Gosart[129], A. T. Goshaw[51], M. I. Gostkin[38], S. Goswami[122], C. A. Gottardo[36], S. A. Gotz[110], M. Gouighri[35b], V. Goumarre[48], A. G. Goussiou[139], N. Govender[33c], I. Grabowska-Bold[86a], K. Graham[34], E. Gramstad[126], S. Grancagnolo[70a,70b], C. M. Grant[1,136], P. M. Gravila[27f], F. G. Gravili[70a,70b], H. M. Gray[17a], M. Greco[70a,70b], C. Grefe[24], A. S. Grefsrud[16], I. M. Gregor[48], K. T. Greif[160], P. Grenier[144], S. G. Grewe[111], A. A. Grillo[137], K. Grimm[31], S. Grinstein[13,r], J.-F. Grivaz[66], E. Gross[170], J. Grosse-Knetter[55], J. C. Grundy[127], L. Guan[107], J. G. R. Guerrero Rojas[164], G. Guerrieri[69a,69c], R. Gugel[101], J. A. M. Guhit[107], A. Guida[18], E. Guilloton[168], S. Guindon[36], F. Guo[14a,14e], J. Guo[62c], L. Guo[48], Y. Guo[107], R. Gupta[130], S. Gurbuz[24], S. S. Gurdasani[54], G. Gustavino[36], M. Guth[56], P. Gutierrez[121], L. F. Gutierrez Zagazeta[129],

M. Gutsche[50], C. Gutschow[97], C. Gwenlan[127], C. B. Gwilliam[93], E. S. Haaland[126], A. Haas[118], M. Habedank[48], C. Haber[17a], H. K. Hadavand[8], A. Hadef[50], S. Hadzic[111], A. I. Hagan[92], J. J. Hahn[142], E. H. Haines[97], M. Haleem[167], J. Haley[122], J. J. Hall[140], G. D. Hallewell[103], L. Halser[19], K. Hamano[166], M. Hamer[24], G. N. Hamity[52], E. J. Hampshire[96], J. Han[62b], K. Han[62a], L. Han[14c], L. Han[62a], S. Han[17a], Y. F. Han[156], K. Hanagaki[84], M. Hance[137], D. A. Hangal[41], H. Hanif[143], M. D. Hank[129], J. B. Hansen[42], P. H. Hansen[42], K. Hara[158], D. Harada[56], T. Harenberg[172], S. Harkusha[37], M. L. Harris[104], Y. T. Harris[127], J. Harrison[13], N. M. Harrison[120], P. F. Harrison[168], N. M. Hartman[111], N. M. Hartmann[110], R. Z. Hasan[96,135], Y. Hasegawa[141], S. Hassan[16], R. Hauser[108], C. M. Hawkes[20], R. J. Hawkings[36], Y. Hayashi[154], S. Hayashida[112], D. Hayden[108], C. Hayes[107], R. L. Hayes[115], C. P. Hays[127], J. M. Hays[95], H. S. Hayward[93], F. He[62a], M. He[14a,14e], Y. He[155], Y. He[48], Y. He[97], N. B. Heatley[95], V. Hedberg[99], A. L. Heggelund[126], N. D. Hehir[95,*], C. Heidegger[54], K. K. Heidegger[54], J. Heilman[34], S. Heim[48], T. Heim[17a], J. G. Heinlein[129], J. J. Heinrich[124], L. Heinrich[111,ab], J. Hejbal[132], A. Held[171], S. Hellesund[16], C. M. Helling[165], S. Hellman[47a,47b], R. C. W. Henderson[92], L. Henkelmann[32], A. M. Henriques Correia[36], H. Herde[99], Y. Hernández Jiménez[146], L. M. Herrmann[24], T. Herrmann[50], G. Herten[54], R. Hertenberger[110], L. Hervas[36], M. E. Hesping[101], N. P. Hessey[157a], M. Hidaoui[35b], E. Hill[156], S. J. Hillier[20], J. R. Hinds[108], F. Hinterkeuser[24], M. Hirose[125], S. Hirose[158], D. Hirschbuehl[172], T. G. Hitchings[102], B. Hiti[94], J. Hobbs[146], R. Hobincu[27e], N. Hod[170], M. C. Hodgkinson[140], B. H. Hodkinson[127], A. Hoecker[36], D. D. Hofer[107], J. Hofer[48], T. Holm[24], M. Holzbock[111], L. B. A. H. Hommels[32], B. P. Honan[102], J. J. Hong[68], J. Hong[62c], T. M. Hong[130], B. H. Hooberman[163], W. H. Hopkins[6], M. C. Hoppesch[163], Y. Horii[112], S. Hou[149], A. S. Howard[94], J. Howarth[59], J. Hoya[6], M. Hrabovsky[123], A. Hrynevich[48], T. Hryn'ova[4], P. J. Hsu[65], S.-C. Hsu[139], T. Hsu[66], M. Hu[17a], Q. Hu[62a], S. Huang[64b], X. Huang[14a,14e], Y. Huang[140], Y. Huang[101], Y. Huang[14a], Z. Huang[102], Z. Hubacek[133], M. Huebner[24], F. Huegging[24], T. B. Huffman[127], C. A. Hugli[48], M. Huhtinen[36], S. K. Huiberts[16], R. Hulsken[105], N. Huseynov[12], J. Huston[108], J. Huth[61], R. Hyneman[144], G. Iacobucci[56], G. Iakovidis[29], L. Iconomidou-Fayard[66], J. P. Iddon[36], P. Iengo[72a,72b], R. Iguchi[154], Y. Iiyama[154], T. Iizawa[127], Y. Ikegami[84], N. Ilic[156], H. Imam[35a], M. Ince Lezki[56], T. Ingebretsen Carlson[47a,47b], G. Introzzi[73a,73b], M. Iodice[77a], V. Ippolito[75a,75b], R. K. Irwin[93], M. Ishino[154], W. Islam[171], C. Issever[18,48], S. Istin[21a,ah], H. Ito[169], R. Iuppa[78a,78b], A. Ivina[170], J. M. Izen[45], V. Izzo[72a], P. Jacka[132], P. Jackson[1], C. S. Jagfeld[110], G. Jain[157a], P. Jain[48], K. Jakobs[54], T. Jakoubek[170], J. Jamieson[59], M. Javurkova[104], L. Jeanty[124], J. Jejelava[150a,y], P. Jenni[54,f], C. E. Jessiman[34], C. Jia[62b], J. Jia[146], X. Jia[61], X. Jia[14a,14e], Z. Jia[14c], C. Jiang[52], S. Jiggins[48], J. Jimenez Pena[13], S. Jin[14c], A. Jinaru[27b], O. Jinnouchi[155], P. Johansson[140], K. A. Johns[7], J. W. Johnson[137], D. M. Jones[147], E. Jones[48], P. Jones[32], R. W. L. Jones[92], T. J. Jones[93], H. L. Joos[36,55], R. Joshi[120], J. Jovicevic[15], X. Ju[17a], J. J. Junggeburth[104], T. Junkermann[63a], A. Juste Rozas[13,r], M. K. Juzek[87], S. Kabana[138e], A. Kaczmarska[87], M. Kado[111], H. Kagan[120], M. Kagan[144], A. Kahn[129], C. Kahra[101], T. Kaji[154], E. Kajomovitz[151], N. Kakati[170], I. Kalaitzidou[54], C. W. Kalderon[29], N. J. Kang[137], D. Kar[33g], K. Karava[127], M. J. Kareem[157b], E. Karentzos[54], O. Karkout[115], S. N. Karpov[38], Z. M. Karpova[38], V. Kartvelishvili[92], A. N. Karyukhin[37], E. Kasimi[153], J. Katzy[48], S. Kaur[34], K. Kawade[141], M. P. Kawale[121], C. Kawamoto[88], T. Kawamoto[62a], E. F. Kay[36], F. I. Kaya[159], S. Kazakos[108], V. F. Kazanin[37], Y. Ke[146], J. M. Keaveney[33a], R. Keeler[166], G. V. Kehris[61], J. S. Keller[34], A. S. Kelly[97], J. J. Kempster[147], P. D. Kennedy[101], O. Kepka[132], B. P. Kerridge[135], S. Kersten[172], B. P. Kerševan[94], L. Keszeghova[28a], S. Ketabchi Haghighat[156], R. A. Khan[130], A. Khanov[122], A. G. Kharlamov[37], T. Kharlamova[37], E. E. Khoda[139], M. Kholodenko[37], T. J. Khoo[18], G. Khoriauli[167], J. Khubua[150b], Y. A. R. Khwaira[128], B. Kibirige[33g], D. W. Kim[47a,47b], Y. K. Kim[39], N. Kimura[97], M. K. Kingston[55], A. Kirchhoff[55], C. Kirfel[24], F. Kirfel[24], J. Kirk[135], A. E. Kiryunin[111], C. Kitsaki[10], O. Kivernyk[24], M. Klassen[159], C. Klein[34], L. Klein[167], M. H. Klein[44], S. B. Klein[56], U. Klein[93], P. Klimek[36], A. Klimentov[29], T. Klioutchnikova[36], P. Kluit[115], S. Kluth[111], E. Kneringer[79], T. M. Knight[156], A. Knue[49], R. Kobayashi[88], D. Kobylianskii[170], S. F. Koch[127], M. Kocian[144], P. Kodyš[134], D. M. Koeck[124], P. T. Koenig[24], T. Koffas[34], O. Kolay[50], I. Koletsou[4], T. Komarek[123], K. Köneke[54], A. X. Y. Kong[1], T. Kono[119], N. Konstantinidis[97], P. Kontaxakis[56], B. Konya[99], R. Kopeliansky[41], S. Koperny[86a], K. Korcyl[87], K. Kordas[153,d], A. Korn[97], S. Korn[55], I. Korolkov[13], N. Korotkova[37], B. Kortman[115], O. Kortner[111], S. Kortner[111], W. H. Kostecka[116], V. V. Kostyukhin[142], A. Kotsokechagia[136], A. Kotwal[51], A. Koulouris[36], A. Kourkoumeli-Charalampidi[73a,73b], C. Kourkoumelis[9], E. Kourlitis[111,ab], O. Kovanda[124], R. Kowalewski[166], W. Kozanecki[136], A. S. Kozhin[37], V. A. Kramarenko[37], G. Kramberger[94], P. Kramer[101], M. W. Krasny[128], A. Krasznahorkay[36], A. C. Kraus[116], J. W. Kraus[172],

J. A. Kremer[48], T. Kresse[50], J. Kretzschmar[93], K. Kreul[18], P. Krieger[156], S. Krishnamurthy[104], M. Krivos[134], K. Krizka[20], K. Kroeninger[49], H. Kroha[111], J. Kroll[132], J. Kroll[129], K. S. Krowpman[108], U. Kruchonak[38], H. Krüger[24], N. Krumnack[81], M. C. Kruse[51], O. Kuchinskaia[37], S. Kuday[3a], S. Kuehn[36], R. Kuesters[54], T. Kuhl[48], V. Kukhtin[38], Y. Kulchitsky[37,a], S. Kuleshov[138d,138b], M. Kumar[33g], N. Kumari[48], P. Kumari[157b], A. Kupco[132], T. Kupfer[49], A. Kupich[37], O. Kuprash[54], H. Kurashige[85], L. L. Kurchaninov[157a], O. Kurdysh[66], Y. A. Kurochkin[37], A. Kurova[37], M. Kuze[155], A. K. Kvam[104], J. Kvita[123], T. Kwan[105], N. G. Kyriacou[107], L. A. O. Laatu[103], C. Lacasta[164], F. Lacava[75a,75b], H. Lacker[18], D. Lacour[128], N. N. Lad[97], E. Ladygin[38], A. Lafarge[40], B. Laforge[128], T. Lagouri[173], F. Z. Lahbabi[35a], S. Lai[55], J. E. Lambert[166], S. Lammers[68], W. Lampl[7], C. Lampoudis[153,d], G. Lamprinoudis[101], A. N. Lancaster[116], E. Lançon[29], U. Landgraf[54], M. P. J. Landon[95], V. S. Lang[54], O. K. B. Langrekken[126], A. J. Lankford[160], F. Lanni[36], K. Lantzsch[24], A. Lanza[73a], J. F. Laporte[136], T. Lari[71a], F. Lasagni Manghi[23b], M. Lassnig[36], V. Latonova[132], A. Laudrain[101], A. Laurier[151], S. D. Lawlor[140], Z. Lawrence[102], R. Lazaridou[168], M. Lazzaroni[71a,71b], B. Le[102], E. M. Le Boulicaut[51], L. T. Le Pottier[17a], B. Leban[23a,23b], A. Lebedev[81], M. LeBlanc[102], F. Ledroit-Guillon[60], S. C. Lee[149], S. Lee[47a,47b], T. F. Lee[93], L. L. Leeuw[33c], H. P. Lefebvre[96], M. Lefebvre[166], C. Leggett[17a], G. Lehmann Miotto[36], M. Leigh[56], W. A. Leight[104], W. Leinonen[114], A. Leisos[153,q], M. A. L. Leite[83c], C. E. Leitgeb[18], R. Leitner[134], K. J. C. Leney[44], T. Lenz[24], S. Leone[74a], C. Leonidopoulos[52], A. Leopold[145], C. Leroy[109], R. Les[108], C. G. Lester[32], M. Levchenko[37], J. Levêque[4], L. J. Levinson[170], G. Levrini[23a,23b], M. P. Lewicki[87], C. Lewis[139], D. J. Lewis[4], A. Li[5], B. Li[62b], C. Li[62a], C.-Q. Li[111], H. Li[62a], H. Li[62b], H. Li[14c], H. Li[14b], H. Li[62b], J. Li[62c], K. Li[139], L. Li[62c], M. Li[14a,14e], S. Li[14a,14e], S. Li[62c,62d], T. Li[5], X. Li[105], Z. Li[127], Z. Li[154], Z. Li[14a,14e], S. Liang[14a,14e], Z. Liang[14a], M. Liberatore[136], B. Liberti[76a], K. Lie[64c], J. Lieber Marin[83e], H. Lien[68], H. Lin[107], K. Lin[108], R. E. Lindley[7], J. H. Lindon[2], E. Lipeles[129], A. Lipniacka[16], A. Lister[165], J. D. Little[68], B. Liu[14a], B. X. Liu[14d], D. Liu[62c,62d], E. H. L. Liu[20], J. B. Liu[62a], J. K. K. Liu[32], K. Liu[62d], K. Liu[62c,62d], M. Liu[62a], M. Y. Liu[62a], P. Liu[14a], Q. Liu[62c,62d,139], X. Liu[62a], X. Liu[62b], Y. Liu[14d,14e], Y. L. Liu[62b], Y. W. Liu[62a], J. Llorente Merino[143], S. L. Lloyd[95], E. M. Lobodzinska[48], P. Loch[7], T. Lohse[18], K. Lohwasser[140], E. Loiacono[48], M. Lokajicek[132,*], J. D. Lomas[20], J. D. Long[163], I. Longarini[160], R. Longo[163], I. Lopez Paz[67], A. Lopez Solis[48], N. Lorenzo Martinez[4], A. M. Lory[110], M. Losada[117a], G. Löschcke Centeno[147], O. Loseva[37], X. Lou[47a,47b], X. Lou[14a,14e], A. Lounis[66], P. A. Love[92], G. Lu[14a,14e], M. Lu[66], S. Lu[129], Y. J. Lu[65], H. J. Lubatti[139], C. Luci[75a,75b], F. L. Lucio Alves[14c], F. Luehring[68], I. Luise[146], O. Lukianchuk[66], O. Lundberg[145], B. Lund-Jensen[145], N. A. Luongo[6], M. S. Lutz[36], A. B. Lux[25], D. Lynn[29], R. Lysak[132], E. Lytken[99], V. Lyubushkin[38], T. Lyubushkina[38], M. M. Lyukova[146], M.Firdaus M. Soberi[52], H. Ma[29], K. Ma[62a], L. L. Ma[62b], W. Ma[62a], Y. Ma[122], J. C. MacDonald[101], P. C. Machado De Abreu Farias[83e], R. Madar[40], T. Madula[97], J. Maeda[85], T. Maeno[29], H. Maguire[140], V. Maiboroda[136], A. Maio[131a,131b,131d], K. Maj[86a], O. Majersky[48], S. Majewski[124], N. Makovec[66], V. Maksimovic[15], B. Malaescu[128], Pa. Malecki[87], V. P. Maleev[37], F. Malek[60,m], M. Mali[94], D. Malito[96], U. Mallik[80], S. Maltezos[10], S. Malyukov[38], J. Mamuzic[13], G. Mancini[53], M. N. Mancini[26], G. Manco[73a,73b], J. P. Mandalia[95], I. Mandić[94], L. Manhaes de Andrade Filho[83a], I. M. Maniatis[170], J. Manjarres Ramos[90], D. C. Mankad[170], A. Mann[110], S. Manzoni[36], L. Mao[62c], X. Mapekula[33c], A. Marantis[153,q], G. Marchiori[5], M. Marcisovsky[132], C. Marcon[71a], M. Marinescu[20], S. Marium[48], M. Marjanovic[121], A. Markhoos[54], M. Markovitch[66], E. J. Marshall[92], Z. Marshall[17a], S. Marti-Garcia[164], J. Martin[97], T. A. Martin[135], V. J. Martin[52], B. Martin dit Latour[16], L. Martinelli[75a,75b], M. Martinez[13,r], P. Martinez Agullo[164], V. I. Martinez Outschoorn[104], P. Martinez Suarez[13], S. Martin-Haugh[135], G. Martinovicova[134], V. S. Martoiu[27b], A. C. Martyniuk[97], A. Marzin[36], D. Mascione[78a,78b], L. Masetti[101], T. Mashimo[154], J. Masik[102], A. L. Maslennikov[37], P. Massarotti[72a,72b], P. Mastrandrea[74a,74b], A. Mastroberardino[43a,43b], T. Masubuchi[154], T. Mathisen[162], J. Matousek[134], N. Matsuzawa[154], J. Maurer[27b], A. J. Maury[66], B. Maček[94], D. A. Maximov[37], A. E. May[102], R. Mazini[149], I. Maznas[116], M. Mazza[108], S. M. Mazza[137], E. Mazzeo[71a,71b], C. Mc Ginn[29], J. P. Mc Gowan[166], S. P. Mc Kee[107], C. C. McCracken[165], E. F. McDonald[106], A. E. McDougall[115], J. A. Mcfayden[147], R. P. McGovern[129], R. P. Mckenzie[33g], T. C. Mclachlan[48], D. J. Mclaughlin[97], S. J. McMahon[135], C. M. Mcpartland[93], R. A. McPherson[166,v], S. Mehlhase[110], A. Mehta[93], D. Melini[164], B. R. Mellado Garcia[33g], A. H. Melo[55], F. Meloni[48], A. M. Mendes Jacques Da Costa[102], H. Y. Meng[156], L. Meng[92], S. Menke[111], M. Mentink[36], E. Meoni[43a,43b], G. Mercado[116], S. Merianos[153], C. Merlassino[69a,69c], L. Merola[72a,72b], C. Meroni[71a,71b], J. Metcalfe[6], A. S. Mete[6], E. Meuser[101], C. Meyer[68], J.-P. Meyer[136], R. P. Middleton[135], L. Mijović[52], G. Mikenberg[170],

M. Mikestikova[132], M. Mikuž[94], H. Mildner[101], A. Milic[36], D. W. Miller[39], E. H. Miller[144], L. S. Miller[34], A. Milov[170], D. A. Milstead[47a,47b], T. Min[14c], A. A. Minaenko[37], I. A. Minashvili[150b], L. Mince[59], A. I. Mincer[118], B. Mindur[86a], M. Mineev[38], Y. Mino[88], L. M. Mir[13], M. Miralles Lopez[59], M. Mironova[17a], A. Mishima[154], M. C. Missio[114], A. Mitra[168], V. A. Mitsou[164], Y. Mitsumori[112], O. Miu[156], P. S. Miyagawa[95], T. Mkrtchyan[63a], M. Mlinarevic[97], T. Mlinarevic[97], M. Mlynarikova[36], S. Mobius[19], P. Mogg[110], M. H. Mohamed Farook[113], A. F. Mohammed[14a,14e], S. Mohapatra[41], G. Mokgatitswane[33g], L. Moleri[170], B. Mondal[142], S. Mondal[133], K. Mönig[48], E. Monnier[103], L. Monsonis Romero[164], J. Montejo Berlingen[13], M. Montella[120], F. Montereali[77a,77b], F. Monticelli[91], S. Monzani[69a,69c], N. Morange[66], A. L. Moreira De Carvalho[48], M. Moreno Llácer[164], C. Moreno Martinez[56], P. Morettini[57b], S. Morgenstern[36], M. Morii[61], M. Morinaga[154], F. Morodei[75a,75b], L. Morvaj[36], P. Moschovakos[36], B. Moser[36], M. Mosidze[150b], T. Moskalets[44], P. Moskvitina[114], J. Moss[31,j], P. Moszkowicz[86a], A. Moussa[35d], E. J. W. Moyse[104], O. Mtintsilana[33g], S. Muanza[103], J. Mueller[130], D. Muenstermann[92], R. Müller[19], G. A. Mullier[162], A. J. Mullin[32], J. J. Mullin[129], D. P. Mungo[156], D. Munoz Perez[164], F. J. Munoz Sanchez[102], M. Murin[102], W. J. Murray[135,168], M. Muškinja[94], C. Mwewa[29], A. G. Myagkov[37,a], A. J. Myers[8], G. Myers[107], M. Myska[133], B. P. Nachman[17a], O. Nackenhorst[49], K. Nagai[127], K. Nagano[84], J. L. Nagle[29,af], E. Nagy[103], A. M. Nairz[36], Y. Nakahama[84], K. Nakamura[84], K. Nakkalil[5], H. Nanjo[125], E. A. Narayanan[113], I. Naryshkin[37], L. Nasella[71a,71b], M. Naseri[34], S. Nasri[117b], C. Nass[24], G. Navarro[22a], J. Navarro-Gonzalez[164], R. Nayak[152], A. Nayaz[18], P. Y. Nechaeva[37], S. Nechaeva[23a,23b], F. Nechansky[48], L. Nedic[127], T. J. Neep[20], A. Negri[73a,73b], M. Negrini[23b], C. Nellist[115], C. Nelson[105], K. Nelson[107], S. Nemecek[132], M. Nessi[36,g], M. S. Neubauer[163], F. Neuhaus[101], J. Neundorf[48], P. R. Newman[20], C. W. Ng[130], Y. W. Y. Ng[48], B. Ngair[117a], H. D. N. Nguyen[109], R. B. Nickerson[127], R. Nicolaidou[136], J. Nielsen[137], M. Niemeyer[55], J. Niermann[55], N. Nikiforou[36], V. Nikolaenko[37,a], I. Nikolic-Audit[128], K. Nikolopoulos[20], P. Nilsson[29], I. Ninca[48], G. Ninio[152], A. Nisati[75a], N. Nishu[2], R. Nisius[111], J.-E. Nitschke[50], E. K. Nkadimeng[33g], T. Nobe[154], T. Nommensen[148], M. B. Norfolk[140], B. J. Norman[34], M. Noury[35a], J. Novak[94], T. Novak[94], L. Novotny[133], R. Novotny[113], L. Nozka[123], K. Ntekas[160], N. M. J. Nunes De Moura Junior[83b], J. Ocariz[128], A. Ochi[85], I. Ochoa[131a], S. Oerdek[48,s], J. T. Offermann[39], A. Ogrodnik[134], A. Oh[102], C. C. Ohm[145], H. Oide[84], R. Oishi[154], M. L. Ojeda[48], Y. Okumura[154], L. F. Oleiro Seabra[131a], I. Oleksiyuk[56], S. A. Olivares Pino[138d], G. Oliveira Correa[13], D. Oliveira Damazio[29], D. Oliveira Goncalves[83a], J. L. Oliver[160], Ö. O. Öncel[54], A. P. O'Neill[19], A. Onofre[131a,131e], P. U. E. Onyisi[11], M. J. Oreglia[39], G. E. Orellana[91], D. Orestano[77a,77b], N. Orlando[13], R. S. Orr[156], L. M. Osojnak[129], R. Ospanov[62a], G. Otero y Garzon[30], H. Otono[89], P. S. Ott[63a], G. J. Ottino[17a], M. Ouchrif[35d], F. Ould-Saada[126], T. Ovsiannikova[139], M. Owen[59], R. E. Owen[135], V. E. Ozcan[21a], F. Ozturk[87], N. Ozturk[8], S. Ozturk[82], H. A. Pacey[127], A. Pacheco Pages[13], C. Padilla Aranda[13], G. Padovano[75a,75b], S. Pagan Griso[17a], G. Palacino[68], A. Palazzo[70a,70b], J. Pampel[24], J. Pan[173], T. Pan[64a], D. K. Panchal[11], C. E. Pandini[115], J. G. Panduro Vazquez[135], H. D. Pandya[1], H. Pang[14b], P. Pani[48], G. Panizzo[69a,69c], L. Panwar[128], L. Paolozzi[56], S. Parajuli[163], A. Paramonov[6], C. Paraskevopoulos[53], D. Paredes Hernandez[64b], A. Pareti[73a,73b], K. R. Park[41], T. H. Park[156], M. A. Parker[32], F. Parodi[57a,57b], E. W. Parrish[116], V. A. Parrish[52], J. A. Parsons[41], U. Parzefall[54], B. Pascual Dias[109], L. Pascual Dominguez[100], E. Pasqualucci[75a], S. Passaggio[57b], F. Pastore[96], P. Patel[87], U. M. Patel[51], J. R. Pater[102], T. Pauly[36], C. I. Pazos[159], J. Pearkes[144], M. Pedersen[126], R. Pedro[131a], S. V. Peleganchuk[37], O. Penc[36], E. A. Pender[52], G. D. Penn[173], K. E. Penski[110], M. Penzin[37], B. S. Peralva[83d], A. P. Pereira Peixoto[139], L. Pereira Sanchez[144], D. V. Perepelitsa[29,af], G. Perera[104], E. Perez Codina[157a], M. Perganti[10], H. Pernegger[36], S. Perrella[75a,75b], O. Perrin[40], K. Peters[48], R. F. Y. Peters[102], B. A. Petersen[36], T. C. Petersen[42], E. Petit[103], V. Petousis[133], C. Petridou[153,d], T. Petru[134], A. Petrukhin[142], M. Pettee[17a], A. Petukhov[37], K. Petukhova[134], R. Pezoa[138f], L. Pezzotti[36], G. Pezzullo[173], T. M. Pham[171], T. Pham[106], P. W. Phillips[135], G. Piacquadio[146], E. Pianori[17a], F. Piazza[124], R. Piegaia[30], D. Pietreanu[27b], A. D. Pilkington[102], M. Pinamonti[69a,69c], J. L. Pinfold[2], B. C. Pinheiro Pereira[131a], A. E. Pinto Pinoargote[136], L. Pintucci[69a,69c], K. M. Piper[147], A. Pirttikoski[56], D. A. Pizzi[34], L. Pizzimento[64b], A. Pizzini[115], M.-A. Pleier[29], V. Pleskot[134], E. Plotnikova[38], G. Poddar[95], R. Poettgen[99], L. Poggioli[128], I. Pokharel[55], S. Polacek[134], G. Polesello[73a], A. Poley[143,157a], A. Polini[23b], C. S. Pollard[168], Z. B. Pollock[120], E. Pompa Pacchi[75a,75b], N. I. Pond[97], D. Ponomarenko[114], L. Pontecorvo[36], S. Popa[27a], G. A. Popeneciu[27d], A. Poreba[36], D. M. Portillo Quintero[157a], S. Pospisil[133], M. A. Postill[140], P. Postolache[27c], K. Potamianos[168], P. A. Potepa[86a], I. N. Potrap[38], C. J. Potter[32], H. Potti[1], J. Poveda[164], M. E. Pozo Astigarraga[36],

A. Prades Ibanez[164], J. Pretel[54], D. Price[102], M. Primavera[70a], M. A. Principe Martin[100], R. Privara[123], T. Procter[59], M. L. Proffitt[139], N. Proklova[129], K. Prokofiev[64c], G. Proto[111], J. Proudfoot[6], M. Przybycien[86a], W. W. Przygoda[86b], A. Psallidas[46], J. E. Puddefoot[140], D. Pudzha[37], D. Pyatiizbyantseva[37], J. Qian[107], D. Qichen[102], Y. Qin[13], T. Qiu[52], A. Quadt[55], M. Queitsch-Maitland[102], G. Quetant[56], R. P. Quinn[165], G. Rabanal Bolanos[61], D. Rafanoharana[54], F. Raffaeli[76a,76b], F. Ragusa[71a,71b], J. L. Rainbolt[39], J. A. Raine[56], S. Rajagopalan[29], E. Ramakoti[37], I. A. Ramirez-Berend[34], K. Ran[48,14e], N. P. Rapheeha[33g], H. Rasheed[27b], V. Raskina[128], D. F. Rassloff[63a], A. Rastogi[17a], S. Rave[101], S. Ravera[57a,57b], B. Ravina[55], I. Ravinovich[170], M. Raymond[36], A. L. Read[126], N. P. Readioff[140], D. M. Rebuzzi[73a,73b], G. Redlinger[29], A. S. Reed[111], K. Reeves[26], J. A. Reidelsturz[172], D. Reikher[152], A. Rej[49], C. Rembser[36], M. Renda[27b], M. B. Rendel[111], F. Renner[48], A. G. Rennie[160], A. L. Rescia[48], S. Resconi[71a], M. Ressegotti[57a,57b], S. Rettie[36], J. G. Reyes Rivera[108], E. Reynolds[17a], O. L. Rezanova[37], P. Reznicek[134], H. Riani[35d], N. Ribaric[92], E. Ricci[78a,78b], R. Richter[111], S. Richter[47a,47b], E. Richter-Was[86b], M. Ridel[128], S. Ridouani[35d], P. Rieck[118], P. Riedler[36], E. M. Riefel[47a,47b], J. O. Rieger[115], M. Rijssenbeek[146], M. Rimoldi[36], L. Rinaldi[23a,23b], T. T. Rinn[29], M. P. Rinnagel[110], G. Ripellino[162], I. Riu[13], J. C. Rivera Vergara[166], F. Rizatdinova[122], E. Rizvi[95], B. R. Roberts[17a], S. H. Robertson[105,v], D. Robinson[32], C. M. Robles Gajardo[138f], M. Robles Manzano[101], A. Robson[59], A. Rocchi[76a,76b], C. Roda[74a,74b], S. Rodriguez Bosca[36], Y. Rodriguez Garcia[22a], A. Rodriguez Rodriguez[54], A. M. Rodríguez Vera[116], S. Roe[36], J. T. Roemer[160], A. R. Roepe-Gier[137], J. Roggel[172], O. Røhne[126], R. A. Rojas[104], C. P. A. Roland[128], J. Roloff[29], A. Romaniouk[37], E. Romano[73a,73b], M. Romano[23b], A. C. Romero Hernandez[163], N. Rompotis[93], L. Roos[128], S. Rosati[75a], B. J. Rosser[39], E. Rossi[127], E. Rossi[72a,72b], L. P. Rossi[61], L. Rossini[54], R. Rosten[120], M. Rotaru[27b], B. Rottler[54], C. Rougier[90], D. Rousseau[66], D. Rousso[48], A. Roy[163], S. Roy-Garand[156], A. Rozanov[103], Z. M. A. Rozario[59], Y. Rozen[151], A. Rubio Jimenez[164], A. J. Ruby[93], V. H. Ruelas Rivera[18], T. A. Ruggeri[1], A. Ruggiero[127], A. Ruiz-Martinez[164], A. Rummler[36], Z. Rurikova[54], N. A. Rusakovich[38], H. L. Russell[166], G. Russo[75a,75b], J. P. Rutherfoord[7], S. Rutherford Colmenares[32], M. Rybar[134], E. B. Rye[126], A. Ryzhov[44], J. A. Sabater Iglesias[56], P. Sabatini[164], H. F.-W. Sadrozinski[137], F. Safai Tehrani[75a], B. Safarzadeh Samani[135], S. Saha[1], M. Sahinsoy[111], A. Saibel[164], M. Saimpert[136], M. Saito[154], T. Saito[154], A. Sala[71a,71b], D. Salamani[36], A. Salnikov[144], J. Salt[164], A. Salvador Salas[152], D. Salvatore[43a,43b], F. Salvatore[147], A. Salzburger[36], D. Sammel[54], E. Sampson[92], D. Sampsonidis[153,d], D. Sampsonidou[124], J. Sánchez[164], V. Sanchez Sebastian[164], H. Sandaker[126], C. O. Sander[48], J. A. Sandesara[104], M. Sandhoff[172], C. Sandoval[22b], L. Sanfilippo[63a], D. P. C. Sankey[135], T. Sano[88], A. Sansoni[53], L. Santi[36,75b], C. Santoni[40], H. Santos[131a,131b], A. Santra[170], E. Sanzani[23a,23b], K. A. Saoucha[161], J. G. Saraiva[131a,131d], J. Sardain[7], O. Sasaki[84], K. Sato[158], C. Sauer[63b], E. Sauvan[4], P. Savard[156,ad], R. Sawada[154], C. Sawyer[135], L. Sawyer[98], C. Sbarra[23b], A. Sbrizzi[23a,23b], T. Scanlon[97], J. Schaarschmidt[139], U. Schäfer[101], A. C. Schaffer[44,66], D. Schaile[110], R. D. Schamberger[146], C. Scharf[18], M. M. Schefer[19], V. A. Schegelsky[37], D. Scheirich[134], M. Schernau[160], C. Scheulen[55], C. Schiavi[57a,57b], M. Schioppa[43a,43b], B. Schlag[144,l], K. E. Schleicher[54], S. Schlenker[36], J. Schmeing[172], M. A. Schmidt[172], K. Schmieden[101], C. Schmitt[101], N. Schmitt[101], S. Schmitt[48], L. Schoeffel[136], A. Schoening[63b], P. G. Scholer[34], E. Schopf[127], M. Schott[24], J. Schovancova[36], S. Schramm[56], T. Schroer[56], H.-C. Schultz-Coulon[63a], M. Schumacher[54], B. A. Schumm[137], Ph. Schune[136], A. J. Schuy[139], H. R. Schwartz[137], A. Schwartzman[144], T. A. Schwarz[107], Ph. Schwemling[136], R. Schwienhorst[108], A. Sciandra[29], G. Sciolla[26], F. Scuri[74a], C. D. Sebastiani[93], K. Sedlaczek[116], S. C. Seidel[113], A. Seiden[137], B. D. Seidlitz[41], C. Seitz[48], J. M. Seixas[83b], G. Sekhniaidze[72a], L. Selem[60], N. Semprini-Cesari[23a,23b], D. Sengupta[56], V. Senthilkumar[164], L. Serin[66], M. Sessa[76a,76b], H. Severini[121], F. Sforza[57a,57b], A. Sfyrla[56], Q. Sha[14a], E. Shabalina[55], A. H. Shah[32], R. Shaheen[145], J. D. Shahinian[129], D. Shaked Renous[170], L. Y. Shan[14a], M. Shapiro[17a], A. Sharma[36], A. S. Sharma[165], P. Sharma[80], P. B. Shatalov[37], K. Shaw[147], S. M. Shaw[102], Q. Shen[62c,5], D. J. Sheppard[143], P. Sherwood[97], L. Shi[97], X. Shi[14a], C. O. Shimmin[173], J. D. Shinner[96], I. P. J. Shipsey[127], S. Shirabe[89], M. Shiyakova[38,t], M. J. Shochet[39], J. Shojaii[106], D. R. Shope[126], B. Shrestha[121], S. Shrestha[120,ag], M. J. Shroff[166], P. Sicho[132], A. M. Sickles[163], E. Sideras Haddad[33g], A. C. Sidley[115], A. Sidoti[23b], F. Siegert[50], Dj. Sijacki[15], F. Sili[91], J. M. Silva[52], I. Silva Ferreira[83b], M. V. Silva Oliveira[29], S. B. Silverstein[47a], S. Simion[66], R. Simoniello[36], E. L. Simpson[102], H. Simpson[147], L. R. Simpson[107], N. D. Simpson[99], S. Simsek[82], S. Sindhu[55], P. Sinervo[156], S. Singh[156], S. Sinha[48], S. Sinha[102], M. Sioli[23a,23b], I. Siral[36], E. Sitnikova[48], J. Sjölin[47a,47b], A. Skaf[55], E. Skorda[20], P. Skubic[121], M. Slawinska[87], V. Smakhtin[170], B. H. Smart[135], S.Yu. Smirnov[37], Y. Smirnov[37], L. N. Smirnova[37,a], O. Smirnova[99], A. C. Smith[41], D. R. Smith[160], E. A. Smith[39], H. A. Smith[127],

J. L. Smith[102], R. Smith[144], M. Smizanska[92], K. Smolek[133], A. A. Snesarev[37], S. R. Snider[156], H. L. Snoek[115], S. Snyder[29], R. Sobie[166,v], A. Soffer[152], C. A. Solans Sanchez[36], E.Yu. Soldatov[37], U. Soldevila[164], A. A. Solodkov[37], S. Solomon[26], A. Soloshenko[38], K. Solovieva[54], O. V. Solovyanov[40], P. Sommer[36], A. Sonay[13], W. Y. Song[157b], A. Sopczak[133], A. L. Sopio[97], F. Sopkova[28b], J. D. Sorenson[113], I. R. Sotarriva Alvarez[155], V. Sothilingam[63a], O. J. Soto Sandoval[138b,138c], S. Sottocornola[68], R. Soualah[161], Z. Soumaimi[35e], D. South[48], N. Soybelman[170], S. Spagnolo[70a,70b], M. Spalla[111], D. Sperlich[54], G. Spigo[36], S. Spinali[92], D. P. Spiteri[59], M. Spousta[134], E. J. Staats[34], R. Stamen[63a], A. Stampekis[20], M. Standke[24], E. Stanecka[87], W. Stanek-Maslouska[48], M. V. Stange[50], B. Stanislaus[17a], M. M. Stanitzki[48], B. Stapf[48], E. A. Starchenko[37], G. H. Stark[137], J. Stark[90], P. Staroba[132], P. Starovoitov[63a], S. Stärz[105], R. Staszewski[87], G. Stavropoulos[46], J. Steentoft[162], P. Steinberg[29], B. Stelzer[143,157a], H. J. Stelzer[130], O. Stelzer-Chilton[157a], H. Stenzel[58], T. J. Stevenson[147], G. A. Stewart[36], J. R. Stewart[122], M. C. Stockton[36], G. Stoicea[27b], M. Stolarski[131a], S. Stonjek[111], A. Straessner[50], J. Strandberg[145], S. Strandberg[47a,47b], M. Stratmann[172], M. Strauss[121], T. Strebler[103], P. Strizenec[28b], R. Ströhmer[167], D. M. Strom[124], R. Stroynowski[44], A. Strubig[47a,47b], S. A. Stucci[29], B. Stugu[16], J. Stupak[121], N. A. Styles[48], D. Su[144], S. Su[62a], W. Su[62d], X. Su[62a], D. Suchy[28a], K. Sugizaki[154], V. V. Sulin[37], M. J. Sullivan[93], D. M. S. Sultan[127], L. Sultanaliyeva[37], S. Sultansoy[3b], T. Sumida[88], S. Sun[171], O. Sunneborn Gudnadottir[162], N. Sur[103], M. R. Sutton[147], H. Suzuki[158], M. Svatos[132], M. Swiatlowski[157a], T. Swirski[167], I. Sykora[28a], M. Sykora[134], T. Sykora[134], D. Ta[101], K. Tackmann[48,s], A. Taffard[160], R. Tafirout[157a], J. S. Tafoya Vargas[66], Y. Takubo[84], M. Talby[103], A. A. Talyshev[37], K. C. Tam[64b], N. M. Tamir[152], A. Tanaka[154], J. Tanaka[154], R. Tanaka[66], M. Tanasini[146], Z. Tao[165], S. Tapia Araya[138f], S. Tapprogge[101], A. Tarek Abouelfadl Mohamed[108], S. Tarem[151], K. Tariq[14a], G. Tarna[27b], G. F. Tartarelli[71a], M. J. Tartarin[90], P. Tas[134], M. Tasevsky[132], E. Tassi[43a,43b], A. C. Tate[163], G. Tateno[154], Y. Tayalati[35e,u], G. N. Taylor[106], W. Taylor[157b], R. Teixeira De Lima[144], P. Teixeira-Dias[96], J. J. Teoh[156], K. Terashi[154], J. Terron[100], S. Terzo[13], M. Testa[53], R. J. Teuscher[156,v], A. Thaler[79], O. Theiner[56], N. Themistokleous[52], T. Theveneaux-Pelzer[103], O. Thielmann[172], D. W. Thomas[96], J. P. Thomas[20], E. A. Thompson[17a], P. D. Thompson[20], E. Thomson[129], R. E. Thornberry[44], C. Tian[62a], Y. Tian[55], V. Tikhomirov[37,a], Yu.A. Tikhonov[37], S. Timoshenko[37], D. Timoshyn[134], E. X. L. Ting[1], P. Tipton[173], A. Tishelman-Charny[29], S. H. Tlou[33g], K. Todome[155], S. Todorova-Nova[134], S. Todt[50], L. Toffolin[69a,69c], M. Togawa[84], J. Tojo[89], S. Tokár[28a], K. Tokushuku[84], O. Toldaiev[68], R. Tombs[32], M. Tomoto[84,112], L. Tompkins[144,l], K. W. Topolnicki[86b], E. Torrence[124], H. Torres[90], E. Torró Pastor[164], M. Toscani[30], C. Tosciri[39], M. Tost[11], D. R. Tovey[140], I. S. Trandafir[27b], T. Trefzger[167], A. Tricoli[29], I. M. Trigger[157a], S. Trincaz-Duvoid[128], D. A. Trischuk[26], B. Trocmé[60], L. Truong[33c], M. Trzebinski[87], A. Trzupek[87], F. Tsai[146], M. Tsai[107], A. Tsiamis[153,d], P. V. Tsiareshka[37], S. Tsigaridas[157a], A. Tsirigotis[153,q], V. Tsiskaridze[156], E. G. Tskhadadze[150a], M. Tsopoulou[153], Y. Tsujikawa[88], I. I. Tsukerman[37], V. Tsulaia[17a], S. Tsuno[84], K. Tsuri[119], D. Tsybychev[146], Y. Tu[64b], A. Tudorache[27b], V. Tudorache[27b], A. N. Tuna[61], S. Turchikhin[57a,57b], I. Turk Cakir[3a], R. Turra[71a], T. Turtuvshin[38,w], P. M. Tuts[41], S. Tzamarias[153,d], E. Tzovara[101], F. Ukegawa[158], P. A. Ulloa Poblete[138b,138c], E. N. Umaka[29], G. Unal[36], A. Undrus[29], G. Unel[160], J. Urban[28b], P. Urrejola[138a], G. Usai[8], R. Ushioda[155], M. Usman[109], Z. Uysal[82], V. Vacek[133], B. Vachon[105], T. Vafeiadis[36], A. Vaitkus[97], C. Valderanis[110], E. Valdes Santurio[47a,47b], M. Valente[157a], S. Valentinetti[23a,23b], A. Valero[164], E. Valiente Moreno[164], A. Vallier[90], J. A. Valls Ferrer[164], D. R. Van Arneman[115], T. R. Van Daalen[139], A. Van Der Graaf[49], P. Van Gemmeren[6], M. Van Rijnbach[36], S. Van Stroud[97], I. Van Vulpen[115], P. Vana[134], M. Vanadia[76a,76b], W. Vandelli[36], E. R. Vandewall[122], D. Vannicola[152], L. Vannoli[53], R. Vari[75a], E. W. Varnes[7], C. Varni[17b], T. Varol[149], D. Varouchas[66], L. Varriale[164], K. E. Varvell[148], M. E. Vasile[27b], L. Vaslin[84], G. A. Vasquez[166], A. Vasyukov[38], L. M. Vaughan[122], R. Vavricka[101], T. Vazquez Schroeder[36], J. Veatch[31], V. Vecchio[102], M. J. Veen[104], I. Veliscek[29], L. M. Veloce[156], F. Veloso[131a,131c], S. Veneziano[75a], A. Ventura[70a,70b], S. Ventura Gonzalez[136], A. Verbytskyi[111], M. Verducci[74a,74b], C. Vergis[95], M. Verissimo De Araujo[83b], W. Verkerke[115], J. C. Vermeulen[115], C. Vernieri[144], M. Vessella[104], M. C. Vetterli[143,ad], A. Vgenopoulos[153,d], N. Viaux Maira[138f], T. Vickey[140], O. E. Vickey Boeriu[140], G. H. A. Viehhauser[127], L. Vigani[63b], M. Villa[23a,23b], M. Villaplana Perez[164], E. M. Villhauer[52], E. Vilucchi[53], M. G. Vincter[34], A. Visibile[115], C. Vittori[36], I. Vivarelli[23a,23b], E. Voevodina[111], F. Vogel[110], J. C. Voigt[50], P. Vokac[133], Yu. Volkotrub[86b], J. Von Ahnen[48], E. Von Toerne[24], B. Vormwald[36], V. Vorobel[134], K. Vorobev[37], M. Vos[164], K. Voss[142], M. Vozak[115], L. Vozdecky[121], N. Vranjes[15], M. Vranjes Milosavljevic[15], M. Vreeswijk[115], N. K. Vu[62c,62d], R. Vuillermet[36], O. Vujinovic[101], I. Vukotic[39], S. Wada[158], C. Wagner[104], J. M. Wagner[17a], W. Wagner[172],

S. Wahdan[172], H. Wahlberg[91], M. Wakida[112], J. Walder[135], R. Walker[110], W. Walkowiak[142], A. Wall[129], E. J. Wallin[99], T. Wamorkar[6], A. Z. Wang[137], C. Wang[101], C. Wang[11], H. Wang[17a], J. Wang[64c], P. Wang[97], R. Wang[61], R. Wang[6], S. M. Wang[149], S. Wang[62b], S. Wang[14a], T. Wang[62a], W. T. Wang[80], W. Wang[14a], X. Wang[14c], X. Wang[163], X. Wang[62c], Y. Wang[62d], Y. Wang[14c], Z. Wang[107], Z. Wang[51,62c,62d], Z. Wang[107], A. Warburton[105], R. J. Ward[20], N. Warrack[59], S. Waterhouse[96], A. T. Watson[20], H. Watson[59], M. F. Watson[20], E. Watton[59,135], G. Watts[139], B. M. Waugh[97], J. M. Webb[54], C. Weber[29], H. A. Weber[18], M. S. Weber[19], S. M. Weber[63a], C. Wei[62a], Y. Wei[54], A. R. Weidberg[127], E. J. Weik[118], J. Weingarten[49], C. Weiser[54], C. J. Wells[48], T. Wenaus[29], B. Wendland[49], T. Wengler[36], N. S. Wenke[111], N. Wermes[24], M. Wessels[63a], A. M. Wharton[92], A. S. White[61], A. White[8], M. J. White[1], D. Whiteson[160], L. Wickremasinghe[125], W. Wiedenmann[171], M. Wielers[135], C. Wiglesworth[42], D. J. Wilbern[121], H. G. Wilkens[36], J. J. H. Wilkinson[32], D. M. Williams[41], H. H. Williams[129], S. Williams[32], S. Willocq[104], B. J. Wilson[102], P. J. Windischhofer[39], F. I. Winkel[30], F. Winklmeier[124], B. T. Winter[54], J. K. Winter[102], M. Wittgen[144], M. Wobisch[98], T. Wojtkowski[60], Z. Wolffs[115], J. Wollrath[160], M. W. Wolter[87], H. Wolters[131a,131c], M. C. Wong[137], E. L. Woodward[41], S. D. Worm[48], B. K. Wosiek[87], K. W. Woźniak[87], S. Wozniewski[55], K. Wraight[59], C. Wu[20], M. Wu[14d], M. Wu[114], S. L. Wu[171], X. Wu[56], Y. Wu[62a], Z. Wu[4], J. Wuerzinger[111,ab], T. R. Wyatt[102], B. M. Wynne[52], S. Xella[42], L. Xia[14c], M. Xia[14b], J. Xiang[64c], M. Xie[62a], S. Xin[14a,14e], A. Xiong[124], J. Xiong[17a], D. Xu[14a], H. Xu[62a], L. Xu[62a], R. Xu[129], T. Xu[107], Y. Xu[14b], Z. Xu[52], Z. Xu[14c], B. Yabsley[148], S. Yacoob[33a], Y. Yamaguchi[155], E. Yamashita[154], H. Yamauchi[158], T. Yamazaki[17a], Y. Yamazaki[85], J. Yan[62c], S. Yan[59], Z. Yan[104], H. J. Yang[62c,62d], H. T. Yang[62a], S. Yang[62a], T. Yang[64c], X. Yang[36], X. Yang[14a], Y. Yang[44], Y. Yang[62a], Z. Yang[62a], W.-M. Yao[17a], H. Ye[14c], H. Ye[55], J. Ye[14a], S. Ye[29], X. Ye[62a], Y. Yeh[97], I. Yeletskikh[38], B. Yeo[17b], M. R. Yexley[97], T. P. Yildirim[127], P. Yin[41], K. Yorita[169], S. Younas[27b], C. J. S. Young[36], C. Young[144], C. Yu[14a,14e], Y. Yu[62a], M. Yuan[107], R. Yuan[62c,62d], L. Yue[97], M. Zaazoua[62a], B. Zabinski[87], E. Zaid[52], Z. K. Zak[87], T. Zakareishvili[164], N. Zakharchuk[34], S. Zambito[56], J. A. Zamora Saa[138b,138d], J. Zang[154], D. Zanzi[54], O. Zaplatilek[133], C. Zeitnitz[172], H. Zeng[14a], J. C. Zeng[163], D. T. Zenger Jr[26], O. Zenin[37], T. Ženiš[28a], S. Zenz[95], S. Zerradi[35a], D. Zerwas[66], M. Zhai[14a,14e], D. F. Zhang[140], J. Zhang[62b], J. Zhang[6], K. Zhang[14a,14e], L. Zhang[62a], L. Zhang[14c], P. Zhang[14a,14e], R. Zhang[171], S. Zhang[107], S. Zhang[90], T. Zhang[154], X. Zhang[62c], X. Zhang[62b], Y. Zhang[62c], Y. Zhang[97], Y. Zhang[14c], Z. Zhang[17a], Z. Zhang[62b], Z. Zhang[66], H. Zhao[139], T. Zhao[62b], Y. Zhao[137], Z. Zhao[62a], Z. Zhao[62a], A. Zhemchugov[38], J. Zheng[14c], K. Zheng[163], X. Zheng[62a], Z. Zheng[144], D. Zhong[163], B. Zhou[107], H. Zhou[7], N. Zhou[62c], Y. Zhou[14b], Y. Zhou[14c], Y. Zhou[7], C. G. Zhu[62b], J. Zhu[107], X. Zhu[62d], Y. Zhu[62c], Y. Zhu[62a], X. Zhuang[14a], K. Zhukov[37], N. I. Zimine[38], J. Zinsser[63b], M. Ziolkowski[142], L. Živković[15], A. Zoccoli[23a,23b], K. Zoch[61], T. G. Zorbas[140], O. Zormpa[46], W. Zou[41], L. Zwalinski[36]

[1] Department of Physics, University of Adelaide, Adelaide, Australia
[2] Department of Physics, University of Alberta, Edmonton, AB, Canada
[3] [(a)]Department of Physics, Ankara University, Ankara, Türkiye; [(b)]Division of Physics, TOBB University of Economics and Technology, Ankara, Türkiye
[4] LAPP, Université Savoie Mont Blanc, CNRS/IN2P3, Annecy, France
[5] APC, Université Paris Cité, CNRS/IN2P3, Paris, France
[6] High Energy Physics Division, Argonne National Laboratory, Argonne, IL, USA
[7] Department of Physics, University of Arizona, Tucson, AZ, USA
[8] Department of Physics, University of Texas at Arlington, Arlington, TX, USA
[9] Physics Department, National and Kapodistrian University of Athens, Athens, Greece
[10] Physics Department, National Technical University of Athens, Zografou, Greece
[11] Department of Physics, University of Texas at Austin, Austin, TX, USA
[12] Institute of Physics, Azerbaijan Academy of Sciences, Baku, Azerbaijan
[13] Institut de Física d'Altes Energies (IFAE), Barcelona Institute of Science and Technology, Barcelona, Spain
[14] [(a)]Institute of High Energy Physics, Chinese Academy of Sciences, Beijing, China; [(b)]Physics Department, Tsinghua University, Beijing, China; [(c)]Department of Physics, Nanjing University, Nanjing, China; [(d)]School of Science, Shenzhen Campus of Sun Yat-sen University, Shenzhen, China; [(e)]University of Chinese Academy of Science (UCAS), Beijing, China
[15] Institute of Physics, University of Belgrade, Belgrade, Serbia

[16] Department for Physics and Technology, University of Bergen, Bergen, Norway
[17] [(a)]Physics Division, Lawrence Berkeley National Laboratory, Berkeley, CA, USA; [(b)]University of California, Berkeley, CA, USA
[18] Institut für Physik, Humboldt Universität zu Berlin, Berlin, Germany
[19] Albert Einstein Center for Fundamental Physics and Laboratory for High Energy Physics, University of Bern, Bern, Switzerland
[20] School of Physics and Astronomy, University of Birmingham, Birmingham, UK
[21] [(a)]Department of Physics, Bogazici University, Istanbul, Türkiye; [(b)]Department of Physics Engineering, Gaziantep University, Gaziantep, Türkiye; [(c)]Department of Physics, Istanbul University, Istanbul, Türkiye
[22] [(a)]Facultad de Ciencias y Centro de Investigaciónes, Universidad Antonio Nariño, Bogotá, Colombia; [(b)]Departamento de Física, Universidad Nacional de Colombia, Bogotá, Colombia
[23] [(a)]Dipartimento di Fisica e Astronomia A. Righi, Università di Bologna, Bologna, Italy; [(b)]INFN Sezione di Bologna, Bologna, Italy
[24] Physikalisches Institut, Universität Bonn, Bonn, Germany
[25] Department of Physics, Boston University, Boston, MA, USA
[26] Department of Physics, Brandeis University, Waltham, MA, USA
[27] [(a)]Transilvania University of Brasov, Brasov, Romania; [(b)]Horia Hulubei National Institute of Physics and Nuclear Engineering, Bucharest, Romania; [(c)]Department of Physics, Alexandru Ioan Cuza University of Iasi, Iasi, Romania; [(d)]Physics Department, National Institute for Research and Development of Isotopic and Molecular Technologies, Cluj-Napoca, Romania; [(e)]National University of Science and Technology Politechnica, Bucharest, Romania; [(f)]West University in Timisoara, Timisoara, Romania; [(g)]Faculty of Physics, University of Bucharest, Bucharest, Romania
[28] [(a)]Faculty of Mathematics, Physics and Informatics, Comenius University, Bratislava, Slovakia; [(b)]Department of Subnuclear Physics, Institute of Experimental Physics of the Slovak Academy of Sciences, Kosice, Slovak Republic
[29] Physics Department, Brookhaven National Laboratory, Upton, NY, USA
[30] Universidad de Buenos Aires, Facultad de Ciencias Exactas y Naturales, Departamento de Física, y CONICET, Instituto de Física de Buenos Aires (IFIBA), Buenos Aires, Argentina
[31] California State University, CA, USA
[32] Cavendish Laboratory, University of Cambridge, Cambridge, UK
[33] [(a)]Department of Physics, University of Cape Town, Cape Town, South Africa; [(b)]iThemba Labs, Western Cape, South Africa; [(c)]Department of Mechanical Engineering Science, University of Johannesburg, Johannesburg, South Africa; [(d)]National Institute of Physics, University of the Philippines Diliman (Philippines), Quezon City, Philippines; [(e)]Department of Physics, University of South Africa, Pretoria, South Africa; [(f)]University of Zululand, KwaDlangezwa, South Africa; [(g)]School of Physics, University of the Witwatersrand, Johannesburg, South Africa
[34] Department of Physics, Carleton University, Ottawa, ON, Canada
[35] [(a)]Faculté des Sciences Ain Chock, Université Hassan II de Casablanca, Morocco; [(b)]Faculté des Sciences, Université Ibn-Tofail, Kénitra, Morocco; [(c)]Faculté des Sciences Semlalia, Université Cadi Ayyad, LPHEA-Marrakech, Marrakech, Morocco; [(d)]LPMR, Faculté des Sciences, Université Mohamed Premier, Oujda, Morocco; [(e)]Faculté des sciences, Université Mohammed V, Rabat, Morocco; [(f)]Institute of Applied Physics, Mohammed VI Polytechnic University, Ben Guerir, Morocco
[36] CERN, Geneva, Switzerland
[37] Affiliated with an institute covered by a cooperation agreement with CERN, Geneva, Switzerland
[38] Affiliated with an international laboratory covered by a cooperation agreement with CERN, Geneva, Switzerland
[39] Enrico Fermi Institute, University of Chicago, Chicago, IL, USA
[40] LPC, Université Clermont Auvergne, CNRS/IN2P3, Clermont-Ferrand, France
[41] Nevis Laboratory, Columbia University, Irvington, NY, USA
[42] Niels Bohr Institute, University of Copenhagen, Copenhagen, Denmark
[43] [(a)]Dipartimento di Fisica, Università della Calabria, Rende, Italy; [(b)]INFN Gruppo Collegato di Cosenza, Laboratori Nazionali di Frascati, Frascati, Italy
[44] Physics Department, Southern Methodist University, Dallas, TX, USA
[45] Physics Department, University of Texas at Dallas, Richardson, TX, USA
[46] National Centre for Scientific Research "Demokritos", Agia Paraskevi, Greece
[47] [(a)]Department of Physics, Stockholm University, Stockholm, Sweden; [(b)]Oskar Klein Centre, Stockholm, Sweden

[48] Deutsches Elektronen-Synchrotron DESY, Hamburg and Zeuthen, Germany
[49] Fakultät Physik, Technische Universität Dortmund, Dortmund, Germany
[50] Institut für Kern- und Teilchenphysik, Technische Universität Dresden, Dresden, Germany
[51] Department of Physics, Duke University, Durham, NC, USA
[52] SUPA - School of Physics and Astronomy, University of Edinburgh, Edinburgh, UK
[53] INFN e Laboratori Nazionali di Frascati, Frascati, Italy
[54] Physikalisches Institut, Albert-Ludwigs-Universität Freiburg, Freiburg, Germany
[55] II. Physikalisches Institut, Georg-August-Universität Göttingen, Göttingen, Germany
[56] Département de Physique Nucléaire et Corpusculaire, Université de Genève, Genève, Switzerland
[57] [(a)]Dipartimento di Fisica, Università di Genova, Genoa, Italy; [(b)]INFN Sezione di Genova, Genoa, Italy
[58] II. Physikalisches Institut, Justus-Liebig-Universität Giessen, Giessen, Germany
[59] SUPA-School of Physics and Astronomy, University of Glasgow, Glasgow, UK
[60] LPSC, Université Grenoble Alpes, CNRS/IN2P3, Grenoble INP, Grenoble, France
[61] Laboratory for Particle Physics and Cosmology, Harvard University, Cambridge, MA, USA
[62] [(a)]Department of Modern Physics and State Key Laboratory of Particle Detection and Electronics, University of Science and Technology of China, Hefei, China; [(b)]Institute of Frontier and Interdisciplinary Science and Key Laboratory of Particle Physics and Particle Irradiation (MOE), Shandong University, Qingdao, China; [(c)]School of Physics and Astronomy, Shanghai Jiao Tong University, Key Laboratory for Particle Astrophysics and Cosmology (MOE), SKLPPC, Shanghai, China; [(d)]Tsung-Dao Lee Institute, Shanghai, China; [(e)]School of Physics and Microelectronics, Zhengzhou University, China
[63] [(a)]Kirchhoff-Institut für Physik, Ruprecht-Karls-Universität Heidelberg, Heidelberg, Germany; [(b)]Physikalisches Institut, Ruprecht-Karls-Universität Heidelberg, Heidelberg, Germany
[64] [(a)]Department of Physics, Chinese University of Hong Kong, Shatin, NT, Hong Kong; [(b)]Department of Physics, University of Hong Kong, Hong Kong, China; [(c)]Department of Physics and Institute for Advanced Study, Hong Kong University of Science and Technology, Clear Water Bay, Kowloon, Hong Kong, China
[65] Department of Physics, National Tsing Hua University, Hsinchu, Taiwan
[66] IJCLab, Université Paris-Saclay, CNRS/IN2P3, 91405, Orsay, France
[67] Centro Nacional de Microelectrónica (IMB-CNM-CSIC), Barcelona, Spain
[68] Department of Physics, Indiana University, Bloomington, IN, USA
[69] [(a)]INFN Gruppo Collegato di Udine, Sezione di Trieste, Udine, Italy; [(b)]ICTP, Trieste, Italy; [(c)]Dipartimento Politecnico di Ingegneria e Architettura, Università di Udine, Udine, Italy
[70] [(a)]INFN Sezione di Lecce, Lecce, Italy; [(b)]Dipartimento di Matematica e Fisica, Università del Salento, Lecce, Italy
[71] [(a)]INFN Sezione di Milano, Milan, Italy; [(b)]Dipartimento di Fisica, Università di Milano, Milan, Italy
[72] [(a)]INFN Sezione di Napoli, Naples, Italy; [(b)]Dipartimento di Fisica, Università di Napoli, Napoli, Italy
[73] [(a)]INFN Sezione di Pavia, Pavia, Italy; [(b)]Dipartimento di Fisica, Università di Pavia, Pavia, Italy
[74] [(a)]INFN Sezione di Pisa, Pisa, Italy; [(b)]Dipartimento di Fisica E. Fermi, Università di Pisa, Pisa, Italy
[75] [(a)]INFN Sezione di Roma, Rome, Italy; [(b)]Dipartimento di Fisica, Sapienza Università di Roma, Rome, Italy
[76] [(a)]INFN Sezione di Roma Tor Vergata, Rome, Italy; [(b)]Dipartimento di Fisica, Università di Roma Tor Vergata, Rome, Italy
[77] [(a)]INFN Sezione di Roma Tre, Rome, Italy; [(b)]Dipartimento di Matematica e Fisica, Università Roma Tre, Rome, Italy
[78] [(a)]INFN-TIFPA, Povo, Italy; [(b)]Università degli Studi di Trento, Trento, Italy
[79] Universität Innsbruck, Department of Astro and Particle Physics, Innsbruck, Austria
[80] University of Iowa, Iowa City, IA, USA
[81] Department of Physics and Astronomy, Iowa State University, Ames, IA, USA
[82] Istinye University, Sariyer, Istanbul, Türkiye
[83] [(a)]Departamento de Engenharia Elétrica, Universidade Federal de Juiz de Fora (UFJF), Juiz de Fora, Brazil; [(b)]Universidade Federal do Rio De Janeiro COPPE/EE/IF, Rio de Janeiro, Brazil; [(c)]Instituto de Física, Universidade de São Paulo, São Paulo, Brazil; [(d)]Rio de Janeiro State University, Rio de Janeiro, Brazil; [(e)]Federal University of Bahia, Bahia, Brazil
[84] KEK, High Energy Accelerator Research Organization, Tsukuba, Japan
[85] Graduate School of Science, Kobe University, Kobe, Japan
[86] [(a)]AGH University of Krakow, Faculty of Physics and Applied Computer Science, Krakow, Poland; [(b)]Marian Smoluchowski Institute of Physics, Jagiellonian University, Krakow, Poland

[87] Institute of Nuclear Physics Polish Academy of Sciences, Krakow, Poland
[88] Faculty of Science, Kyoto University, Kyoto, Japan
[89] Research Center for Advanced Particle Physics and Department of Physics, Kyushu University, Fukuoka , Japan
[90] L2IT, Université de Toulouse, CNRS/IN2P3, UPS, Toulouse, France
[91] Instituto de Física La Plata, Universidad Nacional de La Plata and CONICET, La Plata, Argentina
[92] Physics Department, Lancaster University, Lancaster, UK
[93] Oliver Lodge Laboratory, University of Liverpool, Liverpool, UK
[94] Department of Experimental Particle Physics, Jožef Stefan Institute and Department of Physics, University of Ljubljana, Ljubljana, Slovenia
[95] School of Physics and Astronomy, Queen Mary University of London, London, UK
[96] Department of Physics, Royal Holloway University of London, Egham, UK
[97] Department of Physics and Astronomy, University College London, London, UK
[98] Louisiana Tech University, Ruston, LA, USA
[99] Fysiska institutionen, Lunds universitet, Lund, Sweden
[100] Departamento de Física Teorica C-15 and CIAFF, Universidad Autónoma de Madrid, Madrid, Spain
[101] Institut für Physik, Universität Mainz, Mainz, Germany
[102] School of Physics and Astronomy, University of Manchester, Manchester, UK
[103] CPPM, Aix-Marseille Université, CNRS/IN2P3, Marseille, France
[104] Department of Physics, University of Massachusetts, Amherst, MA, USA
[105] Department of Physics, McGill University, Montreal, QC, Canada
[106] School of Physics, University of Melbourne, Victoria, Australia
[107] Department of Physics, University of Michigan, Ann Arbor, MI, USA
[108] Department of Physics and Astronomy, Michigan State University, East Lansing, MI, USA
[109] Group of Particle Physics, University of Montreal, Montreal, QC, Canada
[110] Fakultät für Physik, Ludwig-Maximilians-Universität München, München, Germany
[111] Max-Planck-Institut für Physik (Werner-Heisenberg-Institut), München, Germany
[112] Graduate School of Science and Kobayashi-Maskawa Institute, Nagoya University, Nagoya, Japan
[113] Department of Physics and Astronomy, University of New Mexico, Albuquerque, NM, USA
[114] Institute for Mathematics, Astrophysics and Particle Physics, Radboud University/Nikhef, Nijmegen, Netherlands
[115] Nikhef National Institute for Subatomic Physics and University of Amsterdam, Amsterdam, Netherlands
[116] Department of Physics, Northern Illinois University, DeKalb, IL, USA
[117] [(a)]New York University Abu Dhabi, Abu Dhabi, United Arab Emirates; [(b)]United Arab Emirates University, Al Ain, United Arab Emirates
[118] Department of Physics, New York University, New York, NY, USA
[119] Ochanomizu University, Otsuka, Bunkyo-ku, Tokyo, Japan
[120] Ohio State University, Columbus, OH, USA
[121] Homer L. Dodge Department of Physics and Astronomy, University of Oklahoma, Norman, OK, USA
[122] Department of Physics, Oklahoma State University, Stillwater, OK, USA
[123] Palacký University, Joint Laboratory of Optics, Olomouc, Czech Republic
[124] Institute for Fundamental Science, University of Oregon, Eugene,, OR, USA
[125] Graduate School of Science, Osaka University, Osaka, Japan
[126] Department of Physics, University of Oslo, Oslo, Norway
[127] Department of Physics, Oxford University, Oxford, UK
[128] LPNHE, Sorbonne Université, Université Paris Cité, CNRS/IN2P3, Paris, France
[129] Department of Physics, University of Pennsylvania, Philadelphia, PA, USA
[130] Department of Physics and Astronomy, University of Pittsburgh, Pittsburgh, PA, USA
[131] [(a)]Laboratório de Instrumentação e Física Experimental de Partículas-LIP, Lisbon, Portugal; [(b)]Departamento de Física, Faculdade de Ciências, Universidade de Lisboa, Lisbon, Portugal; [(c)]Departamento de Física, Universidade de Coimbra, Coimbra, Portugal; [(d)]Centro de Física Nuclear da Universidade de Lisboa, Lisbon, Portugal; [(e)]Departamento de Física, Universidade do Minho, Braga, Portugal; [(f)]Departamento de Física Teórica y del Cosmos, Universidad de Granada, Granada, Spain; [(g)]Departamento de Física, Instituto Superior Técnico, Universidade de Lisboa, Lisbon, Portugal
[132] Institute of Physics of the Czech Academy of Sciences, Prague, Czech Republic
[133] Czech Technical University in Prague, Prague, Czech Republic

[134] Charles University, Faculty of Mathematics and Physics, Prague, Czech Republic
[135] Particle Physics Department, Rutherford Appleton Laboratory, Didcot, UK
[136] IRFU, CEA, Université Paris-Saclay, Gif-sur-Yvette, France
[137] Santa Cruz Institute for Particle Physics, University of California Santa Cruz, Santa Cruz, CA, USA
[138] [(a)]Departamento de Física, Pontificia Universidad Católica de Chile, Santiago, Chile; [(b)]Millennium Institute for Subatomic physics at high energy frontier (SAPHIR), Santiago, Chile; [(c)]Instituto de Investigación Multidisciplinario en Ciencia y Tecnología, y Departamento de Física, Universidad de La Serena, La Serena, Chile; [(d)]Department of Physics, Universidad Andres Bello, Santiago, Chile; [(e)]Instituto de Alta Investigación, Universidad de Tarapacá, Arica, Chile; [(f)]Departamento de Física, Universidad Técnica Federico Santa María, Valparaíso, Chile
[139] Department of Physics, University of Washington, Seattle, WA, USA
[140] Department of Physics and Astronomy, University of Sheffield, Sheffield, UK
[141] Department of Physics, Shinshu University, Nagano, Japan
[142] Department Physik, Universität Siegen, Siegen, Germany
[143] Department of Physics, Simon Fraser University, Burnaby, BC, Canada
[144] SLAC National Accelerator Laboratory, Stanford, CA, USA
[145] Department of Physics, Royal Institute of Technology, Stockholm, Sweden
[146] Departments of Physics and Astronomy, Stony Brook University, Stony Brook, NY, USA
[147] Department of Physics and Astronomy, University of Sussex, Brighton, UK
[148] School of Physics, University of Sydney, Sydney, Australia
[149] Institute of Physics, Academia Sinica, Taipei, Taiwan
[150] [(a)]E. Andronikashvili Institute of Physics, Iv. Javakhishvili Tbilisi State University, Tbilisi, Georgia; [(b)]High Energy Physics Institute, Tbilisi State University, Tbilisi, Georgia; [(c)]University of Georgia, Tbilisi, Georgia
[151] Department of Physics, Technion, Israel Institute of Technology, Haifa, Israel
[152] Raymond and Beverly Sackler School of Physics and Astronomy, Tel Aviv University, Tel Aviv, Israel
[153] Department of Physics, Aristotle University of Thessaloniki, Thessaloniki, Greece
[154] International Center for Elementary Particle Physics and Department of Physics, University of Tokyo, Tokyo, Japan
[155] Department of Physics, Tokyo Institute of Technology, Tokyo, Japan
[156] Department of Physics, University of Toronto, Toronto, ON, Canada
[157] [(a)]TRIUMF, Vancouver, BC, Canada; [(b)]Department of Physics and Astronomy, York University, Toronto, ON, Canada
[158] Division of Physics and Tomonaga Center for the History of the Universe, Faculty of Pure and Applied Sciences, University of Tsukuba, Tsukuba, Japan
[159] Department of Physics and Astronomy, Tufts University, Medford, MA, USA
[160] Department of Physics and Astronomy, University of California Irvine, Irvine, CA, USA
[161] University of Sharjah, Sharjah, United Arab Emirates
[162] Department of Physics and Astronomy, University of Uppsala, Uppsala, Sweden
[163] Department of Physics, University of Illinois, Urbana, IL, USA
[164] Instituto de Física Corpuscular (IFIC), Centro Mixto Universidad de Valencia-CSIC, Valencia, Spain
[165] Department of Physics, University of British Columbia, Vancouver, BC, Canada
[166] Department of Physics and Astronomy, University of Victoria, Victoria, BC, Canada
[167] Fakultät für Physik und Astronomie, Julius-Maximilians-Universität Würzburg, Würzburg, Germany
[168] Department of Physics, University of Warwick, Coventry, UK
[169] Waseda University, Tokyo, Japan
[170] Department of Particle Physics and Astrophysics, Weizmann Institute of Science, Rehovot, Israel
[171] Department of Physics, University of Wisconsin, Madison, WI, USA
[172] Fakultät für Mathematik und Naturwissenschaften, Fachgruppe Physik, Bergische Universität Wuppertal, Wuppertal, Germany
[173] Department of Physics, Yale University, New Haven, CT, USA

[a] Also Affiliated with an institute covered by a cooperation agreement with CERN, Geneva, Switzerland
[b] Also at An-Najah National University, Nablus, Palestine
[c] Also at Borough of Manhattan Community College, City University of New York, New York, NY, USA
[d] Also at Center for Interdisciplinary Research and Innovation (CIRI-AUTH), Thessaloniki, Greece
[e] Also at Centro Studi e Ricerche Enrico Fermi, Rome, Italy

[f] Also at CERN, Geneva, Switzerland
[g] Also at Département de Physique Nucléaire et Corpusculaire, Université de Genève, Genève, Switzerland
[h] Also at Departament de Fisica de la Universitat Autonoma de Barcelona, Barcelona, Spain
[i] Also at Department of Financial and Management Engineering, University of the Aegean, Chios, Greece
[j] Also at Department of Physics, California State University, Sacramento, USA
[k] Also at Department of Physics, King's College London, London, UK
[l] Also at Department of Physics, Stanford University, Stanford, CA, USA
[m] Also at Department of Physics, Stellenbosch University, South Africa
[n] Also at Department of Physics, University of Fribourg, Fribourg, Switzerland
[o] Also at Department of Physics, University of Thessaly, Greece
[p] Also at Department of Physics, Westmont College, Santa Barbara, USA
[q] Also at Hellenic Open University, Patras, Greece
[r] Also at Institucio Catalana de Recerca i Estudis Avancats, ICREA, Barcelona, Spain
[s] Also at Institut für Experimentalphysik, Universität Hamburg, Hamburg, Germany
[t] Also at Institute for Nuclear Research and Nuclear Energy (INRNE) of the Bulgarian Academy of Sciences, Sofia, Bulgaria
[u] Also at Institute of Applied Physics, Mohammed VI Polytechnic University, Ben Guerir, Morocco
[v] Also at Institute of Particle Physics (IPP), Canada
[w] Also at Institute of Physics and Technology, Mongolian Academy of Sciences, Ulaanbaatar, Mongolia
[x] Also at Institute of Physics, Azerbaijan Academy of Sciences, Baku, Azerbaijan
[y] Also at Institute of Theoretical Physics, Ilia State University, Tbilisi, Georgia
[z] Also at Lawrence Livermore National Laboratory, Livermore, USA
[aa] Also at National Institute of Physics, University of the Philippines Diliman (Philippines), Philippines
[ab] Also at Technical University of Munich, Munich, Germany
[ac] Also at The Collaborative Innovation Center of Quantum Matter (CICQM), Beijing, China
[ad] Also at TRIUMF, Vancouver, BC, Canada
[ae] Also at Università di Napoli Parthenope, Napoli, Italy
[af] Also at University of Colorado Boulder, Department of Physics, Colorado, USA
[ag] Also at Washington College, Chestertown, MD, USA
[ah] Also at Yeditepe University, Physics Department, Istanbul, Türkiye
[ai] Also at Faculty of Physics, Sofia University, 'St. Kliment Ohridski', Sofia, Bulgaria
* Deceased